

新 Double-Froude 系統的渾沌現象, 應用 GYC 部分區域穩定理論的渾沌同步及控制, 以 Legendre 函數為參數的 Rössler 系統之超渾沌現象與藉適應控制之 Lü 系統的陰陽廣義同步

學生：陳志銘

指導教授：戈正銘 教授



摘要

本論文由四個部份構成：(1)以相圖、龐卡萊映射圖、分岐圖及 Lyapunov 指數圖等數值方法研究新 Double-Froude 系統的渾沌行爲。(2)應用部分區域穩定性理論研究廣義渾沌同步、渾沌控制。(3)探討 Rössler 系統以 Legendre 函數為參數的超渾沌行爲及同步(4) 藉實用漸進穩定理論為基礎的適應控制來探討陽 Lü 系統和陰 Lü 系統的陰陽廣義同步。

Chaos, and Chaos Synchronization and Control by GYC Partial Region Stability Theory of a New Double-Froude System, Hyperchaos of Rössler System with Legendre Function Parameters and Yin-Yang Generalized Synchronization of Lü System by Adaptive Control

Student: Zhi-Ming Chen

Advisor: Zheng-Ming Ge



ABSTRACT

This thesis consists of four parts: (1) the chaotic behaviors of Double-Froude system are studied numerically by phase portraits, Poincaré maps, bifurcation diagrams and Lyapunov exponent diagrams. (2) generalized synchronization and control of chaos is studied by GYC partial region stability theory. (3) the Rössler system with Legendre function is studied for chaos, hyperchaos and synchronization. (4) Yin-Yang generalized synchronization (YYGS) of Yang Lü and Yin Lü systems are studied by adaptive control based on pragmatical asymptotical stability theory.

誌謝

此篇論文及碩士學業之完成，首先必須感謝指導教授 戈正銘老師的耐心指導與教誨。老師專業領域上的成就以及對於文學和史學上的熱情，都令學生印象深刻且受益匪淺。這兩年的相處，在學術研究之餘也體會到古典文學的美，這都開拓了學生不一樣的視野。

這研究的日子中，承蒙張晉銘、李仕宇、許凱銘、李彥賢、何俊諺和江峻宇學長的熱心指導，同時也感謝瑜韓、育銘、聰文、泳厚、翔平、尙恩、振賓同學的相互勉勵和幫忙，使得本篇論文能夠順利的完成。

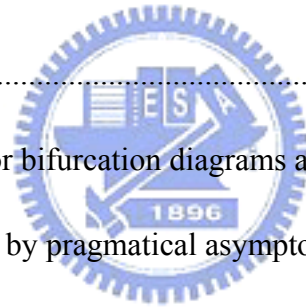
最後感謝我的家人，讓我可以不必擔心課業以外的事物，無後顧之憂的完成學業。最後，僅以此論文獻給你們。



CONTENTS

| | |
|--|-----------|
| CHINESE ABSTRACT..... | i |
| ABSTRACT..... | ii |
| ACKNOWLEDGMENT | iii |
| CONTENTS..... | iv |
| LIST OF FIGURES | vi |
| | |
| Chapter 1 Introduction..... | 1 |
| Chapter 2 Chaos Generalized Synchronization of a New Double-Froude System by GYC Partial Region Stability Theory..... | 4 |
| 2.1 Preliminary | 4 |
| 2.2 Generalized chaos synchronization strategy | 4 |
| 2.3 Chaos of a new double-Froude system..... | 5 |
| 2.4 Numerical simulations examples..... | 6 |
| 2.5 Summary..... | 12 |
| | |
| Chapter 3 Chaos Control of a New Double-Froude Systems System as Functional System by GYC Partial Region Stability Theory | 22 |
| 3.1 Preliminary | 22 |
| 3.2 Chaos control scheme..... | 22 |
| 3.3 Numerical simulations..... | 23 |
| 3.4 Summary..... | 28 |
| | |
| Chapter 4 Hyperchaos of The Rössler System with Legendre Function Parameters..... | 35 |

| | |
|--|-----------|
| 4.1 Preliminary | 35 |
| 4.2 Chaos of The classical Rössler system and Legendre function..... | 35 |
| 4.3 Numerical results..... | 36 |
| 4.4 Summary..... | 38 |
| Chapter 5 Yin-Yang Generalized Synchronization of Chaotic Lü Systems by Pragmatical Asymptotical Stability Theorem..... | 48 |
| 5.1 Preliminary | 48 |
| 5.2 YYGS scheme by adaptive control and pragmatical asymptotical stability theorem..... | 48 |
| 5.3 Yang Lü system..... | 50 |
| 5.4 Yin Lü system..... | 50 |
| 5.5 Simulation results for bifurcation diagrams and Lyapunov exponents | 52 |
| 5.6 YYGS of Lü system by pragmatical asymptotical stability theorem..... | 55 |
| 5.7 Summary..... | 61 |
| Chapter 6 Conclusions..... | 76 |
| Appendix A GYC Partial Region Stability Theory | 78 |
| Appendix B Systems of Positive States..... | 86 |
| Appendix C Pragmatical Asymptotical Stability Theory | 90 |
| References | 93 |



LIST OF FIGURES

| | |
|--|----|
| Fig. 2.1 Chaos of new double-Froude system (a) Phase portrait (b) Time histories of states (c) Power spectrum (d) Bifurcation diagram (e) Lyapunov exponents. | 13 |
| Fig. 2.2 Phase portraits of error dynamics for Case I. | 14 |
| Fig. 2.3 Time histories of errors for Case I. | 15 |
| Fig. 2.4 Time histories of x_i, y_i for Case I. | 15 |
| Fig. 2.5 Phase portraits of error dynamics for Case II. | 16 |
| Fig. 2.6 Time histories of errors for Case II. | 17 |
| Fig. 2.7 Time histories of $x_i - y_i + 10$ and $-m \sin \omega t$ for Case II. | 17 |
| Fig. 2.8 Phase portraits of error dynamics for Case III. | 18 |
| Fig. 2.9 Time histories of errors for Case III. | 19 |
| Fig. 2.10 Time histories of $\frac{x_i^2(t-1)}{4} + 10$ and y_i for Case III. | 19 |
| Fig. 2.11 Phase portraits of error dynamics for Case IV. | 20 |
| Fig. 2.12 Time histories of errors for Case IV. | 21 |
| Fig. 2.13 Time histories of $x_i - y_i + 50$ and $z_i + w_i$ for Case IV. | 21 |
| Fig. 3.1 Phase portraits of error dynamics for Case I. | 29 |
| Fig. 3.2 Time histories of errors for Case I. | 30 |
| Fig. 3.3 Phase portraits of error dynamics for Case II. | 31 |
| Fig. 3.4 Time histories of errors for Case II. | 32 |
| Fig. 3.5 Time histories of x_1, x_2, x_3, x_4 for Case II. | 32 |
| Fig. 3.6 Phase portraits of error dynamics for Case III. | 33 |
| Fig. 3.7 Time histories of errors for Case III. | 34 |
| Fig. 3.8 Time histories of x_1, x_2, x_3, x_4 and z_1, z_2, z_3, z_4 for Case III. | 34 |
| Fig. 4.1 (a) 3D Phase portrait (b) 2D Phase portrait (c) Time histories of states for | |

| | |
|---|----|
| classical Rössler systems..... | 41 |
| Fig. 4.2 Time histories of L_1 and L_3 | 41 |
| Fig. 4.3 The bifurcation diagram for Rössler system with Legendre function parameters with $b=0.2$ and $c=12$ | 42 |
| Fig. 4.4 (a) The Lyapunov exponents for system (4-7). (b) Enlarge diagram of Fig. 4.4(a)..... | 43 |
| Fig. 4.5 Poincaré maps, and time histories for Rössler system with Legendre function parameters when $k=-0.2$ (period 1). | 44 |
| Fig. 4.6 Poincaré maps, and time histories for Rössler system with Legendre function parameters when $k=0.05$ (chaos)..... | 45 |
| Fig. 4.7 (a) The Lyapunov exponents for system (4-7) with $a=0.15$ and $b=0.2$. (b) Enlarged diagram of fig. 4.7(a)..... | 46 |
| Fig. 4.8 Parameter diagram of system (4-7) with varying j, k | 47 |
| Fig. 5.1 Projections of phase portrait and phase portrait of chaotic Yang Lü system with $a=36, b=3$ and $c=20$ | 62 |
| Fig. 5.2 Projection of phase portrait and phase portrait of chaotic Yin Lorenz system with Yin parameters $a=-10, b=-8/3$ and $c=-28$ | 63 |
| Fig. 5.3 Lyapunov exponents and bifurcation diagram of chaotic Yang Lü system with $a=36$ and $b=3$ | 64 |
| Fig. 5.4 Lyapunov exponents and bifurcation diagram of chaotic Yin Lü system with $a=-36$ and $b=-3$ | 65 |
| Fig. 5.5 Lyapunov exponents and bifurcation diagram of chaotic Yang Lü system with $b=-3$ and $c=-20$ | 66 |
| Fig. 5.6 Lyapunov exponents and bifurcation diagram of chaotic Yin Lü system with $c=-20$ and $b=-3$ | 67 |

| | |
|---|----|
| Fig. 5.7 Lyapunov exponents and bifurcation diagram of chaotic Yang Lü system with $a=-36$ and $c=-20$ | 68 |
| Fig. 5.8 Lyapunov exponents and bifurcation diagram of chaotic Yin Lü system with $a=-36$ and $c=-20$ | 69 |
| Fig. 5.9 Time histories of state errors for Yin and Yang Lü chaotic systems..... | 70 |
| Fig. 5.10 Time histories of parameter errors for Yin and Yang Lü chaotic systems... | 70 |
| Fig. 5.11 Time histories of states of Yin and Yang Lü chaotic systems..... | 71 |
| Fig. 5.12 Phase portraits of Yin and Yang Lü chaotic systems..... | 71 |
| Fig. 5.13 Time histories of state errors for Case II..... | 72 |
| Fig. 5.14 Time histories of parameter errors for Case II..... | 72 |
| Fig. 5.15 Time histories of states for Case II..... | 73 |
| Fig. 5.16 Phase portraits for case III..... | 73 |
| Fig. 5.17 Time histories of state errors for Case III..... | 74 |
| Fig. 5.18 Time histories of parameter errors for Case III..... | 74 |
| Fig. 5.19 Time histories of states of Case III..... | 75 |
| Fig. 5.20 Phase portraits for case III..... | 75 |
| Fig. A.1. Partial regions Ω and Ω_1 | 85 |

Chapter 1

Introduction

Synchronization of chaotic systems has become an important topic since the pioneering work of Pecora and Carroll in 1990 [1]. Furthermore, chaos synchronization has many potential applications in laser physics, chemical reactor, secure communication, biomedical and so on [2-4]. Chaos synchronization has been widely investigated in a variety of fields [5-8]. Many chaos synchronization methods have been developed, such as invariant manifold method [9], adaptive control method [10], active control method [11] and synchronization in unidirectionally and bidirectionally coupled systems [12].

Since Ott et al. [13] gave the famous OGY control method in 1990, the applications of the various methods to control a chaotic behavior in natural sciences and engineering are well known. For example, the adaptive control [14-17], the method of chaos control based on sampled data [18], the method of impulse feedback of systematic variable [19], the active control [20-21] and linear error feedback control [22-23].

Chaos is a typical phenomenon in nonlinear dynamic systems whose phase space has a dimension not lower than three. Chaos exists in many physical and engineering systems as a desirable behavior in many systems such as secure communications, liquid mixing, heat transfer and chemical reactions. Therefore, to investigate the hyperchaos and chaos appears to be one of the fundamentally important problems in nonlinear dynamics.

When a chaotic system has more than one positive Lyapunov exponent, the dynamics of the system is expanded in more than one direction, giving rise to a more

complex attractor. Usually, this kind of system is called hyperchaotic. Hyperchaos was first reported by Rössler [24] and received great attention because of its potential in various engineering systems [25-28].

In Chinese philosophy [35-37], Yang is the positive, contemporary or feminine principle in nature, while Yin is the negative, historical or masculine principle in nature. So the contemporary Lü system or chaos may be called Yang Lü system, or Yang chaos, while the historical Lü system and chaos, Yin Lü system, or Yin chaos. There are large amounts of articles in researching Yang Lü system [29-34]. Although the Yang Lü system has been analyzed in detail, there are no articles in looking for the Yin Lü system. In this paper, we find there are rich dynamics in Yin Lü system.

In Chapter 2, a new chaos generalized synchronization strategy by GYC partial region stability theory (Appendix A,B) is proposed [38-40]. By using the GYC partial region stability theory, the controllers are of lower degree than that of controllers by using traditional Lyapunov asymptotical stability theorem [41-49]. The simple linear homogeneous Lyapunov function of error states makes that the controllers introduce less simulation error.

In Chapter 3, a new strategy to achieve chaos control by GYC partial region stability theory is proposed [38-40]. Via the GYC partial region stability theory, the new Lyapunov function is a simple linear homogeneous function of error states and the lower degree controllers are much more simple and introduce less simulation error.

In Chapter 4, hyperchaos and chaos of Rössler system with Legendre function parameters are studied. They are identified by phase portraits, bifurcation diagrams, Lyapunov exponents, time histories of states, Poincaré maps and parameter diagrams. Both hyperchaos and chaos exist abundantly. They give various applications, especially for secret communication.

In Chapter 5, the Yin Lü system is introduced and the chaotic behavior with *Yin* parameters is investigated by phase portrait, Lyapunov exponents and bifurcation diagram in the following simulation results. We use Yang parameters for the Yang Lü system, and Yin parameters for the Yin Lü system. Yin-Yang generalized synchronization of chaotic Lü systems by pragmatical asymptotical stability theorem (Appendix C) is given. Conclusions are presented in Chapter 6.



Chapter 2

Chaos Generalized Synchronization of a New Double-Froude System by GYC Partial Region Stability Theory

2.1 Preliminary

In this Chapter, *GYC partial region stability theory* is used to achieve chaos generalized synchronization for new double-Froude systems. The Lyapunov function of error states becomes a simple linear homogeneous function and the controllers are simpler than that by using traditional Lyapunov theory and so introduce less simulation results. Numerical simulations are provided to show the effectiveness and advantage of this method.

2.2 Generalized chaos synchronization strategy

Consider the following unidirectional coupled chaotic systems

$$\begin{aligned}\dot{\mathbf{x}} &= \mathbf{f}(t, \mathbf{x}) \\ \dot{\mathbf{y}} &= \mathbf{h}(t, \mathbf{y}) + \mathbf{u}\end{aligned}\tag{2-1}$$

where $\mathbf{x} = [x_1, x_2, \dots, x_n]^T \in R^n$, $\mathbf{y} = [y_1, y_2, \dots, y_n]^T \in R^n$ denote the master state vector and slave state vector respectively, \mathbf{f} and \mathbf{h} are nonlinear vector functions, and $\mathbf{u} = [u_1, u_2, \dots, u_n]^T \in R^n$ is a control input vector.

The generalized synchronization can be accomplished when $t \rightarrow \infty$, the limit of the error vector $\mathbf{e} = [e_1, e_2, \dots, e_n]^T$ approaches zero:

$$\lim_{t \rightarrow \infty} \mathbf{e} = 0\tag{2-2}$$

where

$$\mathbf{e} = \mathbf{G}(\mathbf{x}) - \mathbf{y}\tag{2-3}$$

$G(\mathbf{x})$ is a given function of \mathbf{x} .

By using the partial region stability theory, the Lyapunov function is linear homogeneous function of error states. The controllers can be designed in lower degree.

2.3 Chaos of a new double-Froude system

Two double-Froude systems[25] are introduced as typical nonlinear non-autonomous systems:

$$\begin{cases} \frac{dx_1}{dt} = x_2 \\ \frac{dx_2}{dt} = (a - bx_2^2)x_2 - c \sin x_1 - d \cos \omega t \end{cases} \quad (2-4)$$

$$\begin{cases} \frac{dx_3}{dt} = x_4 \\ \frac{dx_4}{dt} = (e - fx_4^2)x_4 - g \sin x_3 - h \cos \omega t \end{cases} \quad (2-5)$$

Exchanging $\cos \omega t$ in Eq. (2-4) and $\cos \omega t$ in Eq. (2-5) with x_3 and x_1 respectively, we obtain an autonomous new double-Froude system:

$$\begin{cases} \frac{dx_1}{dt} = x_2 \\ \frac{dx_2}{dt} = (a - bx_2^2)x_2 - c \sin x_1 - dx_3 \\ \frac{dx_3}{dt} = x_4 \\ \frac{dx_4}{dt} = (e - fx_4^2)x_4 - g \sin x_3 - hx_1 \end{cases} \quad (2-6)$$

where a, b, c, d, e, f, g, h are parameters. This system exhibits chaos when the parameters of system are $a=0.35, b=0.2, c=-1.16, d=1.54, e=0.7525, f=0.2, g=10.5, h=-1.7$ and the initial states of system are $x_1(0)=2, x_2(0)=2.4, x_3(0)=5, x_4(0)=6$. Its chaotic phase portrait, time histories of states, power spectrum, bifurcation diagram and Lyapunov exponents are shown in Fig. 2.1.

2.4 Numerical simulation examples

Two double-Froude systems with unidirectional coupling are given:

$$\begin{cases} \dot{x}_1 = x_2 \\ \dot{x}_2 = (a - bx_2^2)x_2 - c \sin x_1 + dx_3 \\ \dot{x}_3 = x_4 \\ \dot{x}_4 = (e - fx_4^2)x_4 - g \sin x_3 + hx_1 \end{cases} \quad (2-7)$$

$$\begin{cases} \dot{y}_1 = y_2 + u_1 \\ \dot{y}_2 = (a - by_2^2)y_2 - c \sin y_1 + dy_3 + u_2 \\ \dot{y}_3 = y_4 + u_3 \\ \dot{y}_4 = (e - fy_4^2)y_4 - g \sin y_3 + hy_1 + u_4 \end{cases} \quad (2-8)$$

CASE I. The generalized synchronization error function is

$$e_i = x_i - y_i + 10, \quad i = 1, 2, 3, 4 \quad (2-9)$$

The addition of the constant 10 makes the error dynamics always happens in the first quadrant. Our goal is $y_i = x_i + 10$, i.e.

$$\lim_{t \rightarrow \infty} e_i = \lim_{t \rightarrow \infty} (x_i - y_i + 10) = 0, \quad i = 1, 2, 3, 4 \quad (2-10)$$

The error dynamics becomes

$$\begin{cases} \dot{e}_1 = \dot{x}_1 - \dot{y}_1 = x_2 - y_2 - u_1 \\ \dot{e}_2 = \dot{x}_2 - \dot{y}_2 = (a - bx_2^2)x_2 - c \sin x_1 + dx_3 - ((a - by_2^2)y_2 - c \sin y_1 + dy_3) - u_2 \\ \dot{e}_3 = \dot{x}_3 - \dot{y}_3 = x_4 - y_4 - u_3 \\ \dot{e}_4 = \dot{x}_4 - \dot{y}_4 = (e - fx_4^2)x_4 - g \sin x_3 + hx_1 - ((e - fy_4^2)y_4 - g \sin y_3 + hy_1) - u_4 \end{cases} \quad (2-11)$$

Let initial states be $(x_1, x_2, x_3, x_4) = (0.2, 0.35, 0.2, 0.35)$, $(y_1, y_2, y_3, y_4) = (1, 1, 1, 1)$

and system parameters $a = 0.35$, $b = 0.2$, $c = -1.16$, $d = 1.54$, $e = 0.7525$,

$f = 0.2$, $g = 10.5$, $h = -1.7$, we find that the error dynamic always exists in first

quadrant as shown in Fig. 2.2. By GYC partial region asymptotical stability theorem,

one can choose a Lyapunov function in the form of a positive definite function in first

quadrant:

$$V = e_1 + e_2 + e_3 + e_4 \quad (2-12)$$

Its time derivative is

$$\begin{aligned} \dot{V} &= \dot{e}_1 + \dot{e}_2 + \dot{e}_3 + \dot{e}_4 \\ &= (x_2 - y_2 - u_1) \\ &\quad + \left((a - bx_2^2)x_2 - c \sin x_1 + dx_3 - ((a - by_2^2)y_2 - c \sin y_1 + dy_3) - u_2 \right) \\ &\quad + (x_4 - y_4 - u_3) \\ &\quad + \left((e - fx_4^2)x_4 - g \sin x_3 + hx_1 - ((e - fy_4^2)y_4 - g \sin y_3 + hy_1) - u_4 \right) \end{aligned} \quad (2-13)$$

Choose

$$\begin{cases} u_1 = x_2 - y_2 + e_1 \\ u_2 = (a - bx_2^2)x_2 - c \sin x_1 + dx_3 - ((a - by_2^2)y_2 - c \sin y_1 + dy_3) + e_2 \\ u_3 = x_4 - y_4 + e_3 \\ u_4 = (e - fx_4^2)x_4 - g \sin x_3 + hx_1 - ((e - fy_4^2)y_4 - g \sin y_3 + hy_1) + e_4 \end{cases} \quad (2-14)$$

We obtain

$$\dot{V} = -e_1 - e_2 - e_3 - e_4 < 0 \quad (2-15)$$

which is a negative definite function in the first quadrant. Four state errors versus time and time histories of states are shown in Fig. 2.3 and Fig. 2.4.

CASE II. The generalized synchronization error function is

$$e_i = x_i - y_i + m \sin \omega t + 10, \quad i = 1, 2, 3, 4 \quad (2-16)$$

Our goal is $y = x + m \sin \omega t + 10$, i.e.

$$\lim_{t \rightarrow \infty} e_i = \lim_{t \rightarrow \infty} (x_i - y_i + m \sin \omega t + 10) = 0, \quad i = 1, 2, 3, 4 \quad (2-17)$$

The error dynamics becomes

$$\begin{cases} \dot{e}_1 = x_2 - y_2 + m\omega \cos \omega t - u_1 \\ \dot{e}_2 = (a - bx_2^2)x_2 - c \sin x_1 + dx_3 - ((a - by_2^2)y_2 - c \sin y_1 + dy_3) \\ \quad + m\omega \cos \omega t - u_2 \\ \dot{e}_3 = x_4 - y_4 + m\omega \cos \omega t - u_3 \\ \dot{e}_4 = (e - fx_4^2)x_4 - g \sin x_3 + hx_1 - ((e - fy_4^2)y_4 - g \sin y_3 + hy_1) \\ \quad + m\omega \cos \omega t - u_4 \end{cases} \quad (2-18)$$

Let initial states be $(x_1, x_2, x_3, x_4) = (0.2, 0.35, 0.2, 0.35)$, $(y_1, y_2, y_3, y_4) = (1, 1, 1, 1)$ and system parameters $a = 0.35$, $b = 0.2$, $c = -1.16$, $d = 1.54$, $e = 0.7525$, $f = 0.2$, $g = 10.5$, $h = -1.7$, $m = 2$ and $\omega = 1$, we find that the error dynamics always exists in first quadrant as shown in Fig. 2.5. By GYC partial region asymptotical stability theorem, one can choose a Lyapunov function in the form of a positive definite function in first quadrant:

$$V = e_1 + e_2 + e_3 + e_4 \quad (2-19)$$

Its time derivative is

$$\begin{aligned} \dot{V} = & (x_2 - y_2 + m\omega \cos \omega t - u_1) \\ & + \left((a - bx_2^2)x_2 - c \sin x_1 + dx_3 - ((a - by_2^2)y_2 - c \sin y_1 + dy_3) + m\omega \cos \omega t - u_2 \right) \\ & + (x_4 - y_4 + m\omega \cos \omega t - u_3) \\ & + \left((e - fx_4^2)x_4 - g \sin x_3 + hx_1 - ((e - fy_4^2)y_4 - g \sin y_3 + hy_1) + m\omega \cos \omega t - u_4 \right) \end{aligned} \quad (2-20)$$

Choose

$$\begin{cases} u_1 = x_2 - y_2 + m\omega \cos \omega t + e_1 \\ u_2 = (a - bx_2^2)x_2 - c \sin x_1 + dx_3 - ((a - by_2^2)y_2 - c \sin y_1 + dy_3) + m\omega \cos \omega t + e_2 \\ u_3 = x_4 - y_4 + m\omega \cos \omega t + e_3 \\ u_4 = (e - fx_4^2)x_4 - g \sin x_3 + hx_1 - ((e - fy_4^2)y_4 - g \sin y_3 + hy_1) + m\omega \cos \omega t + e_4 \end{cases} \quad (2-21)$$

We obtain

$$\dot{V} = -e_1 - e_2 - e_3 - e_4 < 0 \quad (2-22)$$

which is negative definite function in first quadrant. Four state errors versus time and time histories of states are shown in Fig. 2.6 and Fig. 2.7.

CASE III. The generalized synchronization error function is

$$e_i = \frac{1}{4}x_i^2(t - \tau) - y_i + 10, \quad i = 1, 2, 3, 4 \quad (2-23)$$

where $\tau = 1$ is the time delay.

Our goal is $y_i = \frac{1}{4}x_i^2(t - 1) + 10$, i.e.

$$\lim_{t \rightarrow \infty} e_i = \lim_{t \rightarrow \infty} \left(\frac{1}{4} x_i^2(t-1) - y_i + 10 \right) = 0, \quad i = 1, 2, 3, 4 \quad (2-24)$$

The error dynamics becomes

$$\begin{cases} \dot{e}_1 = \frac{1}{2} x_1(t-1)x_2(t-1) - y_2 - u_1 \\ \dot{e}_2 = \frac{1}{2} x_1 \left((a - bx_2^2(t-1))x_2(t-1) - c \sin x_1(t-1) + dx_3(t-1) \right) \\ \quad - \left((a - by_2^2)y_2 - c \sin y_1 + dy_3 \right) - u_2 \\ \dot{e}_3 = \frac{1}{2} x_3(t-1)x_4(t-1) - y_4 - u_3 \\ \dot{e}_4 = \frac{1}{2} x_3 \left((e - fx_4^2(t-1))x_4(t-1) - g \sin x_3(t-1) + hx_1(t-1) \right) \\ \quad - \left((e - fy_4^2)y_4 - g \sin y_3 + hy_1 \right) - u_4 \end{cases} \quad (2-25)$$

Let initial states be $(x_1, x_2, x_3, x_4) = (0.2, 0.35, 0.2, 0.35)$, $(y_1, y_2, y_3, y_4) = (1, 1, 1, 1)$ and system parameters $a = 0.35$, $b = 0.2$, $c = -1.16$, $d = 1.54$, $e = 0.7525$, $f = 0.2$, $g = 10.5$, $h = -1.7$, we find the error dynamics always exists in first quadrant as shown in Fig. 2.8. By GYC partial region asymptotical stability theorem, one can choose a Lyapunov function in the form of a positive definite function in first quadrant:

$$V = e_1 + e_2 + e_3 + e_4 \quad (2-26)$$

Its time derivative is

$$\begin{aligned} \dot{V} = & \left(\frac{1}{2} x_1(t-1) \times x_2(t-1) - y_2 - u_1 \right) \\ & + \left(\frac{1}{2} x_1(t-1) \times \left((a - bx_2^2(t-1)) \times x_2(t-1) - c \sin x_1(t-1) + dx_3(t-1) \right) \right. \\ & \quad \left. - \left((a - by_2^2)y_2 - c \sin y_1 + dy_3 \right) - u_2 \right) \\ & + \left(\frac{1}{2} x_3(t-1) \times x_4(t-1) - y_4 - u_3 \right) \\ & + \left(\frac{1}{2} x_3(t-1) \times \left((e - fx_4^2(t-1)) \times x_4(t-1) - g \sin x_3(t-1) + hx_1(t-1) \right) - \right. \\ & \quad \left. \left((e - fy_4^2)y_4 - g \sin y_3 + hy_1 \right) - u_4 \right) \end{aligned} \quad (2-27)$$

Choose

$$\begin{cases} u_1 = \frac{1}{2}x_1(t-1)x_2(t-1) - y_2 + e_1 \\ u_2 = \frac{1}{2}x_1(t-1) \times \left((a - bx_2^2(t-1)) \times x_2(t-1) - c \sin x_1(t-1) + dx_3(t-1) \right) \\ \quad - \left((a - by_2^2)y_2 - c \sin y_1 + dy_3 \right) + e_2 \\ u_3 = \frac{1}{2}x_3(t-1) \times x_4(t-1) - y_4 + e_3 \\ u_4 = \frac{1}{2}x_3(t-1) \times \left((e - fx_4^2(t-1)) \times x_4(t-1) - g \sin x_3(t-1) + hx_1(t-1) \right) \\ \quad - \left((e - fy_4^2)y_4 - g \sin y_3 + hy_1 \right) + e_4 \end{cases} \quad (2-28)$$

We obtain

$$\dot{V} = -e_1 - e_2 - e_3 - e_4 < 0 \quad (2-29)$$

which is a negative definite function in first quadrant. Four state errors versus time and time histories of states are shown in Fig. 2.9 and Fig. 2.10.

CASE IV. The generalized synchronization error function is

$$e_i = x_i - y_i + z_i + w_i + 25, \quad i = 1, 2, 3, 4 \quad (2-30)$$

$z = [z_1 \ z_2 \ z_3 \ z_4]^T$ is the state vector of a generalized Lorenz system.

$w = [w_1 \ w_2 \ w_3 \ w_4]^T$ is the state vector of a generalized Chen system.

The goal system for synchronization is the sum of two functional systems, i.e. generalized Lorenz system and generalized Chen system. Let initial states be $(z_1, z_2, z_3, z_4) = (0.2, 0.35, 0.2, 0.35)$, $(w_1, w_2, w_3, w_4) = (5, 6, 5, 6)$ and system parameters $s = 1$, $p = 26$, $q = 0.7$, $r = 1.5$, $a_1 = 36$, $b_1 = 3$, $c_1 = 22$, $d_1 = 16$.

$$\begin{cases} \dot{z}_1 = s(z_2 - z_1) + rz_4 \\ \dot{z}_2 = pz_1 - z_1z_3 - z_2 \\ \dot{z}_3 = z_1z_2 - qz_3 \\ \dot{z}_4 = -z_1 - sz_4 \end{cases} \quad (2-31)$$

$$\begin{cases} \dot{w}_1 = a_1(w_2 - w_1) \\ \dot{w}_2 = -d_1 w_1 - w_1 w_3 + c_1 w_2 - w_4 \\ \dot{w}_3 = w_1 w_2 - b_1 w_3 \\ \dot{w}_4 = w_1 \end{cases} \quad (2-32)$$

We have

$$\lim_{t \rightarrow \infty} e_i = \lim_{t \rightarrow \infty} (x_i - y_i + z_i + w_i + 50) = 0 \quad i=1, 2, 3, 4 \quad (2-33)$$

The error dynamics becomes

$$\begin{cases} \dot{e}_1 = x_2 - y_2 + s(z_2 - z_1) + rz_4 + a_1(w_2 - w_1) - u_1 \\ \dot{e}_2 = (a - bx_2^2)x_2 - c \sin x_1 + dx_3 - ((a - by_2^2)y_2 - c \sin y_1 + dy_3) + (pz_1 - z_1 z_3 - z_2) \\ \quad - d_1 w_1 - w_1 w_3 + c_1 w_2 - w_4 - u_2 \\ \dot{e}_3 = x_4 - y_4 + (z_1 z_2 - qz_3) + w_1 w_2 - b_1 w_3 - u_3 \\ \dot{e}_4 = (e - fx_4^2)x_4 - g \sin x_3 + hx_1 - ((e - fy_4^2)y_4 - g \sin y_3 + hy_1) + (-z_1 - sz_4) \\ \quad + w_1 - u_4 \end{cases} \quad (2-34)$$

Let initial states be $(x_1, x_2, x_3, x_4) = (0.2, 0.35, 0.2, 0.35)$, $(y_1, y_2, y_3, y_4) = (1, 1, 1, 1)$ and system parameters $a = 0.35$, $b = 0.2$, $c = -1.16$, $d = 1.54$, $e = 0.7525$, $f = 0.2$, $g = 10.5$, $h = -1.7$, we find the error dynamics always exists in first quadrant as shown in Fig. 2.11. By GYC partial region asymptotical stability theorem, one can choose a Lyapunov function in the form of a positive definite function in first quadrant:

$$V = e_1 + e_2 + e_3 + e_4 \quad (2-35)$$

Its time derivative is

$$\begin{aligned} \dot{V} = & (x_2 - y_2 + s(z_2 - z_1) + rz_4 + a_1(w_2 - w_1) - u_1) \\ & + \left((a - bx_2^2)x_2 - c \sin x_1 + dx_3 - ((a - by_2^2)y_2 - c \sin y_1 + dy_3) + (pz_1 - z_1 z_3 - z_2) \right) \\ & - \left(d_1 w_1 - w_1 w_3 + c_1 w_2 - w_4 - u_2 \right) \\ & + (x_4 - y_4 + (z_1 z_2 - qz_3) + w_1 w_2 - b_1 w_3 - u_3) \\ & + \left((e - fx_4^2)x_4 - g \sin x_3 + hx_1 - ((e - fy_4^2)y_4 - g \sin y_3 + hy_1) + (-z_1 - sz_4) \right) \\ & + (w_1 - u_4) \end{aligned} \quad (2-36)$$

Choose

$$\begin{cases} u_1 = x_2 - y_2 + s(z_2 - z_1) + rz_4 + a_1(w_2 - w_1) + e_1 \\ u_2 = (a - bx_2^2)x_2 - c \sin x_1 + dx_3 - ((a - by_2^2)y_2 - c \sin y_1 + dy_3) + (pz_1 - z_1z_3 - z_2) \\ \quad - d_1w_1 - w_1w_3 + c_1w_2 - w_4 + e_2 \\ u_3 = x_4 - y_4 + (z_1z_2 - qz_3) - u_3 + w_1w_2 - b_1w_3 + e_3 \\ u_4 = (e - fx_4^2)x_4 - g \sin x_3 + hx_1 - ((e - fy_4^2)y_4 - g \sin y_3 + hy_1) + (-z_1 - sz_4) \\ \quad + w_1 + e_4 \end{cases} \quad (2-37)$$

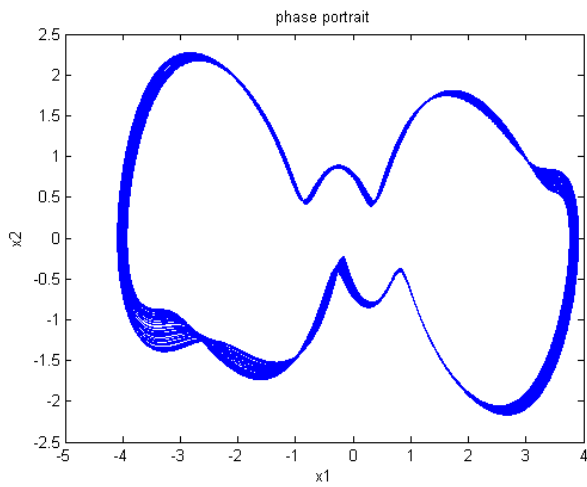
We obtain

$$\dot{V} = -e_1 - e_2 - e_3 - e_4 < 0 \quad (2-38)$$

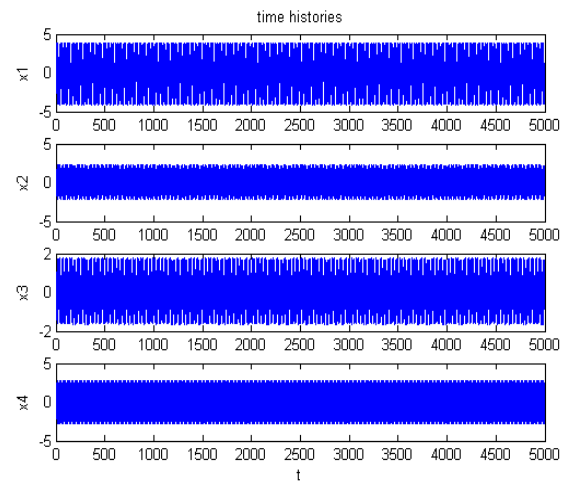
which is a negative definite function in first quadrant. Four state errors versus time and time histories of states are shown in Fig. 2.12 and Fig. 2.13.

2.5 Summary

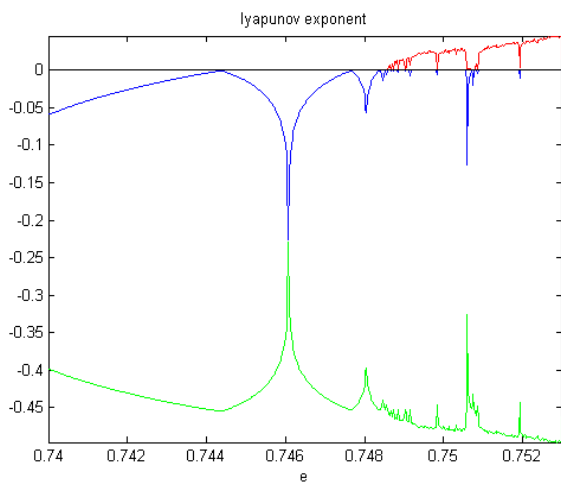
In this Chapter, a new chaos generalized synchronization method by GYC partial region stability theory is proposed. By using the GYC partial region stability theory, the controllers are of lower order than that of controllers by using traditional Lyapunov asymptotical stability theorem. The simple linear homogeneous Lyapunov function of error states makes that the controllers are simpler and introduce less simulation error. In the simulation example, generalized synchronization is extended to time delay system and to two functional chaotic systems. The new double-Froude system, generalized Lorenz system and generalized Chen system are used as simulation examples which verify the effectiveness of the proposed scheme.



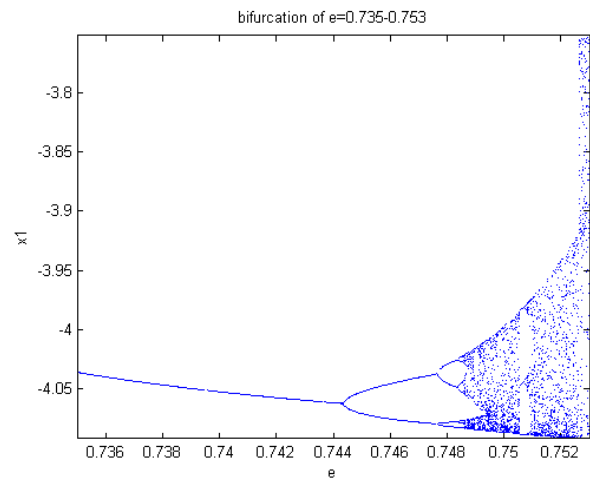
(a)



(b)

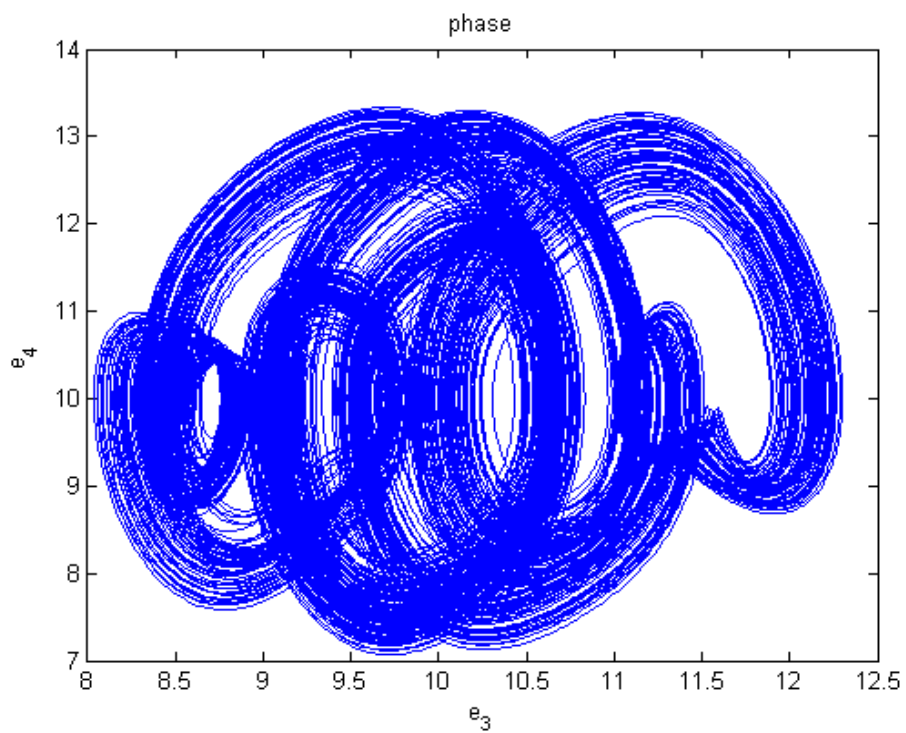
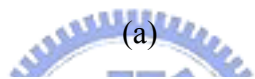
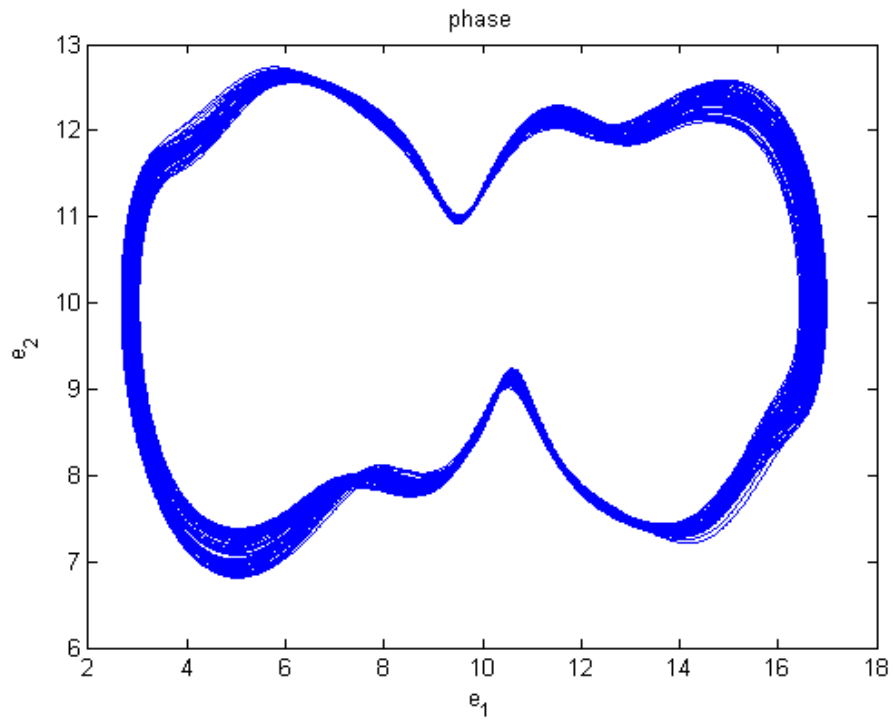


(c)



(d)

Fig. 2.1 Chaos of new double-Froude system (a) Phase portrait (b) Time histories of states (c) Lyapunov exponents (d) Bifurcation diagram.



(b)

Fig. 2.2 Phase portraits of error dynamics for Case I.

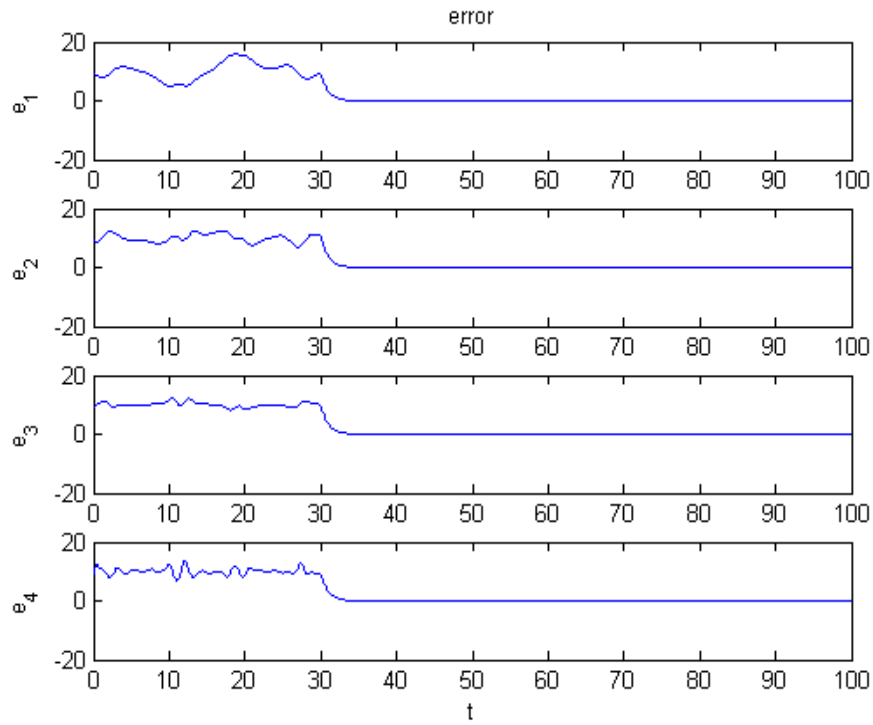


Fig. 2.3 Time histories of errors for Case I.

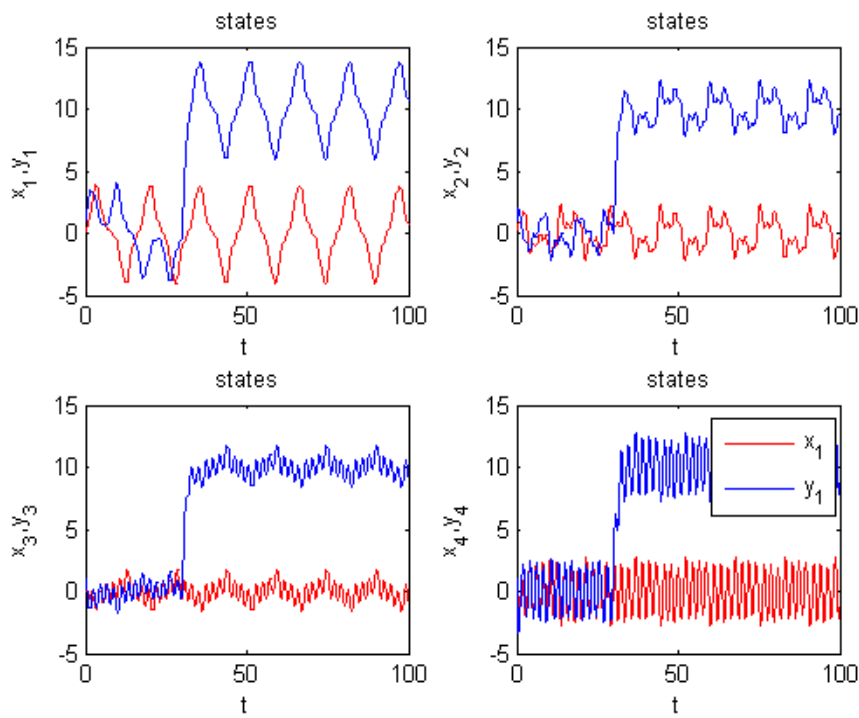
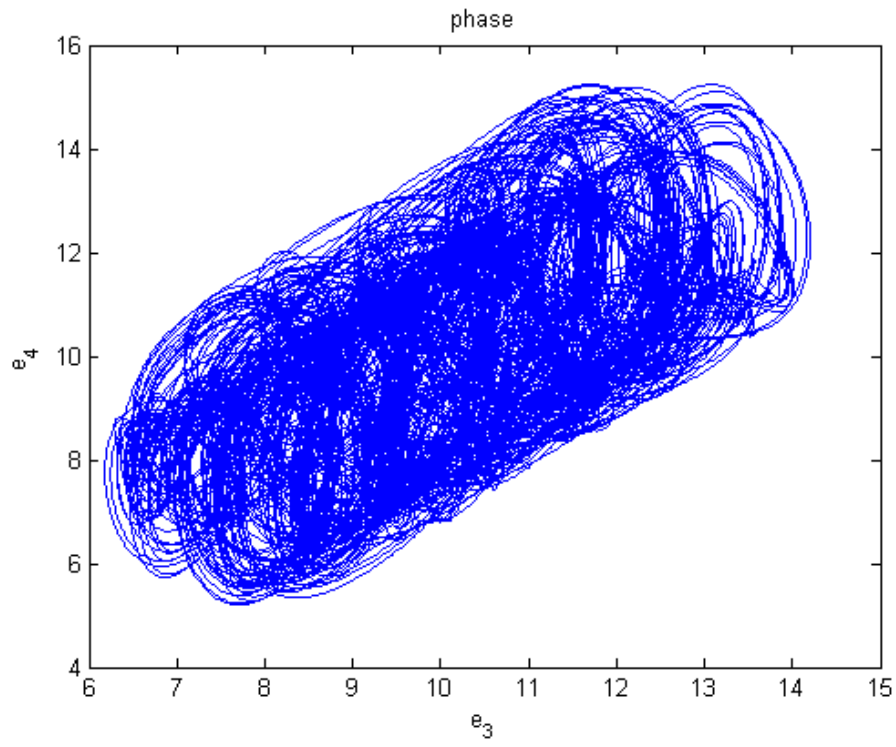
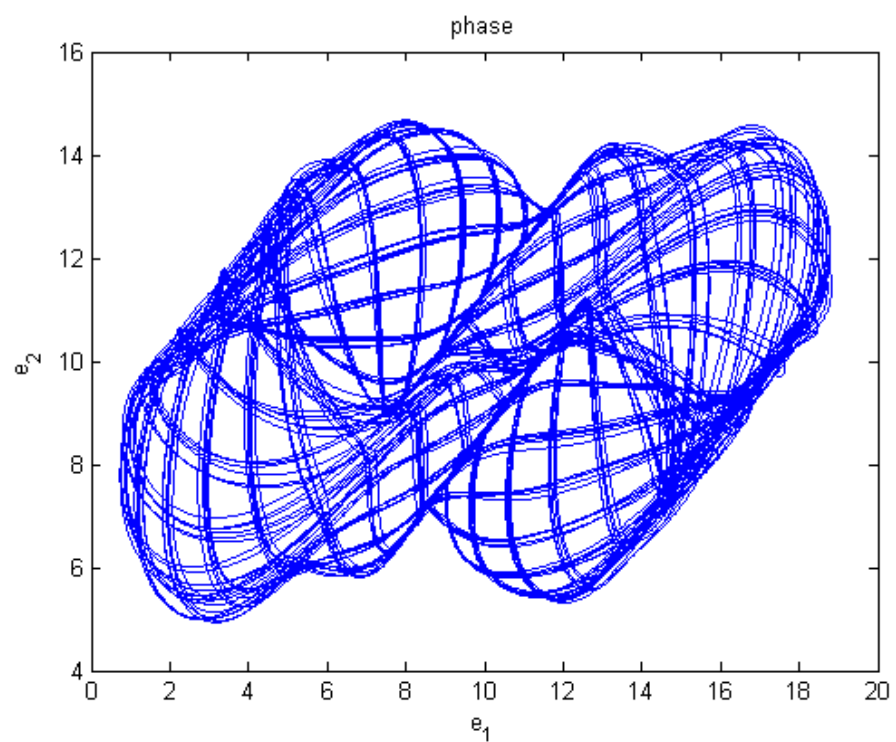


Fig. 2.4 Time histories of x_i, y_i for Case I.



(a)



(b)

Fig. 2.5 Phase portraits of error dynamics for Case II.

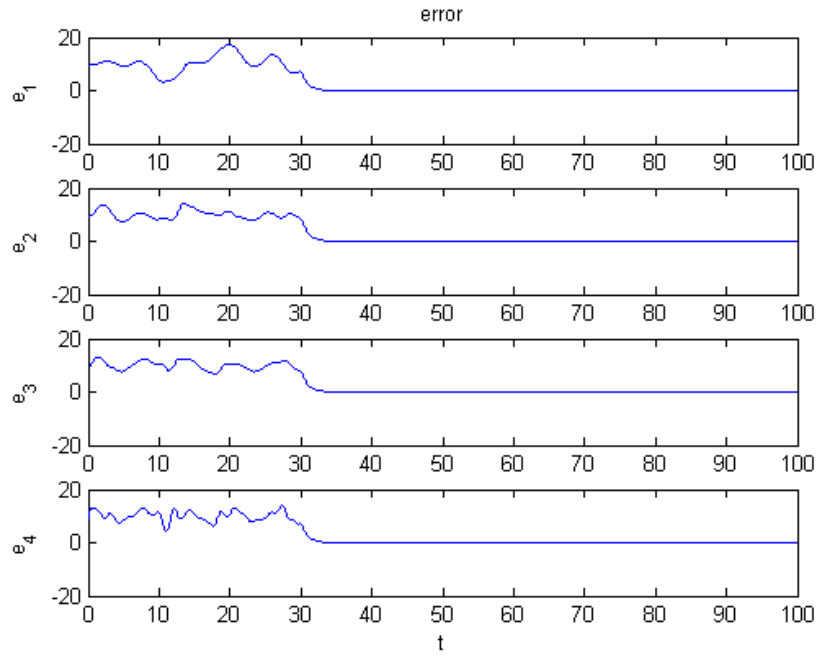


Fig. 2.6 Time histories of errors for Case II.

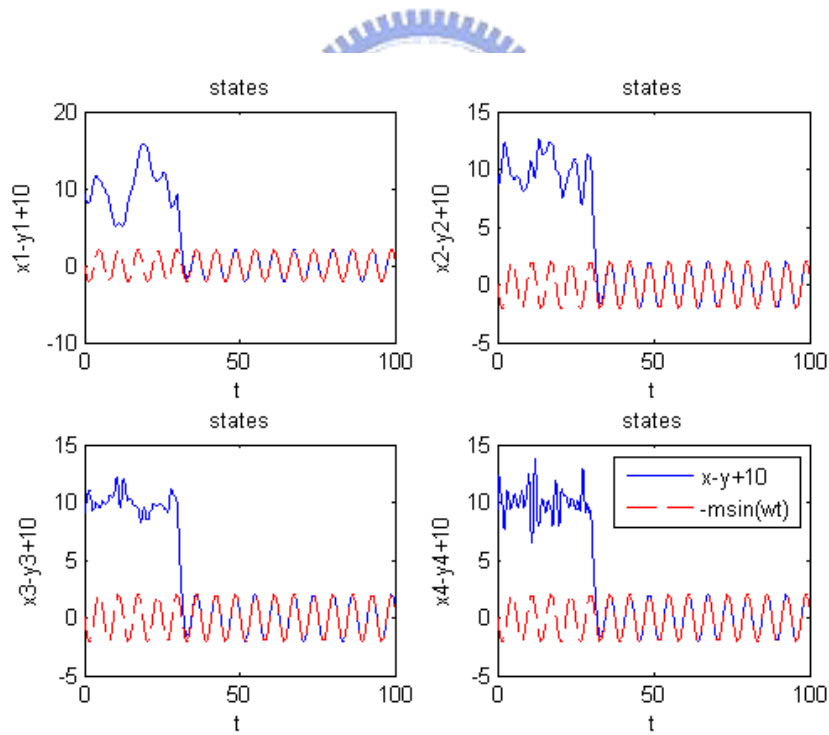
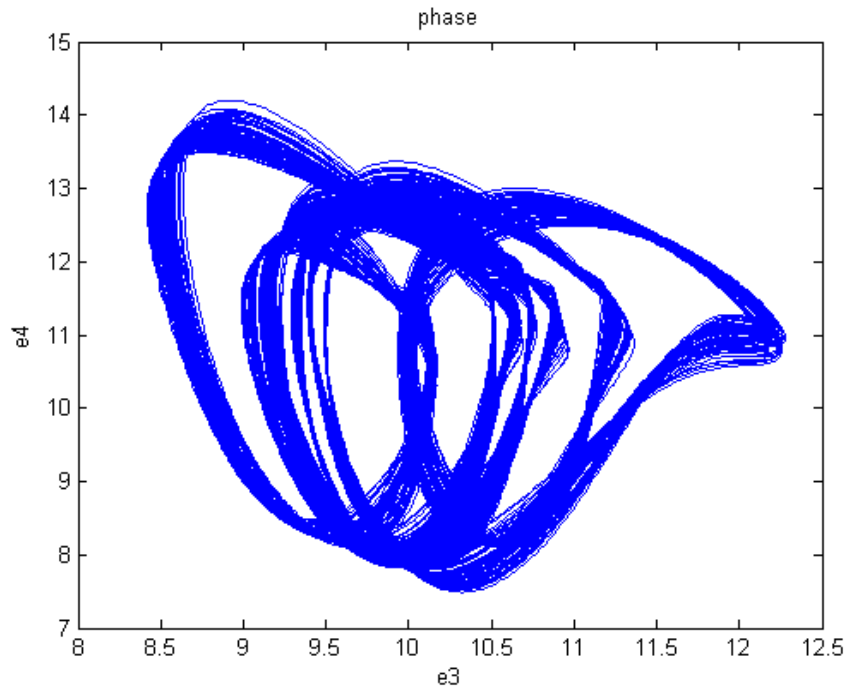
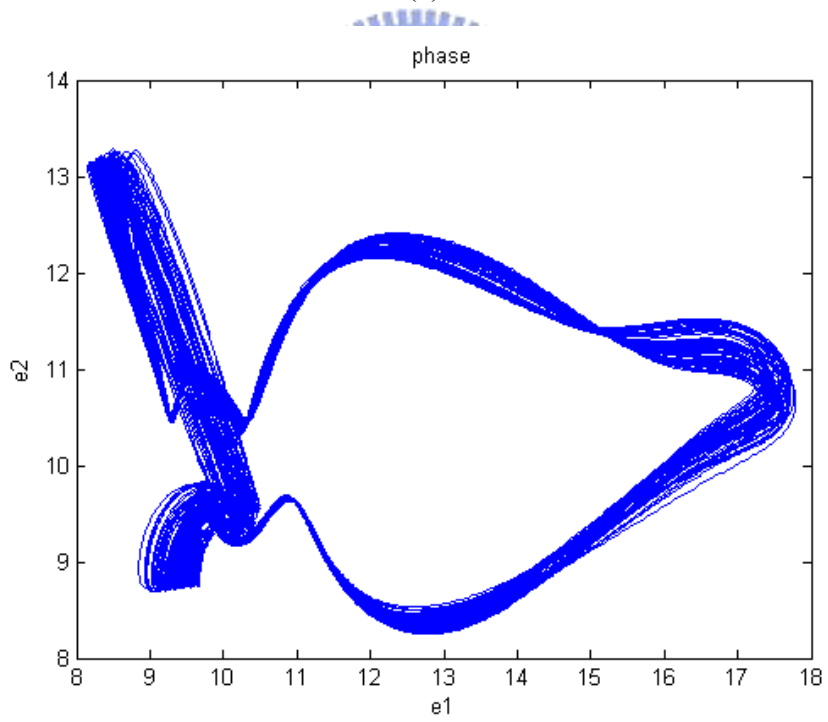


Fig. 2.7 Time histories of $x_i - y_i + 10$ and $-m \sin \omega t$ for Case II.



(a)



(b)

Fig. 2.8 Phase portraits of error dynamics for Case III.

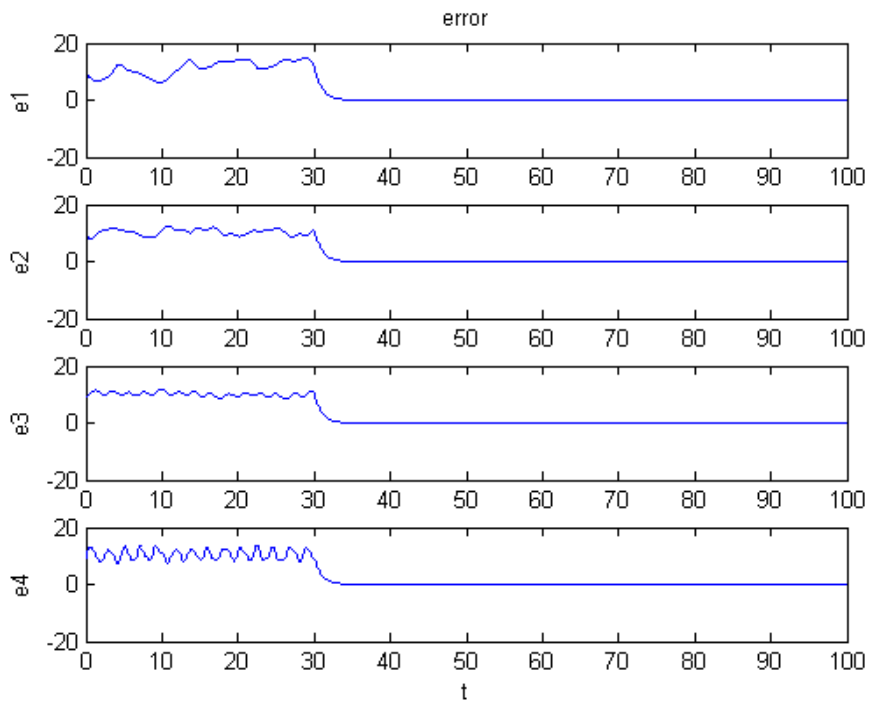


Fig. 2.9 Time histories of errors for Case III.

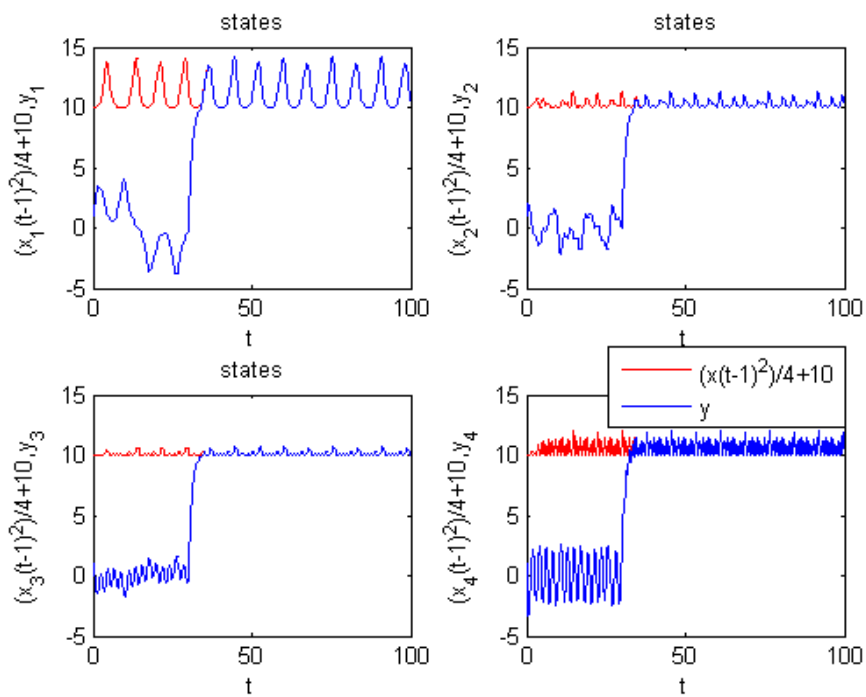


Fig. 2.10 Time histories of $\frac{x_i^2(t-1)}{4} + 10$ and y_i for Case III.

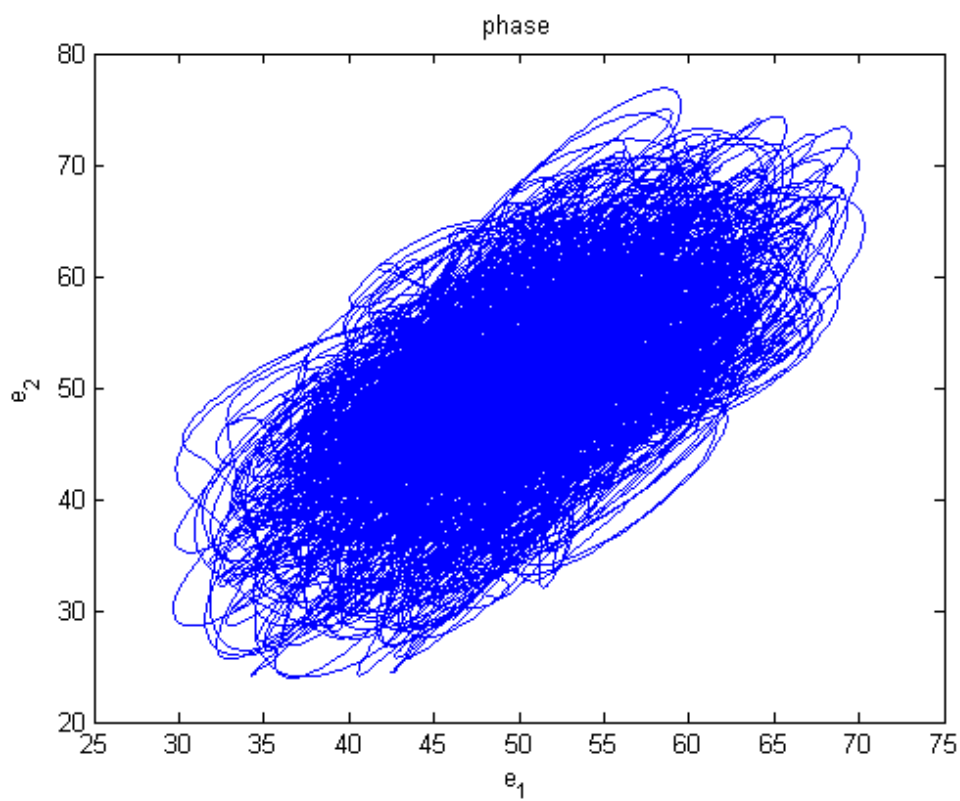
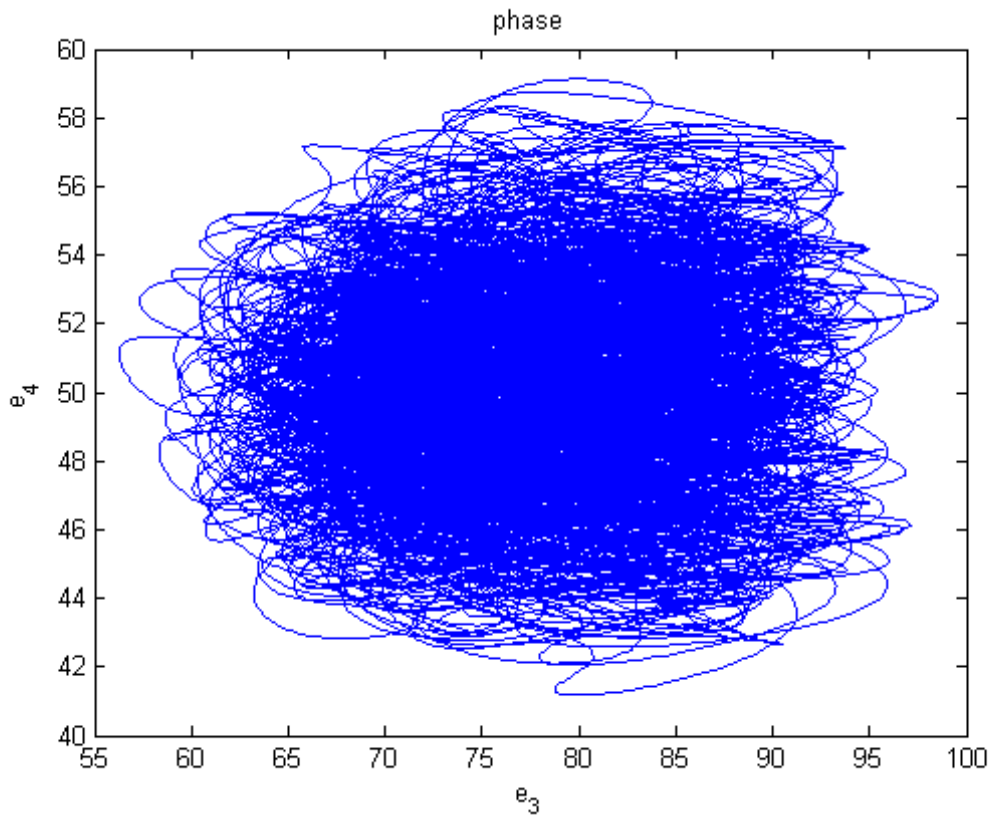


Fig. 2.11 Phase portraits of error dynamics for Case IV.

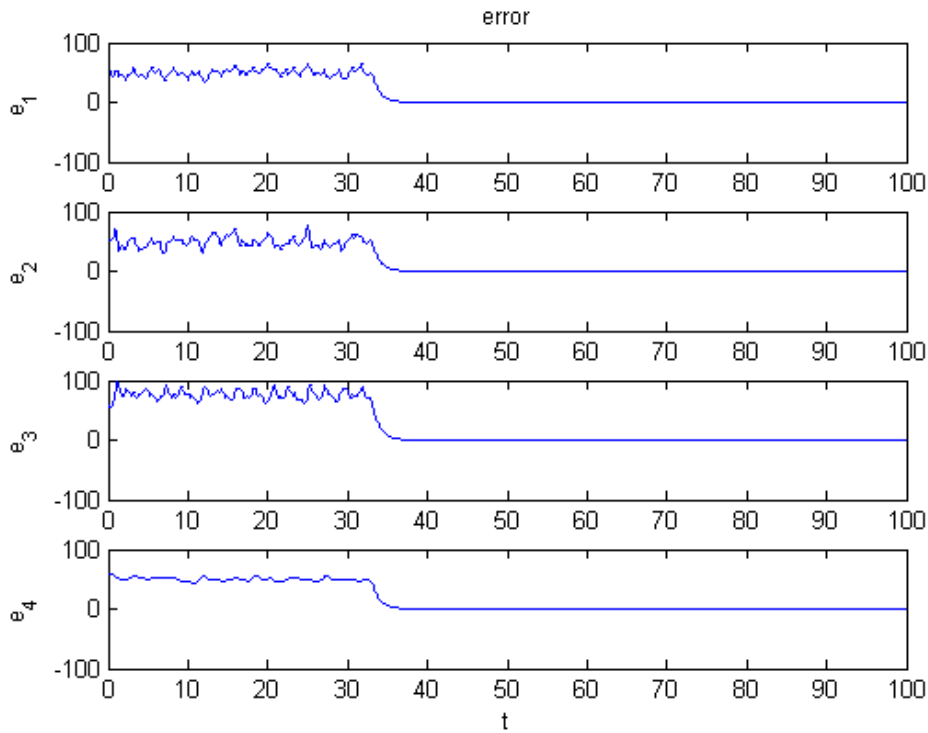


Fig. 2.12 Time histories of errors for Case IV.

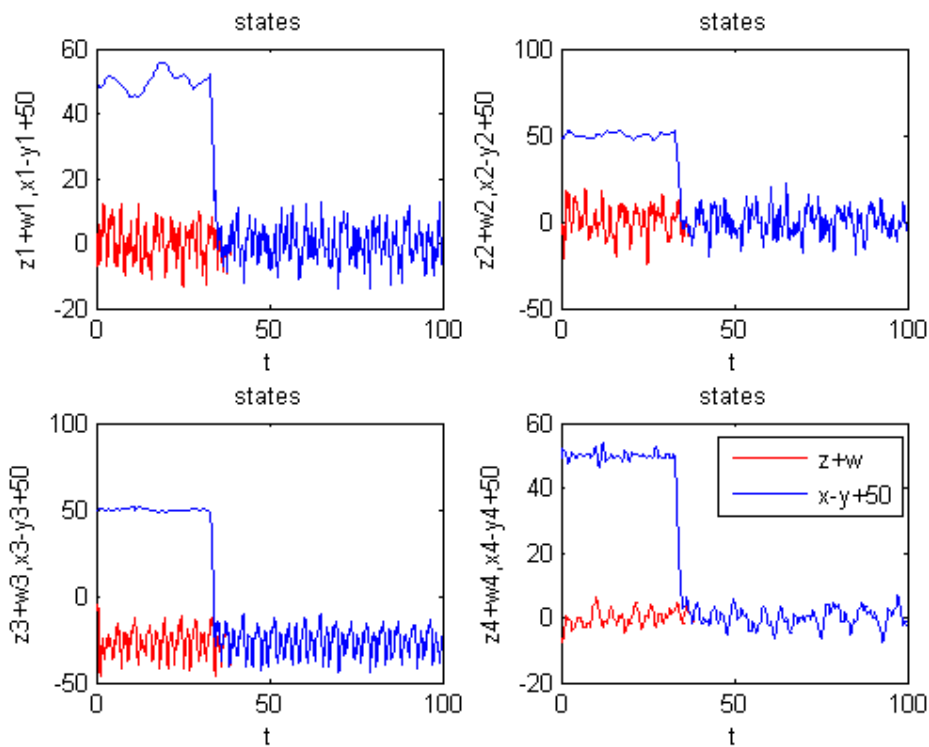


Fig. 2.13 Time histories of $x_i - y_i + 50$ and $z_i + w_i$ for Case IV.

Chapter 3

Chaos Control of a New Double-Froude Systems System as Functional System by GYC Partial Region Stability Theory

3.1 Preliminary

In this Chapter, *GYC partial region stability theory* is used to achieve chaos control for a new double-Froude system. The Lyapunov function of error states becomes a simple linear homogeneous function and the controllers are of lower degree than that by using traditional Lyapunov theory and introduce less simulation error. Numerical simulations are provided to show the effectiveness and advantage of this method.

3.2 Chaos control scheme

Consider the following chaotic systems

$$\dot{\mathbf{x}} = \mathbf{f}(t, \mathbf{x}) \quad (3-1)$$

where $\mathbf{x} = [x_1, x_2, \dots, x_n]^T \in R^n$ is a the state vector, $\mathbf{f} : R_+ \times R^n \rightarrow R^n$ is a vector function.

The goal system which can be either chaotic or regular, is

$$\dot{\mathbf{y}} = \mathbf{g}(t, \mathbf{y}) \quad (3-2)$$

where $\mathbf{y} = [y_1, y_2, \dots, y_n]^T \in R^n$ is a state vector, $\mathbf{g} : R_+ \times R^n \rightarrow R^n$ is a vector function.

In order to make the chaotic state \mathbf{x} approaching the goal state \mathbf{y} , define error $\mathbf{e} = \mathbf{x} - \mathbf{y}$ as the state error. The chaos control is accomplished in the sense that :

$$\lim_{t \rightarrow \infty} \mathbf{e} = \lim_{t \rightarrow \infty} (\mathbf{x} - \mathbf{y}) = 0 \quad (3-3)$$

In this Chapter, we will use examples in which the error dynamics happens in the first quadrant of coordinate system and use the partial region stability theory. The Lyapunov function is a simple linear homogeneous function of error states and the controllers are simpler because they are in lower degree than that of traditional controllers.

3.3 Numerical simulations

The following chaotic system

$$\begin{cases} \frac{dx_1}{dt} = x_2 - 10 \\ \frac{dx_2}{dt} = (a - b(x_2 - 10)^2)(x_2 - 10) - c \sin(x_1 - 10) - d(x_3 - 10) \\ \frac{dx_3}{dt} = x_4 - 10 \\ \frac{dx_4}{dt} = (e - f(x_4 - 10)^2)(x_4 - 10) - g \sin(x_3 - 10) - h(x_1 - 10) \end{cases} \quad (3-4)$$

is the new double-Froude system of which the old origin is translated to $(x_1, x_2, x_3, x_4) = (10, 10, 10, 10)$ in order that the error dynamics happens always in the first quadrant of error state coordinate system. This translated new double-Froude system presents chaotic motion when initial conditions is $(x_1, x_2, x_3, x_4) = (10.2, 10.35, 10.2, 10.35)$ and the parameters are $a = 0.35$, $b = 0.2$, $c = -1.16$, $d = 1.54$, $e = 0.7525$, $f = 0.2$, $g = 10.5$, $h = -1.7$.

In order to lead (x_1, x_2, x_3, x_4) to the goal, we add control terms u_1 , u_2 , u_3 and u_4 to each equation of Eq. (3-4), respectively.

$$\begin{cases} \dot{x}_1 = x_2 - 10 + u_1 \\ \dot{x}_2 = (a - b(x_2 - 10)^2)(x_2 - 10) - c \sin(x_1 - 10) - d(x_3 - 10) + u_2 \\ \dot{x}_3 = x_4 - 10 + u_3 \\ \dot{x}_4 = (e - f(x_4 - 10)^2)(x_4 - 10) - g \sin(x_3 - 10) - h(x_1 - 10) + u_4 \end{cases} \quad (3-5)$$

CASE I. Control the chaotic motion to zero.

In this case we will control the chaotic motion of the new double-Froude system to zero. The goal is $y=0$. The state error is $e_i = x_i - y_i = x_i$, ($i=1, 2, 3, 4$) and error dynamics becomes

$$\begin{cases} \dot{e}_1 = \dot{x}_1 = x_2 - 10 + u_1 \\ \dot{e}_2 = \dot{x}_2 = (a - b(x_2 - 10)^2)(x_2 - 10) - c \sin(x_1 - 10) - d(x_3 - 10) + u_2 \\ \dot{e}_3 = \dot{x}_3 = x_4 - 10 + u_3 \\ \dot{e}_4 = \dot{x}_4 = (e - f(x_4 - 10)^2)(x_4 - 10) - g \sin(x_3 - 10) - h(x_1 - 10) + u_4 \end{cases} \quad (3-6)$$

In Fig. 3.1, we see that the error dynamics always exists in first quadrant.

By GYC partial region asymptotical stability theorem, one can easily choose a Lyapunov function in the form of a positive definite function in first quadrant as:

$$V = e_1 + e_2 + e_3 + e_4 \quad (3-7)$$

Its time derivative through error dynamics (3-6) is

$$\begin{aligned} \dot{V} &= \dot{e}_1 + \dot{e}_2 + \dot{e}_3 + \dot{e}_4 \\ &= x_2 - 10 + u_1 \\ &\quad + (a - b(x_2 - 10)^2)(x_2 - 10) - c \sin(x_1 - 10) - d(x_3 - 10) + u_2 \\ &\quad + x_4 - 10 + u_3 \\ &\quad + (e - f(x_4 - 10)^2)(x_4 - 10) - g \sin(x_3 - 10) - h(x_1 - 10) + u_4 \end{aligned} \quad (3-8)$$

Choose

$$\begin{aligned} u_1 &= -(x_2 - 10) - e_1 \\ u_2 &= -((a - b(x_2 - 10)^2)(x_2 - 10) - c \sin(x_1 - 10) - d(x_3 - 10)) - e_2 \\ u_3 &= -(x_4 - 10) - e_3 \\ u_4 &= -((e - f(x_4 - 10)^2)(x_4 - 10) - g \sin(x_3 - 10) - h(x_1 - 10)) - e_4 \end{aligned} \quad (3-9)$$

We obtain

$$\dot{V} = \dot{e}_1 + \dot{e}_2 + \dot{e}_3 + \dot{e}_4 < 0$$

which is negative definite function in first quadrant. The numerical results are shown in Fig.3.2. After 30 sec, the error trajectories approach the origin.

CASE II. Control the chaotic motion to a regular function.

In this case we will control the chaotic motion of the new double-Froude system (3-4) to regular function of time. The goal is $y_i = m \sin \omega_i t$, ($i=1, 2, 3, 4$). The error equation

$$e_i = x_i - y_i = x_i - m \sin \omega_i t, \quad (i=1, 2, 3, 4) \quad (3-10)$$

$$\lim_{t \rightarrow \infty} e_i = \lim_{t \rightarrow \infty} (x_i - m \sin \omega_i t) = 0, \quad (i=1, 2, 3, 4)$$

where $m = 10$ and $\omega_1 = 0.5, \omega_2 = 0.3, \omega_3 = 0.4, \omega_4 = 0.6$

The error dynamics is

$$\begin{cases} \dot{e}_1 = x_2 - 10 + u_1 - m\omega_1 \cos \omega_1 t \\ \dot{e}_2 = (a - b(x_2 - 10)^2)(x_2 - 10) - c \sin(x_1 - 10) - d(x_3 - 10) + u_2 - m\omega_2 \cos \omega_2 t \\ \dot{e}_3 = x_4 - 10 + u_3 - m\omega_3 \cos \omega_3 t \\ \dot{e}_4 = (e - f(x_4 - 10)^2)(x_4 - 10) - g \sin(x_3 - 10) - h(x_1 - 10) + u_4 - m\omega_4 \cos \omega_4 t \end{cases} \quad (3-11)$$

In Fig. 3.3, the error dynamics always exists in first quadrant.

By GYC partial region asymptotical stability theorem, one can easily choose a Lyapunov function in the form of a positive definite function in first quadrant as:

$$V = e_1 + e_2 + e_3 + e_4$$

Its time derivative is

$$\begin{aligned} V = \dot{e}_1 + \dot{e}_2 + \dot{e}_3 + \dot{e}_4 = & (x_2 - 10 + u_1 - m\omega_1 \cos \omega_1 t) \\ & + ((a - b(x_2 - 10)^2)(x_2 - 10) - c \sin(x_1 - 10) \\ & - d(x_3 - 10) + u_2 - m\omega_2 \cos \omega_2 t) \\ & + (x_4 - 10 + u_3 - m\omega_3 \cos \omega_3 t) \\ & + ((e - f(x_4 - 10)^2)(x_4 - 10) - g \sin(x_3 - 10) \\ & - h(x_1 - 10) + u_4 - m\omega_4 \cos \omega_4 t) \end{aligned} \quad (3-12)$$

Choose

$$\begin{aligned} u_1 = & -(x_2 - 10 - m\omega_1 \cos \omega_1 t) - e_1 \\ u_2 = & -((a - b(x_2 - 10)^2)(x_2 - 10) - c \sin(x_1 - 10) - d(x_3 - 10) \\ & - m\omega_2 \cos \omega_2 t) - e_2 \\ u_3 = & -(x_4 - 10 - m\omega_3 \cos \omega_3 t) - e_3 \\ u_4 = & -((e - f(x_4 - 10)^2)(x_4 - 10) - g \sin(x_3 - 10) - h(x_1 - 10) \\ & - m\omega_4 \cos \omega_4 t) - e_4 \end{aligned} \quad (3-13)$$

We obtain

$$\dot{V} = -e_1 - e_2 - e_3 - e_4 < 0$$

which is a negative definite function in first quadrant. The numerical results are shown in Fig. 3.4 and Fig. 3.5. After 30 sec., the errors approach zero and the chaotic trajectories approach to regular motions.

CASE III. Control the chaotic motion of the new double-Froude system to the sum of the chaotic motions of a generalized Lorenz system and of a generalized Chen system.

In this case we will control chaotic motion of the new double-Froude system (3-4) to the sum of the chaotic motions of the generalized Lorenz system and of the generalized Chen system. The goal system for control is the sum of the generalized Lorenz system and the generalized Chen system with initial states $(z_1, z_2, z_3, z_4) = (0.2, 0.35, 0.2, 0.35)$, $(w_1, w_2, w_3, w_4) = (5, 6, 5, 6)$ and system parameters $s = 1$, $p = 26$, $q = 0.7$, $r = 1.5$, $a_1 = 36$, $b_1 = 3$, $c_1 = 22$, $d_1 = 16$.

$$\begin{cases} \dot{z}_1 = s(z_2 - z_1) + rz_4 \\ \dot{z}_2 = pz_1 - z_1z_3 - z_2 \\ \dot{z}_3 = z_1z_2 - qz_3 \\ \dot{z}_4 = -z_1 - sz_4 \end{cases} \quad (3-14)$$

$$\begin{cases} \dot{w}_1 = a_1(w_2 - w_1) \\ \dot{w}_2 = -d_1w_1 - w_1w_3 + c_1w_2 - w_4 \\ \dot{w}_3 = w_1w_2 - b_1w_3 \\ \dot{w}_4 = w_1 \end{cases}$$

The error equation is $e_i = x_i - z_i - w_i$, $(i=1, 2, 3, 4)$. Our aim is $\lim_{t \rightarrow 0} e_i = 0$, $(i=1, 2, 3, 4)$.

The error dynamics becomes

$$\begin{cases} \dot{e}_1 = \dot{x}_1 - \dot{z}_1 - \dot{w}_1 = (x_2 - 10 - s(z_2 - z_1) - rz_4 - a_1(w_2 - w_1)) + u_1 \\ \dot{e}_2 = \dot{x}_2 - \dot{z}_2 - \dot{w}_2 = ((a - b(x_2 - 10)^2)(x_2 - 10) - c \sin(x_1 - 10) - d(x_3 - 10) \\ \quad - (pz_1 - z_1z_3 - z_2) - (-d_1w_1 - w_1w_3 + c_1w_2 - w_4)) + u_2 \\ \dot{e}_3 = \dot{x}_3 - \dot{z}_3 - \dot{w}_3 = (x_4 - 10 - z_1z_2 + qz_3 - w_1w_2 + b_1w_3) + u_3 \\ \dot{e}_4 = \dot{x}_4 - \dot{z}_4 - \dot{w}_4 = ((e - f(x_4 - 10)^2)(x_4 - 10) - g \sin(x_3 - 10) - h(x_1 - 10) \\ \quad + z_1 + sz_4 - w_1) + u_4 \end{cases} \quad (3-15)$$

In Fig. 3.6, the error dynamics always exists in first quadrant.

By GYC partial region asymptotical stability theorem, one can easily choose a Lyapunov function in the form of a positive definite function in first quadrant as:

$$V = e_1 + e_2 + e_3 + e_4$$

Its time derivative is

$$\begin{aligned} \dot{V} = \dot{e}_1 + \dot{e}_2 + \dot{e}_3 + \dot{e}_4 = & ((x_2 - 10 - s(z_2 - z_1) - rz_4 - a_1(w_2 - w_1)) + u_1) \\ & + (((a - b(x_2 - 10)^2)(x_2 - 10) - c \sin(x_1 - 10) - d(x_3 - 10) \\ & - (pz_1 - z_1z_3 - z_2) - (-d_1w_1 - w_1w_3 + c_1w_2 - w_4)) + u_2) \\ & + ((x_4 - 10 - z_1z_2 + qz_3 - w_1w_2 + b_1w_3) + u_3) \\ & + (((e - f(x_4 - 10)^2)(x_4 - 10) - g \sin(x_3 - 10) - h(x_1 - 10) \\ & + z_1 + sz_4 - w_1) + u_4) \end{aligned} \quad (3-16)$$

Choose

$$\begin{aligned} u_1 = & -(x_2 - 10 - s(z_2 - z_1) - rz_4 - a_1(w_2 - w_1)) - e_1 \\ u_2 = & -((a - b(x_2 - 10)^2)(x_2 - 10) - c \sin(x_1 - 10) - d(x_3 - 10) \\ & - (pz_1 - z_1z_3 - z_2) - (-d_1w_1 - w_1w_3 + c_1w_2 - w_4)) - e_2 \\ u_3 = & -(x_4 - 10 - z_1z_2 + qz_3 - w_1w_2 + b_1w_3) - e_3 \\ u_4 = & -((e - f(x_4 - 10)^2)(x_4 - 10) - g \sin(x_3 - 10) - h(x_1 - 10) \\ & + z_1 + sz_4 - w_1) - e_4 \end{aligned} \quad (3-17)$$

We obtain

$$\dot{V} = -e_1 - e_2 - e_3 - e_4 < 0$$

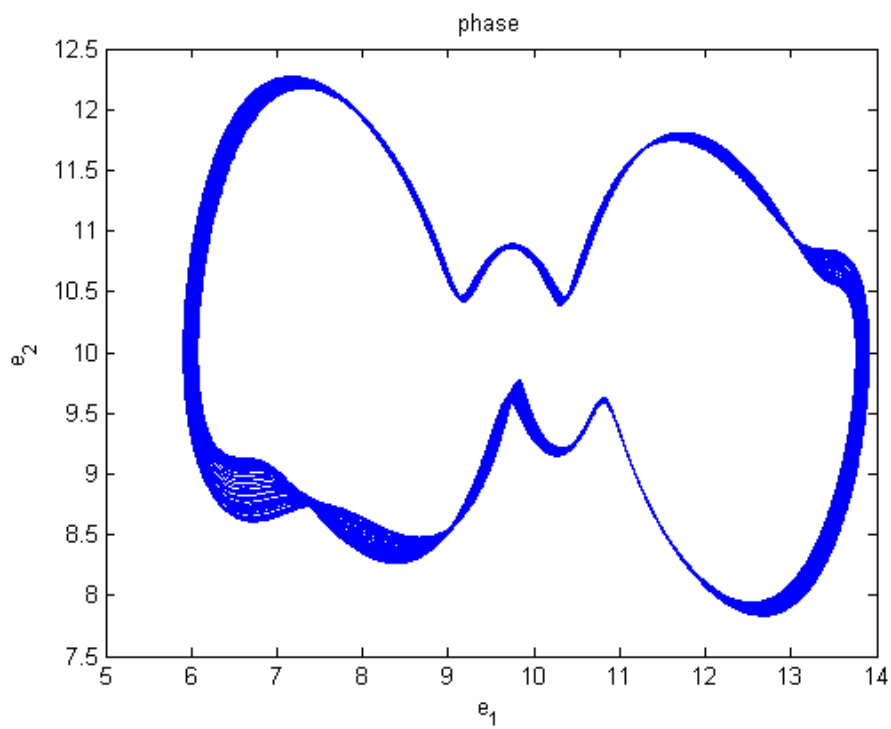
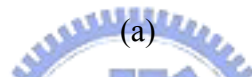
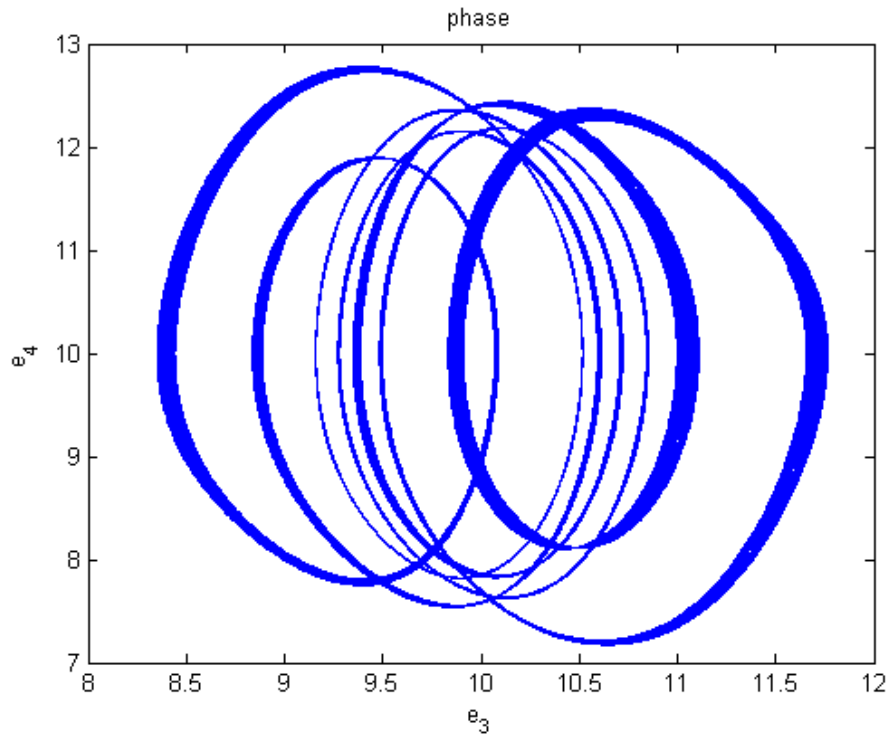
which is negative definite function in first quadrant. The numerical results are shown in Fig.3.7 and Fig. 3.8. After 30 sec., the errors approach zero and the chaotic trajectories of the new double-Froude system approach to the sum of the chaotic

motions of the generalized Lorenz system and of the generalized Chen system.

3.4 Summary

In this Chapter, a new strategy by using GYC partial region stability theory is proposed to achieve chaos control. Via GYC partial region stability theory, the new Lyapunov function used is a simple linear homogeneous function of error states and the lower degree controllers are much more simple and introduce less simulation error. A new chaotic double-Froude system and a generalized Lorenz system and a generalized Chen system are used as simulation examples which confirm the scheme effectively.





(b)

Fig. 3.1 Phase portraits of error dynamics for Case I.

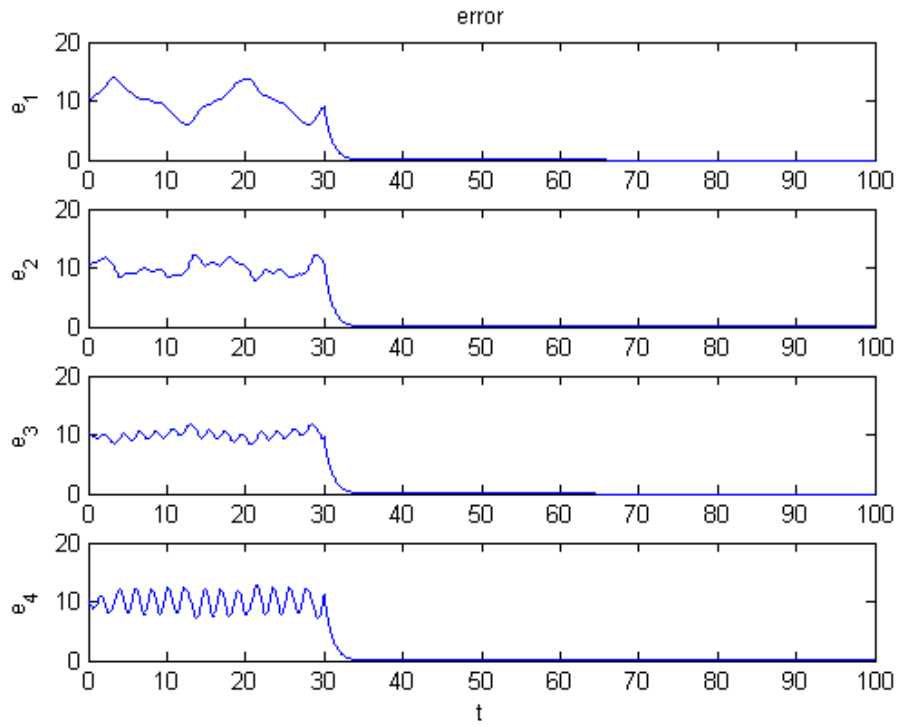
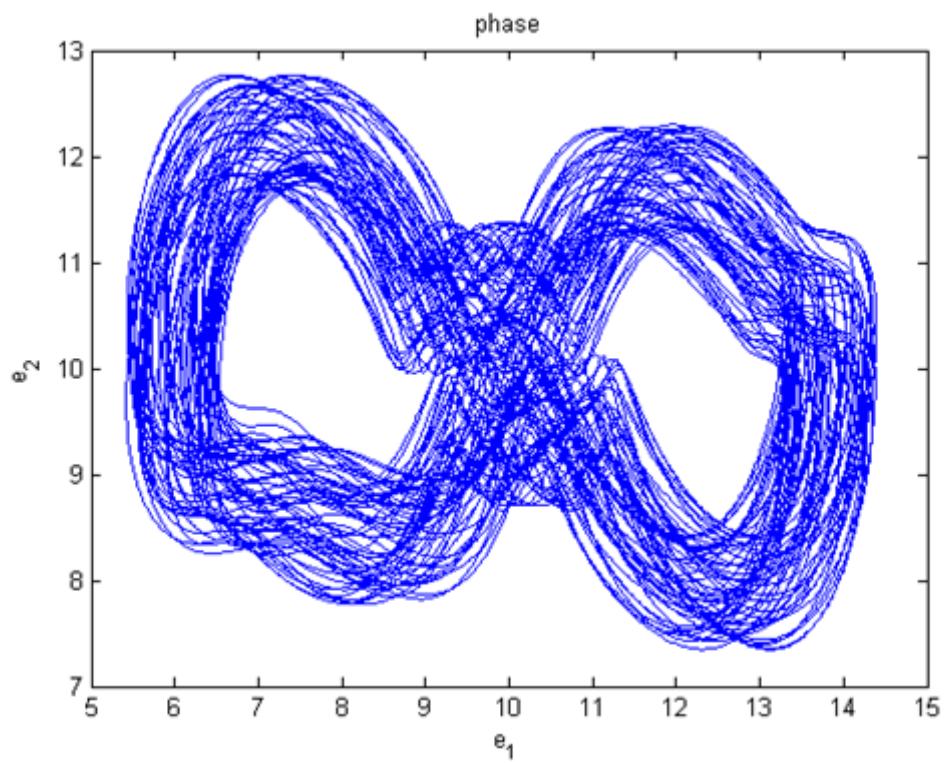
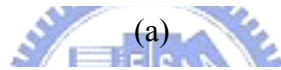
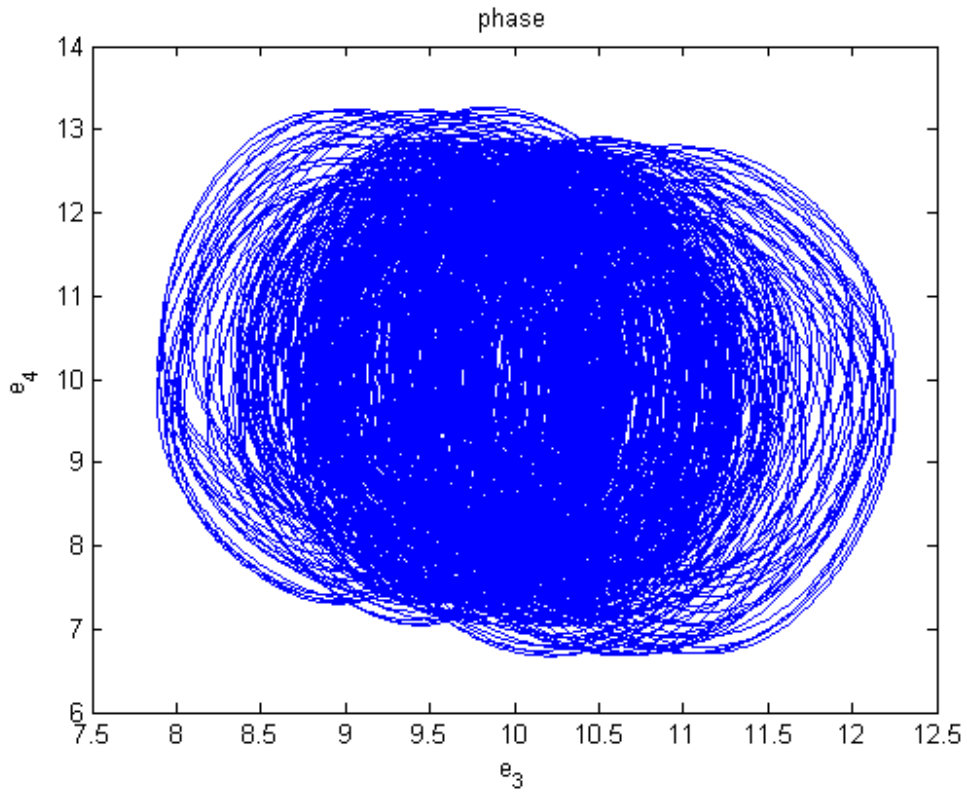


Fig. 3.2 Time histories of errors for Case I.





(b)

Fig. 3.3 Phase portraits of error dynamics for Case II.

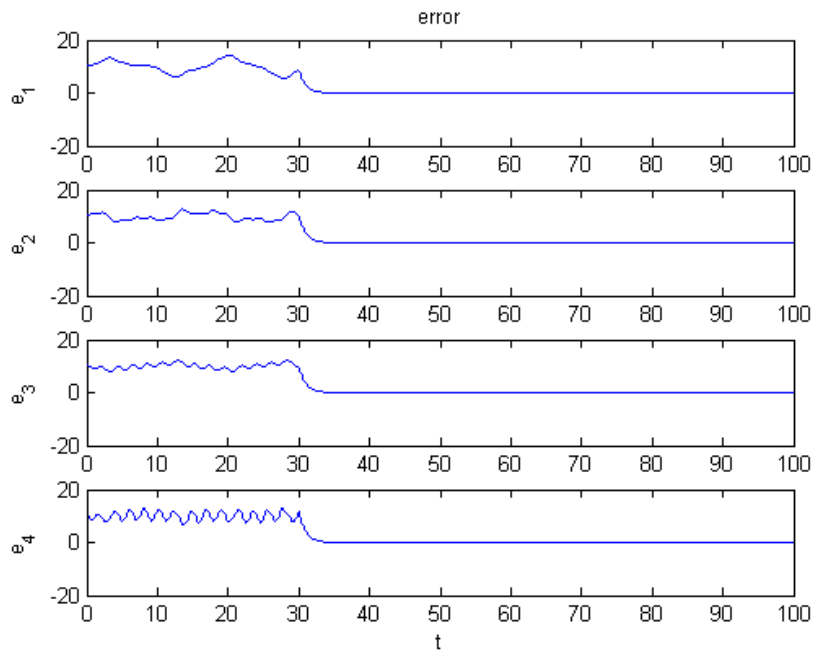


Fig. 3.4 Time histories of errors for Case II.

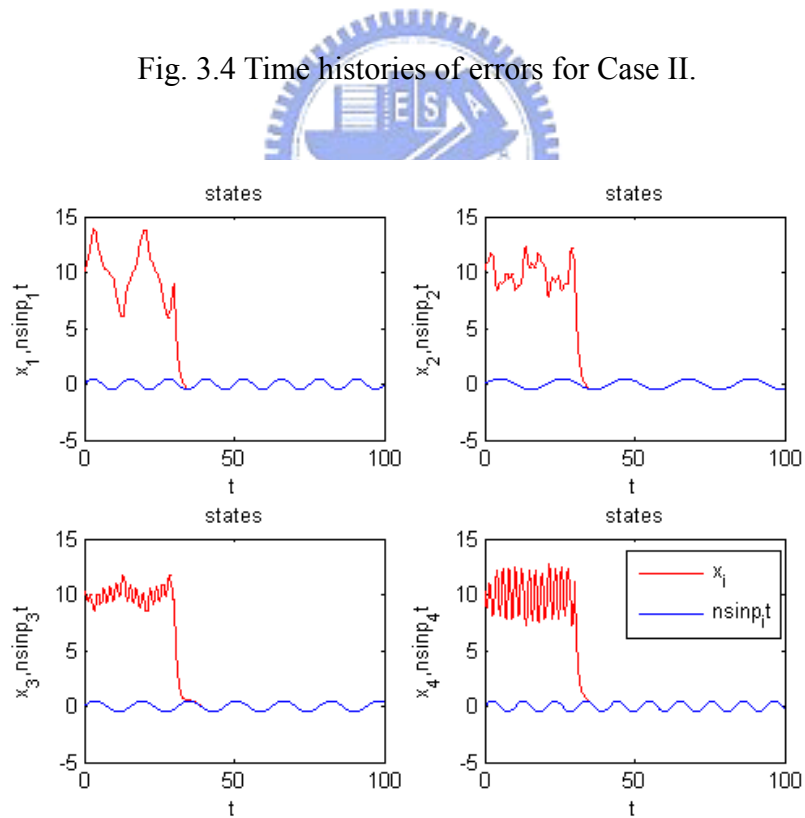


Fig. 3.5 Time histories of x_1, x_2, x_3, x_4 for Case II.

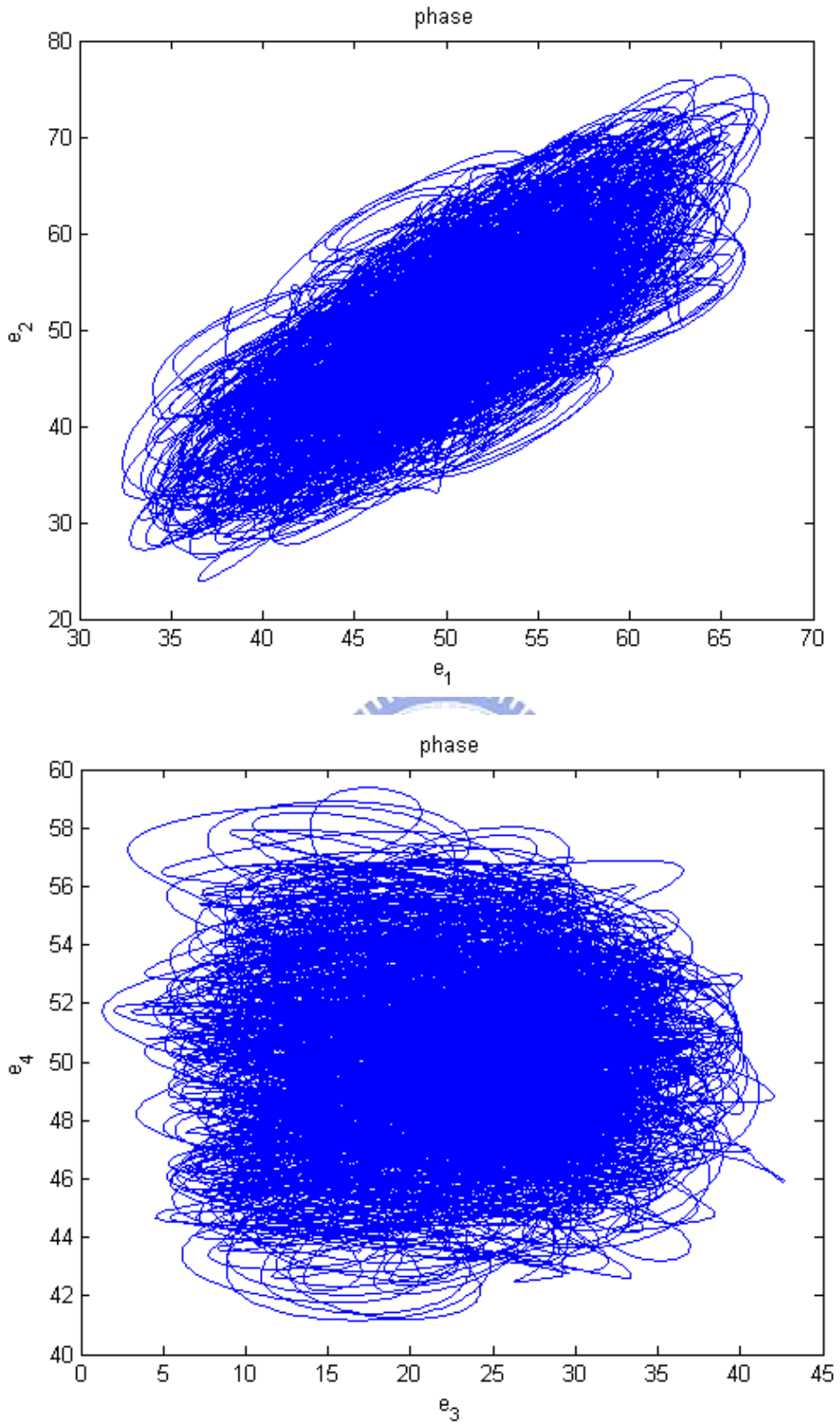


Fig. 3.6 Phase portraits of error dynamics for Case III.

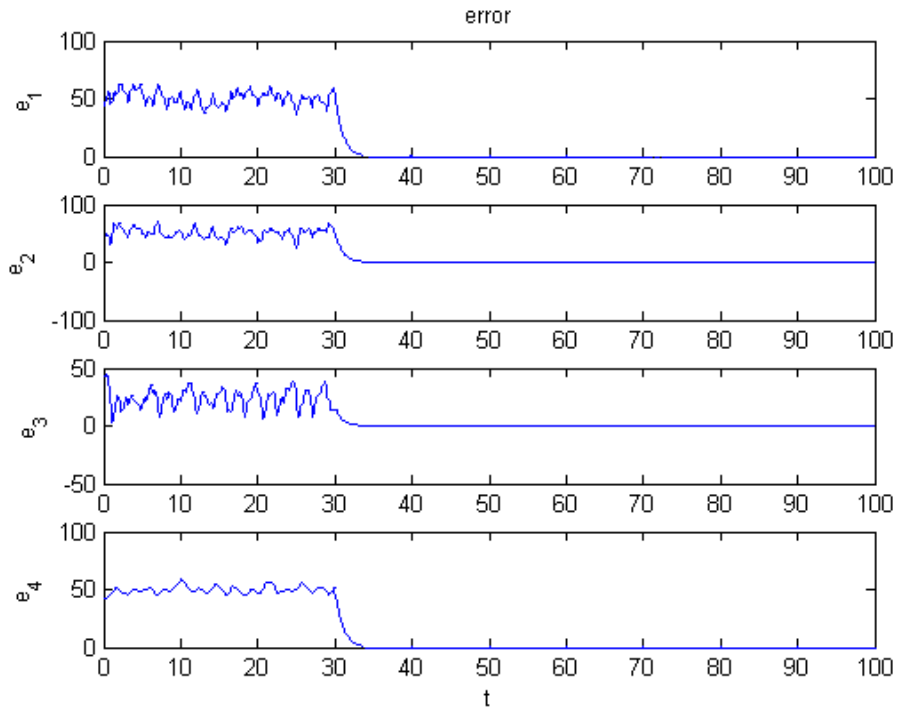


Fig. 3.7 Time histories of errors for Case III.

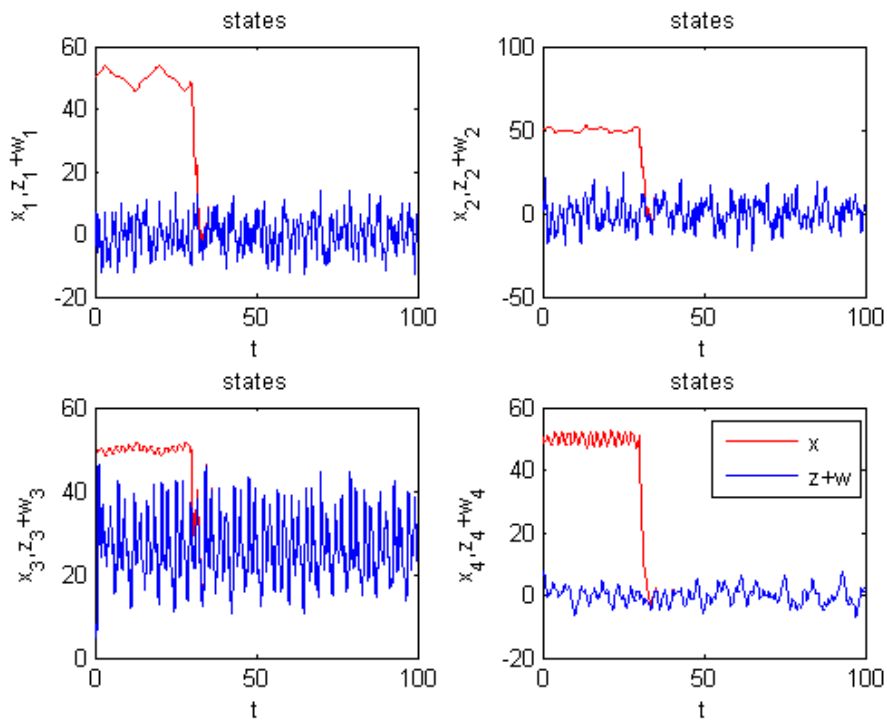


Fig. 3.8 Time histories of x_1, x_2, x_3, x_4 and z_1, z_2, z_3, z_4 for Case III.

Chapter 4

Hyperchaos of The Rössler System with Legendre Function Parameters

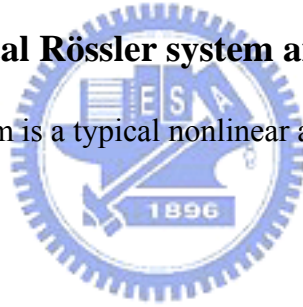
4.1 Preliminary

Hyperchaos and chaos of Rössler system with Legendre function parameters are studied. They are identified by phase portraits, bifurcation diagram, Lyapunov exponents, time histories of states, Poincaré maps and parameter diagram. Both hyperchaos and chaos exist abundantly. They give various applications, especially for secret communication.

4.2 Chaos of The classical Rössler system and Legendre function

A classical Rössler system is a typical nonlinear autonomous system:

$$\begin{cases} \frac{dx_1}{dt} = -(x_2 + x_3) \\ \frac{dx_2}{dt} = x_1 + ax_2 \\ \frac{dx_3}{dt} = b + x_1x_3 - cx_3 \end{cases} \quad (4-1)$$



where a, b, c are constant parameters. When the parameters of system are $a = 0.15, b = 0.2, c = 10$ and the initial states of system are $x_1(0) = 2, x_2(0) = 2.4, x_3(0) = 5$, its chaotic phase portraits and time histories are shown in Fig. 4.1.

We shall use Legendre functions [26] as parameters of the system in next section. The Legendre functions are defined by

$$P_n^m(x) = (-1)^m (1-x^2)^{m/2} \frac{d^m}{dx^m} P_n(x) \quad (4-2)$$

where $P_n(x)$ is the Legendre polynomial of degree n .

$$P_n(x) = \frac{1}{2^n n!} \left[\frac{d^n}{dx^n} (x^2 - 1)^n \right] \quad (4-3)$$

Choosing $n=2$, we obtain

$$\begin{cases} L_1(x) = P_2^0(x) = P_2(x) \\ L_3(x) = P_2^2(x) = (-1)^2 (1-x^2) \frac{d^2}{dx^2} P_2(x) \\ P_2(x) = \frac{1}{2^2 \cdot 2!} \left[\frac{d^2}{dx^2} (x^2 - 1)^2 \right] \end{cases} \quad (4-4)$$

Changing the variable

$$x = \cos t, \quad -1 \leq x \leq 1 \quad (4-5)$$

The Legendre functions become given periodic functions of time t :

$$\begin{cases} L_1(t) = P_2^0(\cos t) = P_2(\cos t) \\ L_3(t) = P_2^2(\cos t) = (-1)^2 (1-x^2) \frac{d^2}{dx^2} P_2(\cos t) \\ P_2(t) = \frac{1}{2^2 \cdot 2!} \left[\frac{d^2}{dx^2} (x^2 - 1)^2 \right] \end{cases} \quad (4-6)$$

as shown in Fig. 4.2.

4.3 Numerical results

CASE I :

$$\begin{cases} \frac{dx_1}{dt} = -(x_2 + x_3) \\ \frac{dx_2}{dt} = x_1 + Ax_2 \\ \frac{dx_3}{dt} = B + x_1x_3 - Cx_3 \end{cases} \quad (4-7)$$

Now, the parameters of Rössler system are taken as $A=0.1L_3 + k$, $B=b$, $C=c + 0.1L_1$, and the initial states of system are $x_1(0) = 2, x_2(0) = 2.4, x_3(0) = 5$, the bifurcation diagram by changing parameter k is shown in Fig. 4.3 with $b=0.2, c=12$. Its

corresponding Lyapunov exponents are shown in Fig. 4.4. The phase portraits, time histories, and Poincaré maps of the systems are showed in Fig. 4.5 and Fig. 4.6. When $k=-0.2$, period 1 phenomena are shown in Fig. 4.5. When $k=0.1$, the chaotic behaviors are given in Fig.4.6.

When $b=0.2$ and $c=12$ are fixed while parameter k varies, system (4-7) is chaotic in the range $-0.12 \leq k \leq -0.09$, $-0.085 \leq k \leq 0.1$ for increment of 0.01. Some typical values of parameter k that generate hyperchaos, and the range of k for different system behaviors, are listed in Table 4.1. System (4-7) is chaotic in the above ranges.

Table 4.1 The ranges of k for different system dynamics.

| System dynamics | Ranges of k |
|-------------------------------------|---|
| • Periodic | $-0.2 \leq k \leq -0.15$, $-0.15 \leq k \leq -0.12$, $-0.09 \leq k \leq -0.085$ |
| • Chaotic | $-0.12 \leq k \leq -0.09$, $-0.085 \leq k \leq 0.03$ |
| • Hyperchaotic | $0.03 \leq k \leq 0.08$ |
| • Chaotic-hyperchaotic interweaving | $0.08 \leq k \leq 0.1$ |

CASE II :

When the parameters of system are $A=0.1L_3 + a$, $B=b$, $C=k + 0.1L_1$, and the initial states of system are $x_1(0) = 2, x_2(0) = 2.4, x_3(0) = 5$, $a=0.15$ and $b=0.2$ are fixed while parameter k varies, system (4-7) is chaotic in the range $2 \leq k \leq 15$, for increment of 0.028. Some typical values of parameter k that generate hyperchaos, and the range of k for different system behaviors, are listed in Table 4.2. The Lyapunov exponents are shown in Fig. 4.7.

Table 4.2 The ranges of k for different system dynamics.

| System dynamics | Ranges of k |
|-----------------|---|
| • Periodic | $0.8 \leq k \leq 1, 1.05 \leq k \leq 1.15, 1.2 \leq k \leq 2, 3 \leq k \leq 3.1$ |
| • Chaotic | $1 \leq k \leq 1.05, 1.15 \leq k \leq 1.2, 2 \leq k \leq 3, 3.1 \leq k \leq 10.5$ |
| • Hyperchaotic | $10.5 \leq k \leq 14.3$ |

CASE III :

When the parameters of system are $A=0.1L_3 + j$, $B=b$, $C=c + kL_1$, and the initial states of system are $x_1(0) = 2, x_2(0) = 2.4, x_3(0) = 5$.

When $b=0.2$ and $c=12$ are fixed while parameter j, k varies. Some typical values of parameter j, k that generate hyperchaos, and the ranges of j, k for different system behaviors, are listed in Table 4.3. System (4-7) is chaotic in the above range. The parameter diagram is shown in Fig. 4.8.

Table 4.3 The ranges of j, k for different system dynamics.

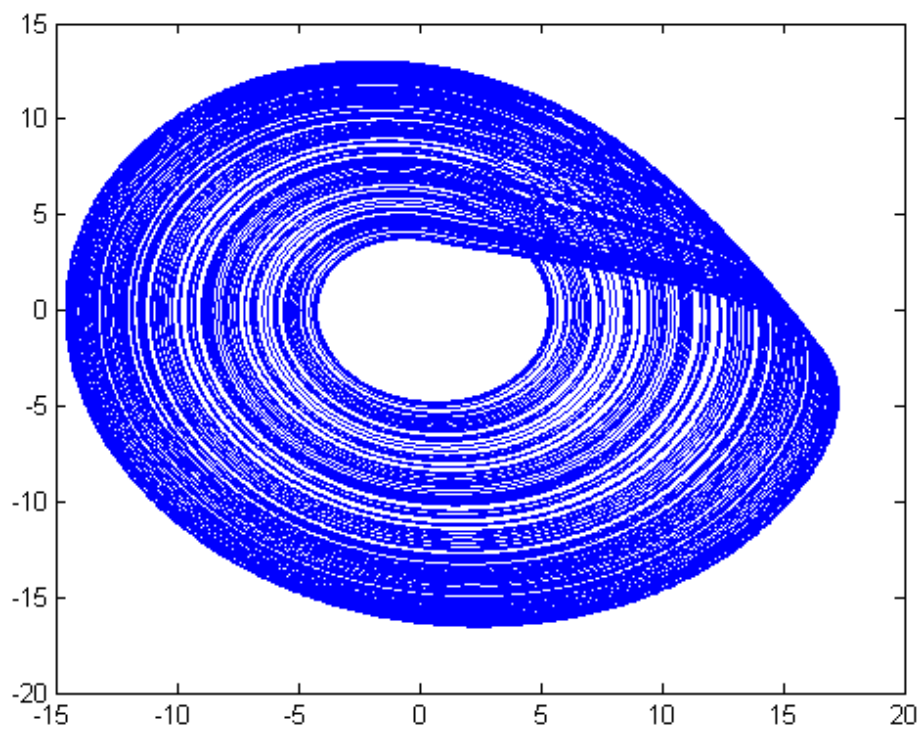
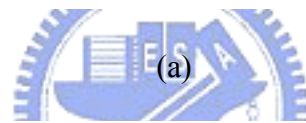
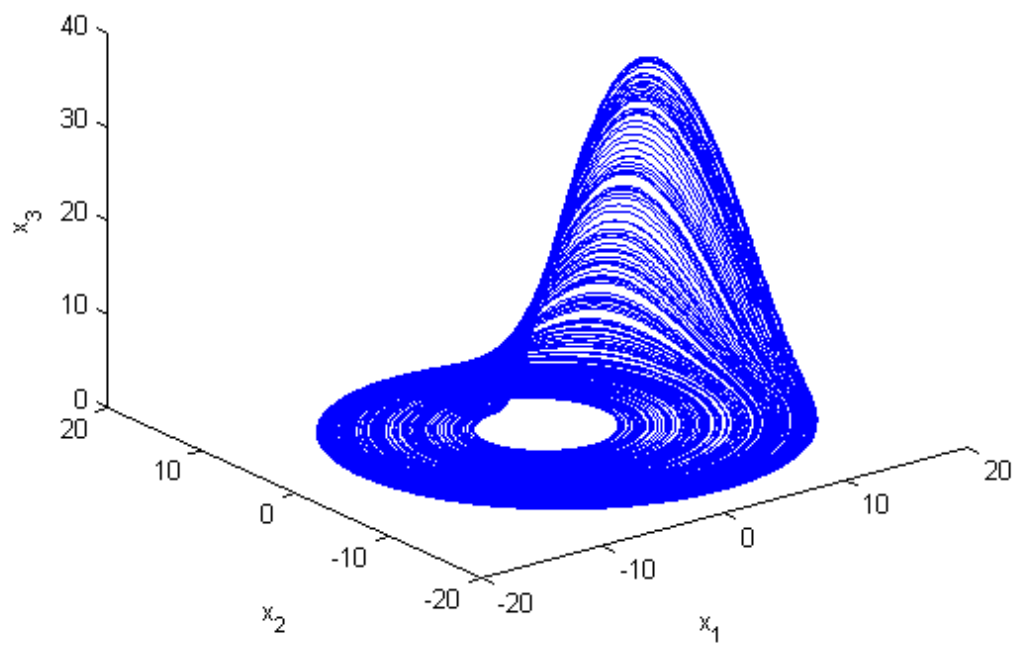
| System dynamics | Ranges of j | Ranges of k |
|-----------------|--|----------------------------|
| • Periodic | $-0.2 \leq j \leq -0.135$ | $-10 \leq k \leq 10$ |
| • Periodic | $-0.135 \leq j \leq -0.07$ | $-0.135 \leq k \leq -0.07$ |
| • Chaotic | $-0.135 \leq j \leq 0.1$ | $-5 \leq k \leq 10$ |
| • Chaotic | $-0.07 \leq j \leq 0.1$ | $-10 \leq k \leq -5$ |
| • Hyperchaotic | $-0.02 \leq j \leq 0.03, 0.08 \leq j \leq 0.1$ | $8 \leq k \leq 10$ |
| • Hyperchaotic | $0 \leq j \leq 0.1$ | $0 \leq k \leq 5$ |
| • Hyperchaotic | $-0.03 \leq j \leq 0.03$ | $-10 \leq k \leq -6.5$ |

4.4 Summary

Hyperchaos and chaos of a Rössler system with Legendre function parameters are studied firstly. The results are verified by time histories of states, phase portraits,

Poincaré maps, bifurcation analysis, Lyapunov exponents and parametric diagram. Abundant hyperchaos is found for this system, which gives potential in various applications, particularly in secret communication.





(b)

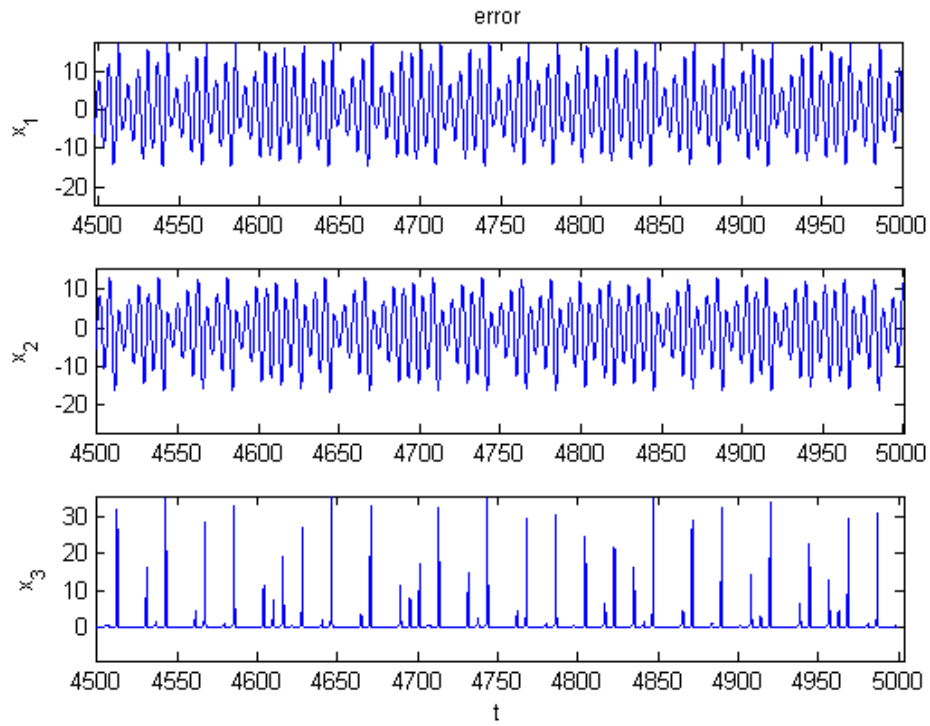


Fig. 4.1 (a) 3D Phase portrait (b) 2D Phase portrait (c) Time histories of states for classical Rössler systems.

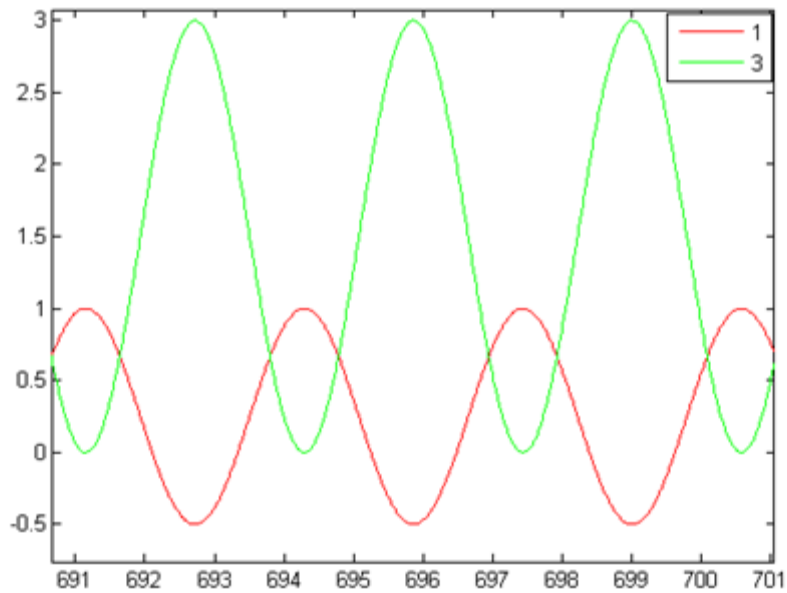


Fig. 4.2 Time histories of L_1 and L_3 .

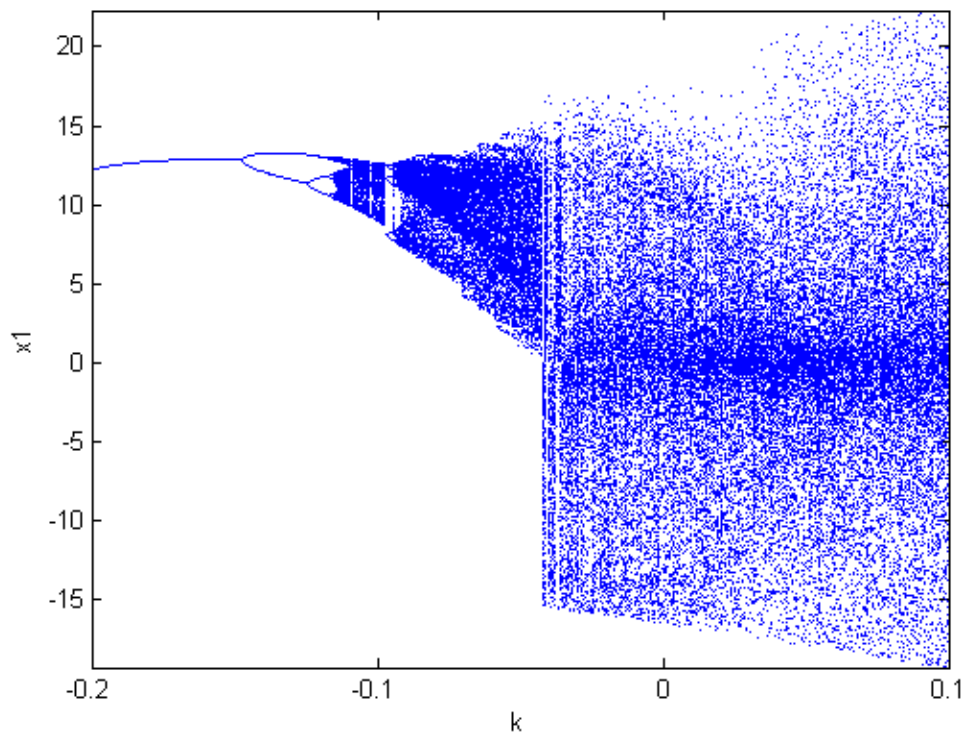
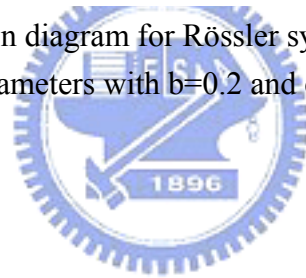
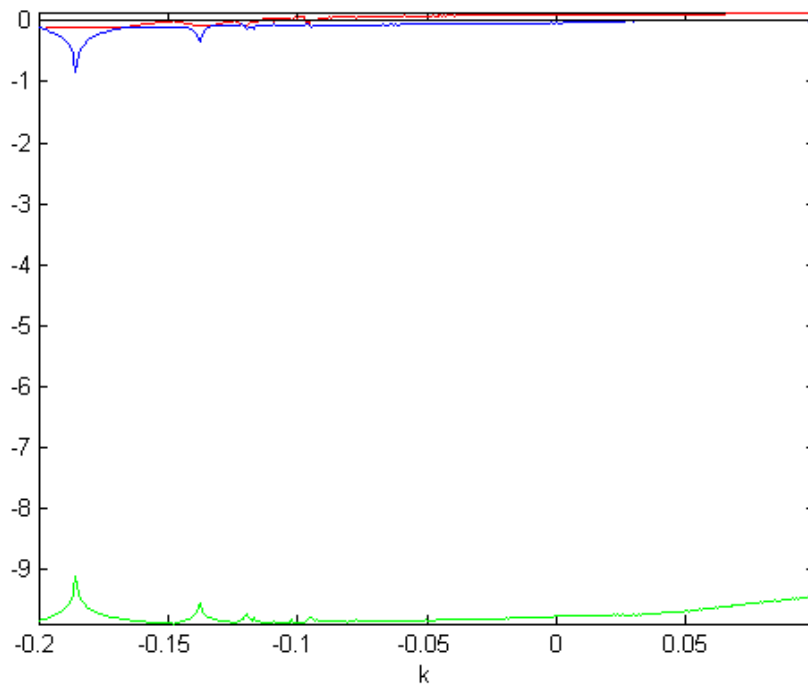
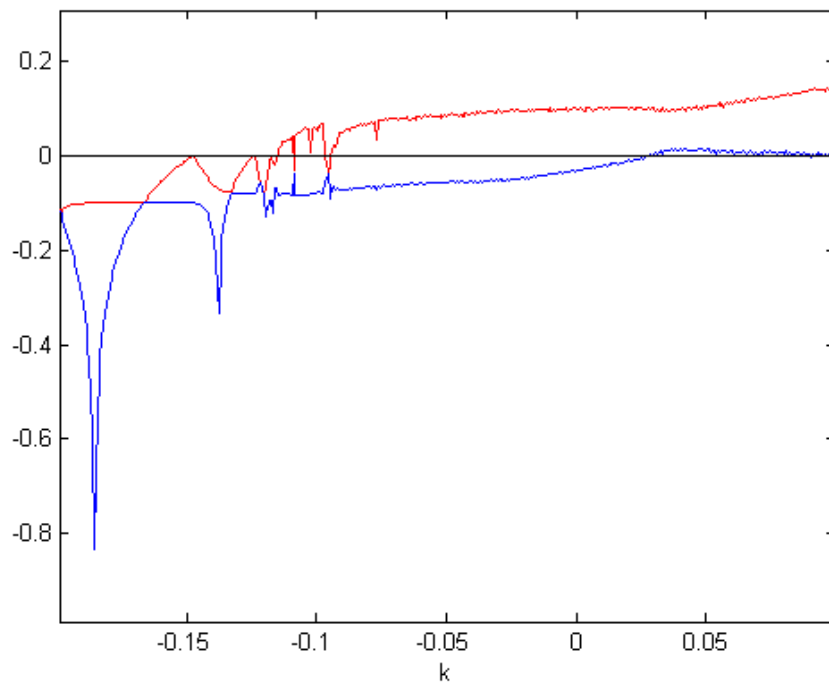


Fig. 4.3 The bifurcation diagram for Rössler system with Legendre function parameters with $b=0.2$ and $c=12$.





(a)



(b)

Fig. 4.4 (a) The Lyapunov exponents for system (4-7). (b) Enlarge diagram of Fig. 4.4(a)

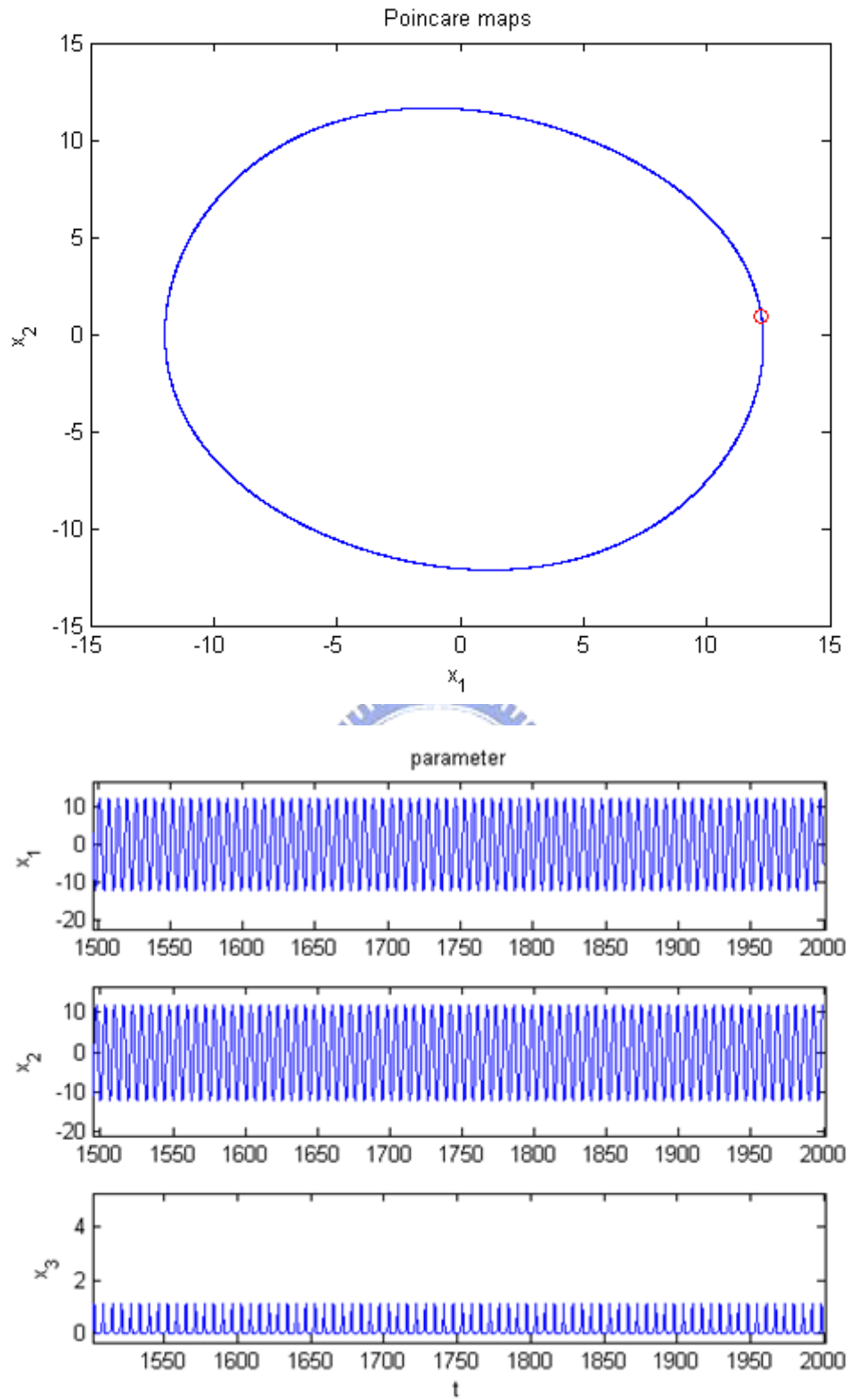


Fig. 4.5 Poincaré maps, and time histories for Rössler system with Legendre function parameters when $k=-0.2$ (period 1).

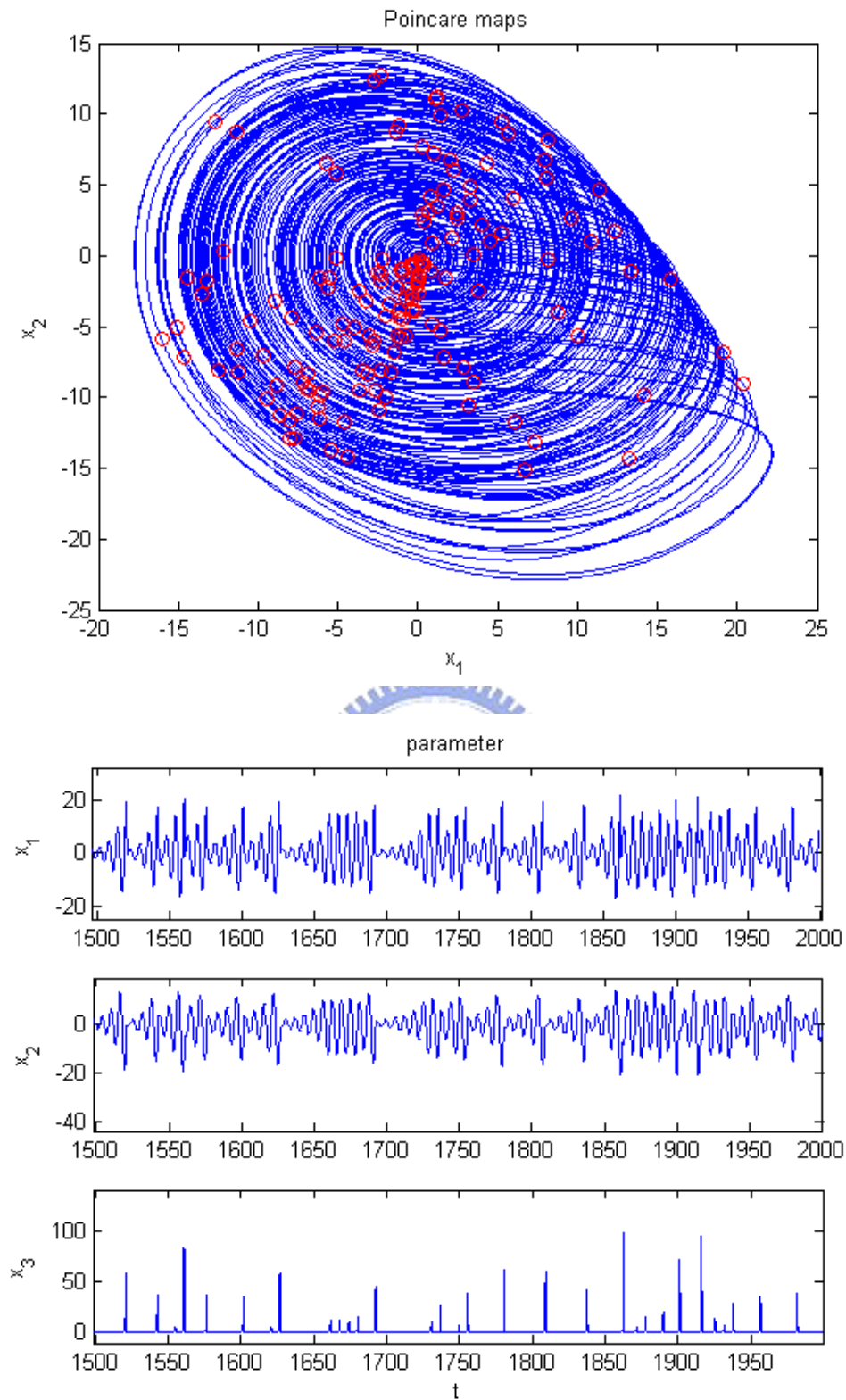
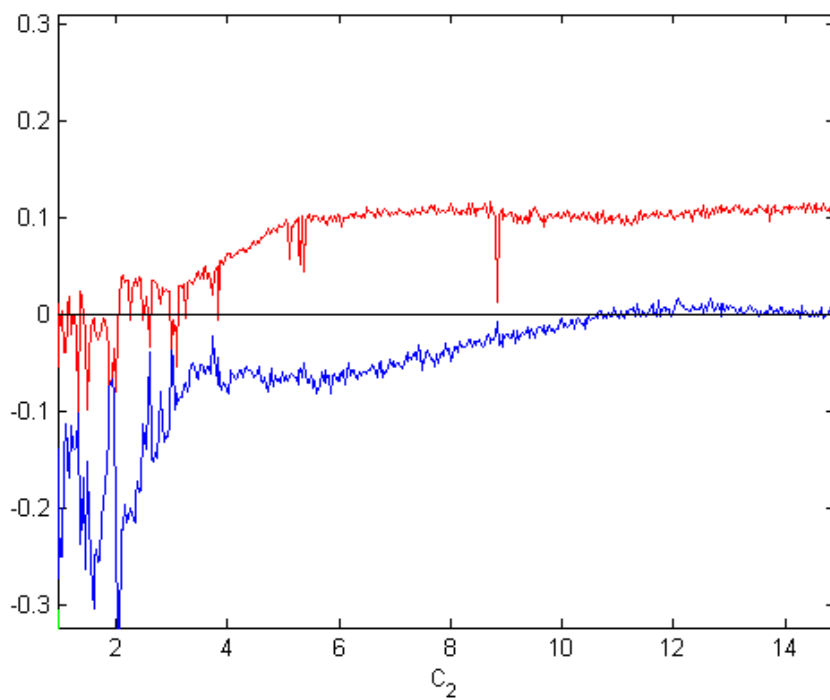
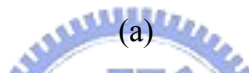
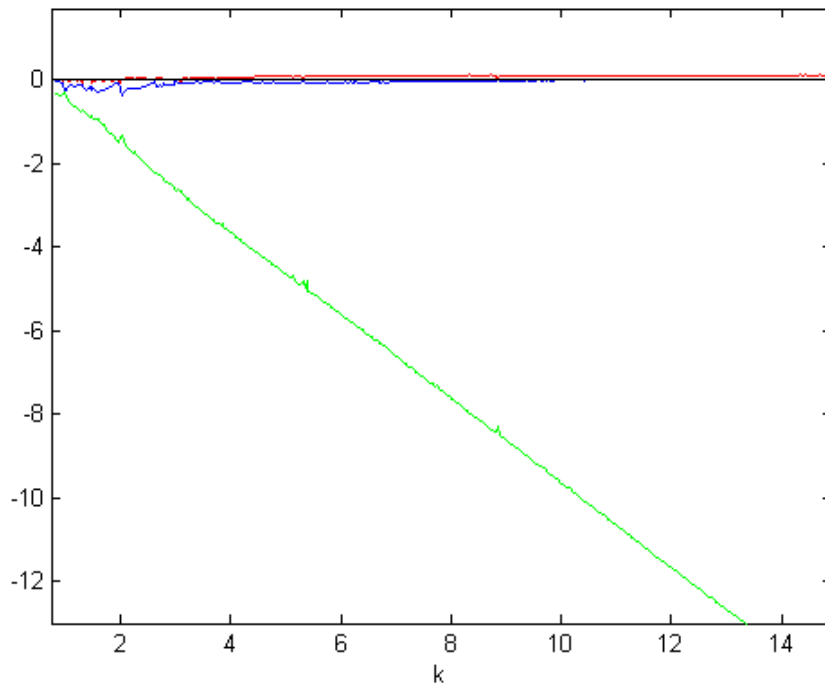


Fig. 4.6 Poincaré maps, and time histories for Rössler system with Legendre function parameters when $k=0.05$ (chaos).



(b)

Fig. 4.7 (a) The Lyapunov exponents for system (4-7) with $a=0.15$ and $b=0.2$. (b) Enlarged diagram of fig. 4.7(a).

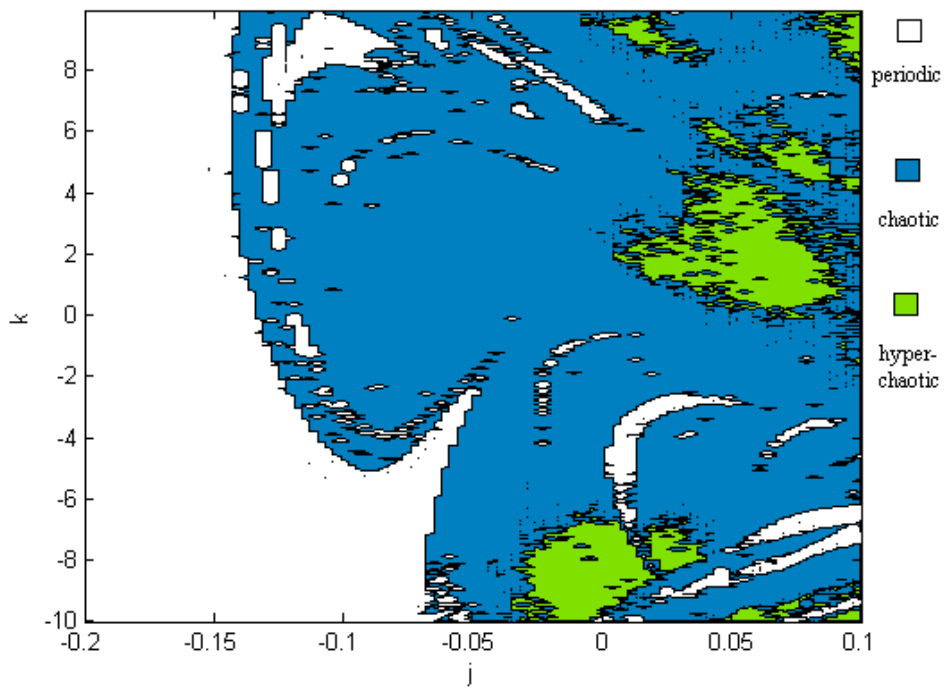


Fig. 4.8 Parameter diagram of system (4-7) with varying j, k .



Chapter 5

Yin-Yang Generalized Synchronization of Chaotic Lü Systems by Pragmatical Asymptotical Stability Theorem

5.1 Preliminary

In this Chapter, the history of Lü system is studied in the first time. Simulation results are shown that chaos of historical, i.e. negative time Lü system is appeared when using “*Yin*”, i.e. negative parameters. Yin Lü system is studied in this paper and the behavior of Yin Lü system is investigated by Lyapunov exponents, phase portraits and bifurcation diagrams.

Projective Yin-Yang generalized synchronization of chaotic Lü systems is accomplished by pragmatical asymptotical stability theorem.

5.2 YYGS scheme by adaptive control and pragmatical asymptotical stability theorem

There are two identical nonlinear dynamical systems, and the master system controls the slave system. The master system is given by

$$\frac{dx(t)}{dt} = Ax(t) + f(x(t), B) \quad (5-1)$$

where $x(t) = [x_1(t), x_2(t), \dots, x_n(t)]^T \in R^n$ denotes a state vector, A is an $n \times n$ uncertain constant coefficient matrix, f is a nonlinear vector function, and B is a vector of uncertain constant coefficients in f . The slave system is given by

$$\frac{dy(-t)}{d(-t)} = \hat{A}y(-t) + f(y(-t), \hat{B}) + u(t) \quad (5-2)$$

where $y(-t) = [y_1(-t), y_2(-t), \dots, y_n(-t)]^T \in R^n$ denotes a state vector, \hat{A} is an $n \times n$ estimated coefficient matrix, \hat{B} is a vector of estimated coefficients in f , and $u(t) = [u_1(t), u_2(t), \dots, u_n(t)]^T \in R^n$ is a control input vector.

Our goal is to design a controller $u(t)$ so that the state vector of the slave system (5-2) asymptotically approaches the state vector of the master system (5-1) plus a given chaotic vector function $F(t) = [F_1(t), F_2(t), \dots, F_n(t)]^T$. This is a special kind of generalized synchronization, $y(-t)$ is a given function for $x(t)$

$$y(-t) = G(x, t) = x(t) + F(t) \quad (5-3)$$

The synchronization can be accomplished when $t \rightarrow \infty$, the limit of the error vector $e(t) = [e_1(t), e_2(t), \dots, e_n(t)]^T$ approaches zero:

$$\lim_{t \rightarrow \infty} e_i(t) = 0 \quad (i = 1, 2, \dots, n) \quad (5-4)$$

where

$$e(t) = [x(t) + F(t)] - y(-t) \quad (5-5)$$

The error dynamics is

$$\frac{de(t)}{dt} = \left[\frac{dx(t)}{dt} + \frac{dF(t)}{dt} \right] - \frac{dy(-t)}{dt} = \left[\frac{dx(t)}{dt} + \frac{dF(t)}{dt} \right] + \frac{dy(-t)}{d(-t)} \quad (5-6)$$

$$\frac{de(t)}{dt} = Ax(t) + \hat{A}y(-t) + f(x(t), B) + f(y(-t), \hat{B}) + \dot{F}(t) + u(t). \quad (5-7)$$

A Lyapunov function $V(e, \tilde{A}, \tilde{B})$ is chosen as a positive definite function of e, \tilde{A}, \tilde{B} :

$$V(e, \tilde{A}, \tilde{B}) = \frac{1}{2} e^T e + \frac{1}{2} \tilde{A}^T \tilde{A} + \frac{1}{2} \tilde{B}^T \tilde{B} \quad (5-8)$$

where $\tilde{A} = A - \hat{A}$, $\tilde{B} = B - \hat{B}$, Its time derivative along any solution of Eq. (5-7) and update parameter differential equations for \tilde{A} and \tilde{B} is

$$\dot{V}(e, \tilde{A}, \tilde{B}) = e^T \left[Ax(t) - \hat{A}y(-t) + f(x(t), B) + f(y(-t), \hat{B}) + \dot{F}(t) + u(t) \right] + \tilde{A}\dot{\tilde{A}} + \tilde{B}\dot{\tilde{B}} \quad (5-9)$$

where $u(t)$, $\dot{\tilde{A}}$ and $\dot{\tilde{B}}$ are chosen so that $\dot{V} = e^T C e$, where C is a diagonal negative definite matrix. \dot{V} is a negative semi-definite function of e and parameter differences \tilde{A} and \tilde{B} . In current scheme of adaptive synchronization [57-60], traditional Lyapunov stability theorem and Babalat lemma are used to prove the error vector approaches zero, as time approaches infinity. But the question, that the estimated parameters also approach to the uncertain parameters, remains no answer. By pragmatism asymptotical stability theorem, the question can be answered strictly.

5.3 Yang Lü system

Before introducing the Yin Lü system, the Yang Lü system can be recalled firstly as follow:



$$\begin{cases} \frac{dx_1}{dt} = a(x_2 - x_1) \\ \frac{dx_2}{dt} = -x_1x_3 + cx_2 \\ \frac{dx_3}{dt} = x_1x_2 - bx_3 \end{cases} \quad (5-10)$$

When initial condition $(x_{10}, x_{20}, x_{30}) = (0.2, 0.35, 0.2)$ and parameters $a=36$, $b=3$ and $c=20$, chaos of the Yang Lü system is appeared. The chaotic behaviors of Eq. (5-9) is shown in Fig. 5.1.

5.4 Yin Lü system

Yin Lü system is

$$\begin{cases} \frac{dy_1(-t)}{d(-t)} = a(y_2(-t) - y_1(-t)) \\ \frac{dy_2(-t)}{d(-t)} = -y_1(-t)y_3(-t) + cy_2(-t) \\ \frac{dy_3(-t)}{d(-t)} = y_1(-t)y_2(-t) - by_3(-t) \end{cases} \quad (5-11)$$

It is clear that in the left hand sides, the derivatives are taken with the back-time. It means we aim to find out the Yin behavior of the Lü system and to comprehend the relation between history and presence. The simulation results are arranged in Table 5.1:

Table 5.1 Dynamic behaviors of Yin Lü system for different signs of parameters

| a | b | c | states |
|---|---|---|----------------------|
| - | + | + | Approach to infinity |
| + | - | + | Approach to infinity |
| - | - | + | Approach to infinity |
| - | + | - | Approach to infinity |
| - | - | - | Chaotic and periodic |

Table 5.1 shows the dynamic behaviors of Yin Lü system for different signs of parameters. An awe-inspiring phenomenon is discovered. When initial condition $(x_{10}, x_{20}, x_{30}) = (0.2, 0.35, 0.2)$ and parameters $a=-36$, $b=-3$ and $c=-20$, chaos of the Yin Lü system appears. Therefore, we call these parameters *Yin* parameters. The chaotic behavior of Eq. (5-11) is shown in Fig. 5.2. In Chinese philosophy, Yin is the negative, past or feminine principle in nature, while Yang is the positive, present or masculine principle in nature. Yin and Yang are two fundamental opposites in Chinese philosophy. Consequently, the positive value of parameters, $a=36$, $b=3$ and $c=20$, in Yang Lü system are called Yang parameters.

5.5 Simulation results for bifurcation diagrams and Lyapunov exponents

In order to research the difference and similarity between Yang and Yin Lü system, the bifurcation diagram and Lyapunov exponents are used. The simulation results are divided into three parts:

Part I: parameter c is varied and $a=-36$, $b=-3$:

Table 5.2 Contrast between Yin and Yang Lü system for Lyapunov exponents

| c | Yin Lü system | | | c | Yang Lü system | | |
|----------------|-----------------|-----------------|-----------------|---------------|-----------------|-----------------|-----------------|
| -29.764 | 0.000197 | -4.61405 | -4.62215 | 29.764 | -0.0002 | -4.61547 | -4.62033 |
| -29.5 | -0.000007 | -1.20339 | -8.29661 | 29.5 | 0.000295 | -0.23415 | -9.26615 |
| -29.456 | 0.000022 | -0.92901 | -8.61497 | 29.456 | 0.000156 | -0.81612 | -8.72803 |
| -29.368 | 0.555732 | 0.000253 | -10.188 | 29.368 | 0.00074 | -0.23754 | -9.3952 |
| -29.324 | 0.000801 | -0.01166 | -9.66514 | 29.324 | 0.896088 | 0.000456 | -10.5725 |
| -29.28 | 0.001811 | -0.51764 | -9.20417 | 29.28 | 0.001913 | -0.5179 | -9.20401 |
| -29.236 | 0.001535 | -1.90309 | -7.86244 | 29.236 | -3.7E-05 | -1.90473 | -7.85923 |
| -29.192 | -0.000025 | -1.11772 | -8.69025 | 29.192 | 0.000522 | -1.11769 | -8.69084 |

Table 5.3 Range of parameter c of Yin Lü system

| | |
|--------------|---------------------|
| -13.0~-29.06 | Chaos |
| -29.06~-35 | Periodic trajectory |

Table 5.2 shows different Lyapunov exponents in the some values of parameter c of Yang and Yin Lü system. Different behaviors at $c=-29.324$ and $c=29.324$ are especially interesting. When c is -29.324 , Yin Lü system is periodic, while c is 29.324 ,

Yang Lü system is hyperchaotic. Table 5.3 shows that when ranges of parameter c is $-13.0 \sim -29.06$, the chaotic behavior is shown in Yin Lü system. while when the range of parameter c is $-29.06 \sim -35$, the periodic behavior of Yin Lü system is shown. Bifurcation diagrams and Lyapunov exponents of chaotic Yang and Yin Lü systems are shown in Fig. 5.3 and Fig. 5.4.

Part2: parameter a is varied and $b=-3$, $c=-20$:

Table 5.4 Contrast between Yin and Yang Lü system for Lyapunov exponents

| a | | | | a | | | |
|---------------|--------------|--------------|--------------|----------------|-------------|--------------|--------------|
| Yin Lü system | | | | Yang Lü system | | | |
| -53.2 | 0.393326116 | 0.000172417 | -36.59349757 | 53.2 | 0.391750789 | -0.000611097 | -36.59113873 |
| -52.996 | 0.414701286 | 0.00010234 | -36.41080268 | 52.996 | 0.388522269 | -0.00004713 | -36.38447419 |
| -52.86 | 0.414233756 | -0.00006142 | -36.2741714 | 52.86 | 0.430180767 | 0.000363957 | -36.29054378 |
| -52.316 | -0.000230724 | -0.247495794 | -35.06827262 | 52.316 | 0.000699843 | -0.247791492 | -35.06890748 |
| -52.18 | 0.419583056 | -0.00123092 | -35.59835126 | 52.18 | 0.430830963 | 0.000434407 | -35.61126449 |
| -51.976 | 0.495389391 | 0.000004097 | -35.47139263 | 51.976 | 0.503320761 | -0.000608358 | -35.47871155 |
| -51.84 | 0.489573289 | -0.000173319 | -35.32939913 | 51.84 | 0.500249518 | -0.000213826 | -35.34003485 |
| -51.772 | 0.513902832 | -0.000152537 | -35.28574945 | 51.772 | 0.490941389 | 0.000160239 | -35.26310078 |
| -51.704 | 0.641579463 | -0.00005584 | -35.34552277 | 51.704 | 0.633573271 | -0.00026471 | -35.33730771 |

Table 5.4 shows that the behaviors of Yang and Yin Lü system are similar but not the same. Bifurcation diagrams and Lyapunov exponents of chaotic Yang and Yin Lü system are shown in Fig. 5.5 and Fig. 5.6.

Part3: parameter b is varied and a=-36, c=-20:

Table 5.5 Contrast between Yin and Yang Lü system for Lyapunov exponents

| b | Yin Lü system | | | b | Yang Lü system | | |
|----------------|-----------------|----------------|-----------------|---------------|-----------------|-----------------|-----------------|
| -13.578 | 0.908798 | 0.000179 | -30.487 | 13.578 | 0.911833 | -0.000095 | -30.4897 |
| -13.73 | 0.922892 | -0.0001 | -30.6528 | 13.73 | 0.921613 | 0.000422 | -30.652 |
| -13.844 | 0.939375 | -0.000046 | -30.7833 | 13.844 | 0.939861 | 0.000249 | -30.7841 |
| -13.882 | 0.944978 | -0.000018 | -30.827 | 13.882 | 0.946319 | -0.00022 | -30.8281 |
| -13.92 | 0.950611 | -0.00023 | -30.8704 | 13.92 | 0.950943 | -0.00053 | -30.8704 |
| -13.958 | 0.000771 | -0.1725 | -29.7863 | 13.958 | 0.946901 | 0.000038 | -30.9049 |
| -13.996 | 0.00052 | -0.18495 | -29.8116 | 13.996 | 0.000881 | -0.18479 | -29.8121 |
| -14.11 | 0.000235 | -0.22197 | -29.8883 | 14.11 | 0.000539 | -0.22204 | -29.8885 |

Table 5.6 Range of parameter b of Yin Lü system and Yang Lü system

| Yin Lü system (b) | | Yang Lü system (b) |
|-------------------|---------------------|--------------------|
| -20~-13.938242 | Periodic trajectory | 20~13.97 |
| -13.938241~-11.6 | Quasi-periodic | 13.97~11.6 |
| -11.6~-1.8 | Chaos | 11.6~1.8 |
| -1.8~-1.08 | Periodic trajectory | 1.8~1.08 |
| -1.08~-1 | Chaos | 1.08~1 |

In Table 5.5 and 5.6, the behaviors of Yang and Yin Lü system are quite different. In Table 5.6, periodic trajectory behavior exists in Yang Lü system in ranges 20~13.97 and 1.8~1.08, while periodic trajectory behavior exists in Yin Lü system in range of -20~-13.938242 and -1.8~-1.08. Bifurcation diagrams and Lyapunov exponents of chaotic Yang and Yin Lü systems are shown in Fig. 5.7 and Fig. 5.8.

5.6 YYGS of Lü system by pragmatistical asymptotical stability

theorem

In this Section, adaptive synchronization from Yin Lü chaos to Yang Lü chaos is proposed. The Yin Lü system is considered as slave system and the Yang Lü system is regarded as master system. These two equations are shown as follow.

Master system is a Yang Lü system:

$$\begin{cases} \frac{dx_1(t)}{dt} = a(x_2(t) - x_1(t)) \\ \frac{dx_2(t)}{dt} = -x_1(t)x_3(t) + cx_2(t) \\ \frac{dx_3(t)}{dt} = x_1(t)x_2(t) - bx_3(t) \end{cases} \quad (5-12)$$

Slave system is a Yin Lü system:

$$\begin{cases} \frac{dy_1(-t)}{d(-t)} = \hat{a}(y_2(-t) - y_1(-t)) + u_1 \\ \frac{dy_2(-t)}{d(-t)} = -y_1(-t)y_3(-t) + \hat{c}y_2(-t) + u_2 \\ \frac{dy_3(-t)}{d(-t)} = y_1(-t)y_2(-t) - \hat{b}y_3(-t) + u_3 \end{cases} \quad (5-13)$$

where $x_i(t)$ and $y_i(-t)$ stands for states variables of the master system and the slave system, respectively. a, b and c are the uncertain parameters of master system, $\hat{a}, \hat{b}, \hat{c}$ are the estimated parameters of slave system. u_1, u_2 and u_3 are nonlinear controllers used for synchronization.

Let we define the error signal as:

$$e_i(t) = x_i(t) - y_i(-t) \quad i = 1, 2, 3 \quad (5-14)$$

Our aim is

$$\lim_{t \rightarrow \infty} \|x_i(t) - y_i(-t)\| = 0 \quad (i = 1, 2, 3) \quad (5-15)$$

Case I

Eq. (5-14) is used. Error dynamics is

$$\frac{de(t)}{dt} = \frac{dx(t)}{dt} + \frac{dy(-t)}{d(-t)}$$

$$\begin{cases} \dot{e}_1 = [a(x_2 - x_1) + (\hat{a}(y_2(-t) - y_1(-t)) - u_1)] \\ \dot{e}_2 = [-x_1x_3 + cx_2 + (-y_1(-t)y_3(-t) + \hat{c}y_2(-t) - u_2)] \\ \dot{e}_3 = [x_1x_2 - bx_3 + (y_1(-t)y_2(-t) - \hat{b}y_3(-t) - u_3)] \end{cases} \quad (5-16)$$

Choose a Lyapunov function in the form of a positive definite function:

$$V(e_1, e_2, e_3, \tilde{a}, \tilde{b}, \tilde{c}) = \frac{1}{2}(e_1^2 + e_2^2 + e_3^2 + \tilde{a}^2 + \tilde{b}^2 + \tilde{c}^2) \quad (5-17)$$

where $\tilde{a} = a - \hat{a}, \tilde{b} = b - \hat{b}, \tilde{c} = c - \hat{c}$ and $\hat{a}, \hat{b}, \hat{c}$ are estimates of uncertain parameters a, b, c.

Its time derivative is

$$\begin{aligned} \dot{V} &= e_1\dot{e}_1 + e_2\dot{e}_2 + e_3\dot{e}_3 + \tilde{a}\dot{\tilde{a}} + \tilde{b}\dot{\tilde{b}} + \tilde{c}\dot{\tilde{c}} \\ &= e_1[a(x_2 - x_1) + (\hat{a}(y_2(-t) - y_1(-t)) - u_1)] \\ &\quad + e_2[-x_1x_3 + cx_2 + (-y_1(-t)y_3(-t) + \hat{c}y_2(-t) - u_2)] \\ &\quad + e_3[x_1x_2 - bx_3 + (y_1(-t)y_2(-t) - \hat{b}y_3(-t) - u_3)] \\ &\quad + \tilde{a}\dot{\tilde{a}} + \tilde{b}\dot{\tilde{b}} + \tilde{c}\dot{\tilde{c}} \end{aligned} \quad (5-18)$$

We choose

$$\begin{cases} \dot{\tilde{a}} = -\dot{\hat{a}} = \tilde{a}e_1 \\ \dot{\tilde{b}} = -\dot{\hat{b}} = \tilde{b}e_3 \\ \dot{\tilde{c}} = -\dot{\hat{c}} = \tilde{c}e_2 \end{cases} \quad (5-19)$$

$$\begin{cases} u_1 = [a(x_2 - x_1) + \hat{a}(y_2(-t) + y_1(-t)) + e_1] + \tilde{a}^2 \\ u_2 = [-x_1x_3 + cx_2 - y_1(-t)y_3(-t) + \hat{c}y_2(-t) + e_2] + \tilde{c}^2 \\ u_3 = [x_1x_2 - bx_3 + y_1(-t)y_2(-t) - \hat{b}y_3(-t) + e_3] + \tilde{b}^2 \end{cases} \quad (5-20)$$

Obtain

$$\dot{V} = -e_1^2 - e_2^2 - e_3^2 < 0 \quad (5-21)$$

which is negative semi-definite function of $e_1, e_2, e_3, \tilde{a}, \tilde{b}$ and \tilde{c} . The Lyapunov asymptotical stability theorem is not satisfied. We cannot obtain that common origin of error dynamics (5-16) and parameter dynamics (5-19) is asymptotically stable. By pragmatical asymptotically stability theorem (see Appendix C), D is a 6-manifold, $n = 6$ and the number of error state variables $p = 3$. When $e_1 = e_2 = e_3 = 0$ and $\tilde{a}, \tilde{b}, \tilde{c}$ take arbitrary values, $\dot{V} = 0$, so X is of 3 dimensions, $m = n - p = 6 - 3 = 3$, $m + 1 < n$ is satisfied. According to the pragmatical asymptotically stability theorem, error vector e approaches zero and the estimated parameters also approach the uncertain parameters. The equilibrium point is pragmatically asymptotically stable. Under the assumption of equal probability, it is actually asymptotically stable. The simulation results are shown in Fig. 5.9~5.12.

Case II

We choose the following Rössler system as the given system which gives $F(t)$:

$$\begin{cases} \frac{dz_1(t)}{dt} = -(z_2(t) + z_3(t)) \\ \frac{dz_2(t)}{dt} = z_1(t) + mz_2(t) \\ \frac{dz_3(t)}{dt} = n + z_1(t)z_3(t) - oz_3(t) \end{cases} \quad (5-22)$$

where $m=0.15, n=0.2, o=10$.

Let we define the error signals as:

$$e_i(t) = [x_i(t) + F_i(t)] - y_i(-t) \quad i = 1, 2, 3$$

Error dynamics is

$$\frac{de(t)}{dt} = \left[\frac{dx(t)}{dt} + \frac{dF(t)}{dt} \right] + \frac{dy(-t)}{d(-t)}$$

$$\begin{aligned}
\dot{e}_1 &= [a(x_2 - x_1) - (z_2 + z_3) + (\hat{a}(y_2(-t) - y_1(-t)) - u_1)] \\
\dot{e}_2 &= [-x_1x_3 + cx_2 + z_1 + mz_2 + (-y_1(-t)y_3(-t) + \hat{c}y_2(-t) - u_2)] \\
\dot{e}_3 &= [x_1x_2 - bx_3 + n + z_1z_3 - oz_3 + (y_1(-t)y_2(-t) - \hat{b}y_3(-t) - u_3)]
\end{aligned} \tag{5-23}$$

Choose a Lyapunov function in the form of a positive definite function:

$$V(e_1, e_2, e_3, \tilde{a}, \tilde{b}, \tilde{c}) = \frac{1}{2}(e_1^2 + e_2^2 + e_3^2 + \tilde{a}^2 + \tilde{b}^2 + \tilde{c}^2) \tag{5-24}$$

where $\tilde{a} = a - \hat{a}, \tilde{b} = b - \hat{b}, \tilde{c} = c - \hat{c}$ and $\hat{a}, \hat{b}, \hat{c}$ are estimates of uncertain parameters a, b, c.

Its time derivative is

$$\begin{aligned}
\dot{V} &= e_1\dot{e}_1 + e_2\dot{e}_2 + e_3\dot{e}_3 + \tilde{a}\dot{\tilde{a}} + \tilde{b}\dot{\tilde{b}} + \tilde{c}\dot{\tilde{c}} \\
&= e_1 [a(x_2 - x_1) - (z_2 + z_3) + (\hat{a}(y_2(-t) - y_1(-t)) - u_1)] \\
&\quad + e_2 [-x_1x_3 + cx_2 + z_1 + mz_2 + (-y_1(-t)y_3(-t) + \hat{c}y_2(-t) - u_2)] \\
&\quad + e_3 [x_1x_2 - bx_3 + n + z_1z_3 - oz_3 + (y_1(-t)y_2(-t) - \hat{b}y_3(-t) - u_3)] \\
&\quad + \tilde{a}\dot{\tilde{a}} + \tilde{b}\dot{\tilde{b}} + \tilde{c}\dot{\tilde{c}}
\end{aligned} \tag{5-25}$$

We choose

$$\begin{cases} \dot{\tilde{a}} = -\dot{\hat{a}} = \tilde{a}e_1 \\ \dot{\tilde{b}} = -\dot{\hat{b}} = \tilde{b}e_3 \\ \dot{\tilde{c}} = -\dot{\hat{c}} = \tilde{c}e_2 \end{cases} \tag{5-26}$$

$$\begin{cases} u_1 = [a(x_2 - x_1) + \hat{a}(y_2(-t) + y_1(-t)) + e_1 + \tilde{a}^2 - (z_2 + z_3)] \\ u_2 = [-x_1x_3 + cx_2 - y_1(-t)y_3(-t) + \hat{c}y_2(-t) + e_2 + \tilde{c}^2 + z_1 + mz_2] \\ u_3 = [x_1x_2 - bx_3 - y_1(-t)y_2(-t) - \hat{b}y_3(-t) + e_3 + \tilde{b}^2 + n + z_1z_3 - oz_3] \end{cases} \tag{5-27}$$

Obtain

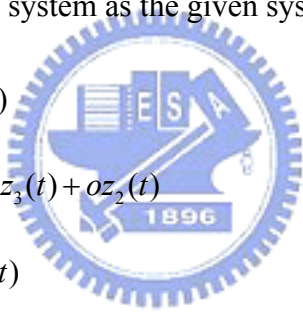
$$\dot{V} = -e_1^2 - e_2^2 - e_3^2 < 0 \tag{5-28}$$

which is negative semi-definite function of $e_1, e_2, e_3, \tilde{a}, \tilde{b}$ and \tilde{c} . The Lyapunov asymptotical stability theorem is not satisfied. We cannot obtain that common origin of error dynamics (5-23) and parameter dynamics (5-26) is asymptotically stable. By

pragmatical asymptotically stability theorem, D is a 6-manifold, $n=6$ and the number of error state variables $p=3$. When $e_1=e_2=e_3=0$ and $\tilde{a}, \tilde{b}, \tilde{c}$ take arbitrary values, $\dot{V}=0$, so X is of 3 dimensions, $m=n-p=6-3=3$, $m+1 < n$ is satisfied. According to the pragmatical asymptotically stability theorem, error vector e approaches zero and the estimated parameters also approach the uncertain parameters. The equilibrium point is pragmatically asymptotically stable. Under the assumption of equal probability, it is actually asymptotically stable. The simulation results are shown in Fig. 5.13-5.16.

Case III

We choose the following Chen system as the given system which gives $F(t)$

$$\begin{cases} \frac{dz_1(t)}{dt} = -m(z_2(t) - z_1(t)) \\ \frac{dz_2(t)}{dt} = (o - m)z_1(t) - z_1z_3(t) + oz_2(t) \\ \frac{dz_3(t)}{dt} = z_1(t)z_2(t) - nz_3(t) \end{cases} \quad (5-29)$$


where $m=35$, $n=3$, $o=28$

Let we define the error signals as:

$$e_i(t) = [x_i(t) + F(t)] - y_i(-t) \quad i = 1, 2, 3$$

Error dynamics is

$$\begin{aligned} \frac{de(t)}{dt} &= \left[\frac{dx(t)}{dt} + \frac{dF(t)}{dt} \right] + \frac{dy(-t)}{d(-t)} \\ \dot{e}_1 &= [a(x_2 - x_1) - m(z_2 - z_1) + (-\hat{a}(y_2(-t) - y_1(-t)) - u_1)] \\ \dot{e}_2 &= [-x_1x_3 + cx_2 + (o - m)z_1 - z_1z_3 + oz_2 + (-y_1(-t)y_3(-t) + \hat{c}y_2(-t) - u_2)] \\ \dot{e}_3 &= [x_1x_2 - bx_3 + z_1z_2 - nz_3 + (y_1(-t)y_2(-t) - \hat{b}y_3(-t) - u_3)] \end{aligned} \quad (5-30)$$

Choose a Lyapunov function in the form of a positive definite function:

$$V(e_1, e_2, e_3, \tilde{a}_1, \tilde{b}_1, \tilde{c}_1) = \frac{1}{2}(e_1^2 + e_2^2 + e_3^2 + \tilde{a}^2 + \tilde{b}^2 + \tilde{c}^2) \quad (5-31)$$

where $\tilde{a} = a - \hat{a}, \tilde{b} = b - \hat{b}, \tilde{c} = c - \hat{c}$ and $\hat{a}, \hat{b}, \hat{c}$ are estimates parameters, a, b, c are uncertain parameters of master system.

Its time derivative is

$$\begin{aligned} \dot{V} &= e_1 \dot{e}_1 + e_2 \dot{e}_2 + e_3 \dot{e}_3 + \tilde{a} \dot{\tilde{a}} + \tilde{b} \dot{\tilde{b}} + \tilde{c} \dot{\tilde{c}} \\ &= e_1 [a(x_2 - x_1) - m(z_2 - z_1) + (-\hat{a}(y_2(-t) - y_1(-t)) - u_1)] \\ &\quad + e_2 [-x_1 x_3 + c x_2 + (o - m)z_1 - z_1 z_3 + o z_2 + (-y_1(-t)y_3(-t) + \hat{c}y_2(-t) - u_2)] \\ &\quad + e_3 [x_1 x_2 - b x_3 + z_1 z_2 - n z_3 + (y_1(-t)y_2(-t) - \hat{b}y_3(-t) - u_3)] \\ &\quad + \tilde{a} \dot{\tilde{a}} + \tilde{b} \dot{\tilde{b}} + \tilde{c} \dot{\tilde{c}} \end{aligned} \quad (5-32)$$

We choose

$$\begin{cases} \dot{\tilde{a}} = -\dot{\hat{a}} = \tilde{a}e_1 \\ \dot{\tilde{b}} = -\dot{\hat{b}} = \tilde{b}e_3 \\ \dot{\tilde{c}} = -\dot{\hat{c}} = \tilde{c}e_2 \end{cases} \quad (5-33)$$

$$\begin{cases} u_1 = [a(x_2 - x_1) + \hat{a}(y_2(-t) + y_1(-t)) + e_1 + \tilde{a}^2 - m(z_2 - z_1)] \\ u_2 = [-x_1 x_3 + c x_2 - y_1(-t)y_3(-t) + \hat{c}y_2(-t) + e_2 + \tilde{c}^2 + (o - m)z_1 - z_1 z_3 + o z_2] \\ u_3 = [x_1 x_2 - b x_3 - y_1(-t)y_2(-t) - \hat{b}y_3(-t) + e_3 + \tilde{b}^2 + z_1 z_2 - n z_3] \end{cases} \quad (5-34)$$

Obtain

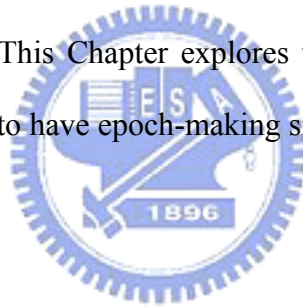
$$\dot{V} = -e_1^2 - e_2^2 - e_3^2 < 0 \quad (5-35)$$

which is a negative semi-definite function of $e_1, e_2, e_3, \hat{a}, \hat{b}$ and \hat{c} . The Lyapunov asymptotical stability theorem is not satisfied. We cannot obtain that common origin of error dynamics (5-30) and parameter dynamics (5-33) is asymptotically stable. By pragmatcal asymptotically stability theorem, D is a 6-manifold, $n=6$ and the number of error state variables $p=3$. When $e_1 = e_2 = e_3 = 0$ and $\hat{a}, \hat{b}, \hat{c}$ take arbitrary values, $\dot{V} = 0$, so X is of 3 dimensions, $m = n - p = 6 - 3 = 3$, $m + 1 < n$ is satisfied.

According to the pragmatical asymptotically stability theorem, error vector e approaches zero and the estimated parameters also approach the uncertain parameters. The equilibrium point is pragmatically asymptotically stable. Under the assumption of equal probability, it is actually asymptotically stable. The simulation results are shown in Fig. 5-17-5-20.

5.7 Summary

In this Chapter, the Yin Lü system is firstly introduced. Via numerical simulation, the Yin Lü system is compared with the Yang Lü system and we find out there are similarity and difference between history and presence. In this Chapter, YYGS of Yang Lü and Yin Lü system are accomplished by adaptive control based on pragmatical asymptotical stability theory. This Chapter explores the another half battle field for chaos study, would be proved to have epoch-making significance in future.



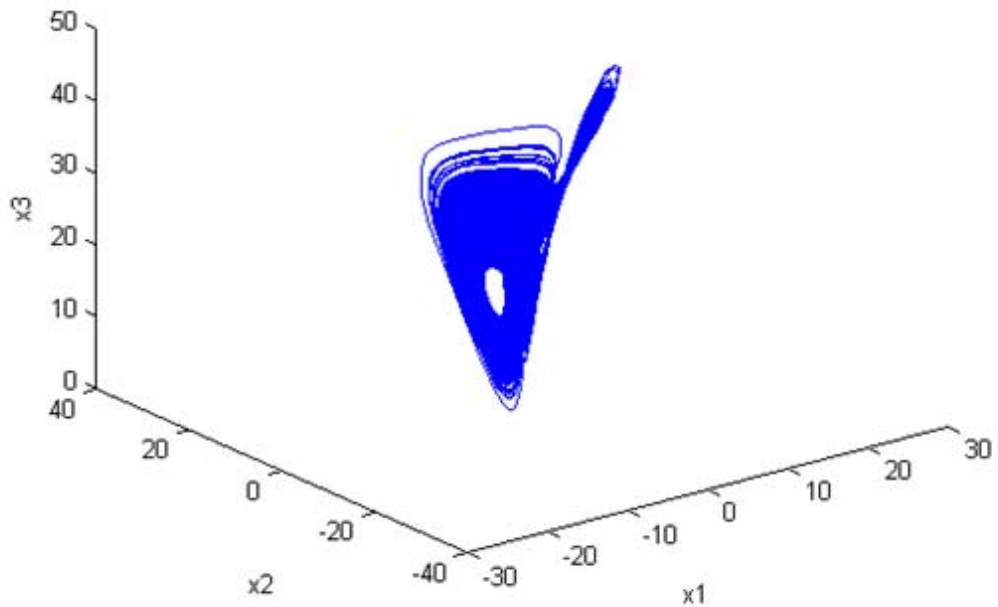
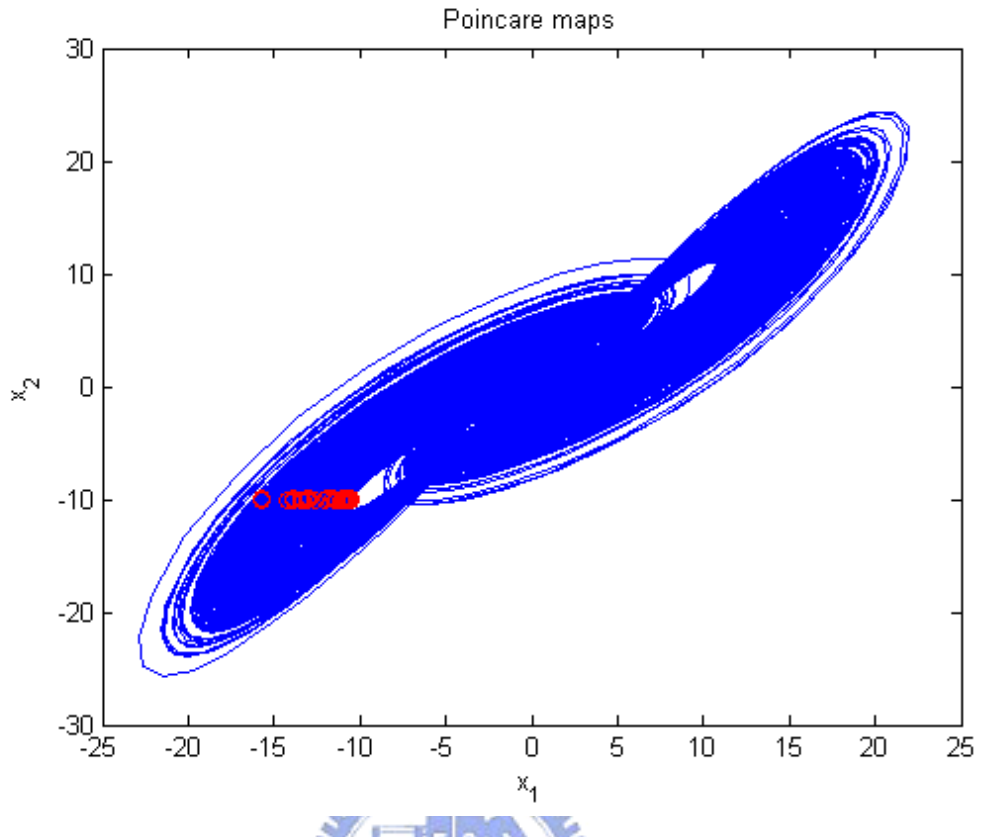


Fig. 5.1 Projections of phase portrait and phase portrait of chaotic Yang Lü system with $a=36$, $b=3$ and $c=20$.

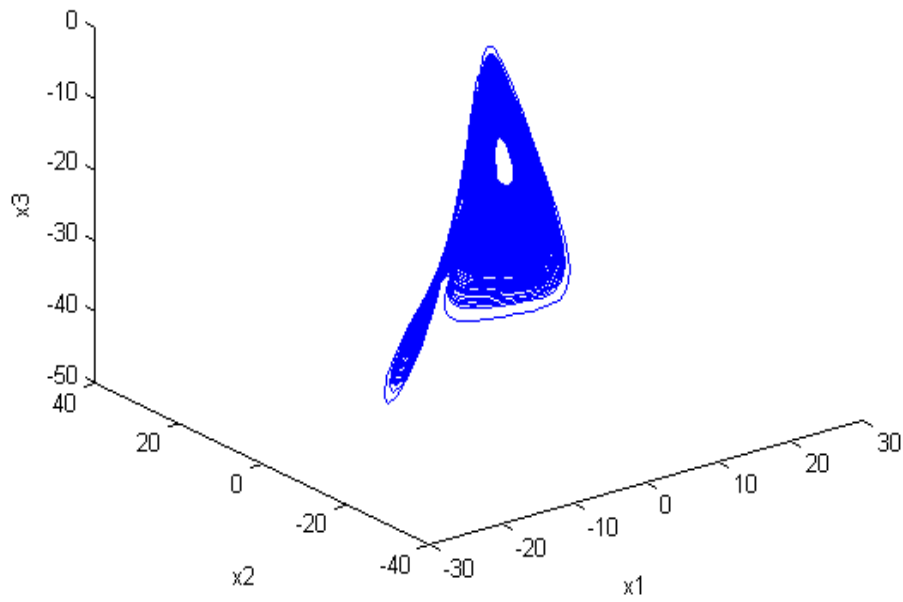
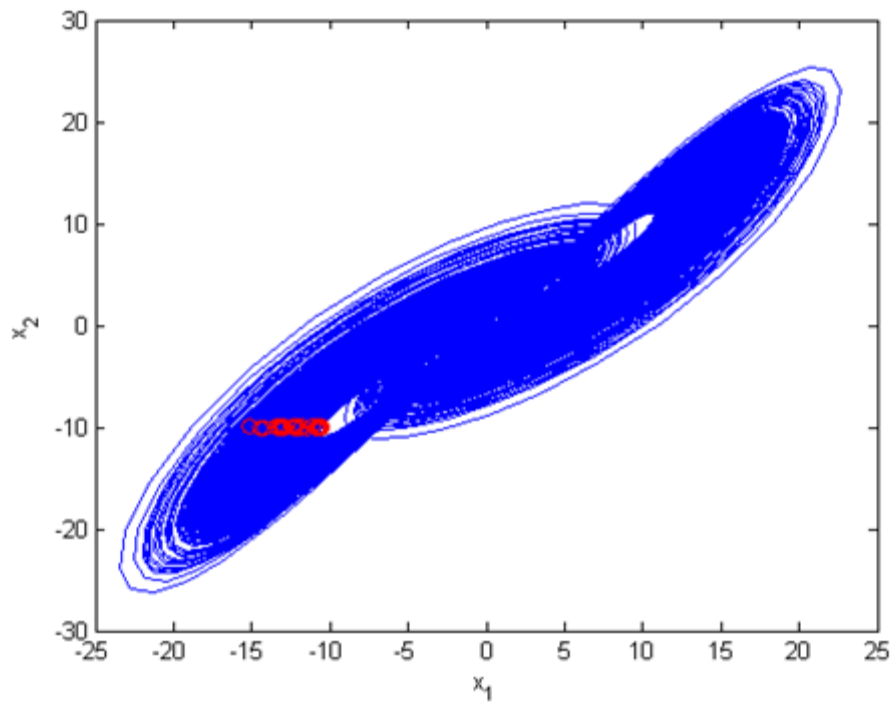


Fig. 5.2 Projection of phase portrait and phase portrait of chaotic Yin Lorenz system with Yin parameters $a=-10$, $b=-8/3$ and $c=-28$.

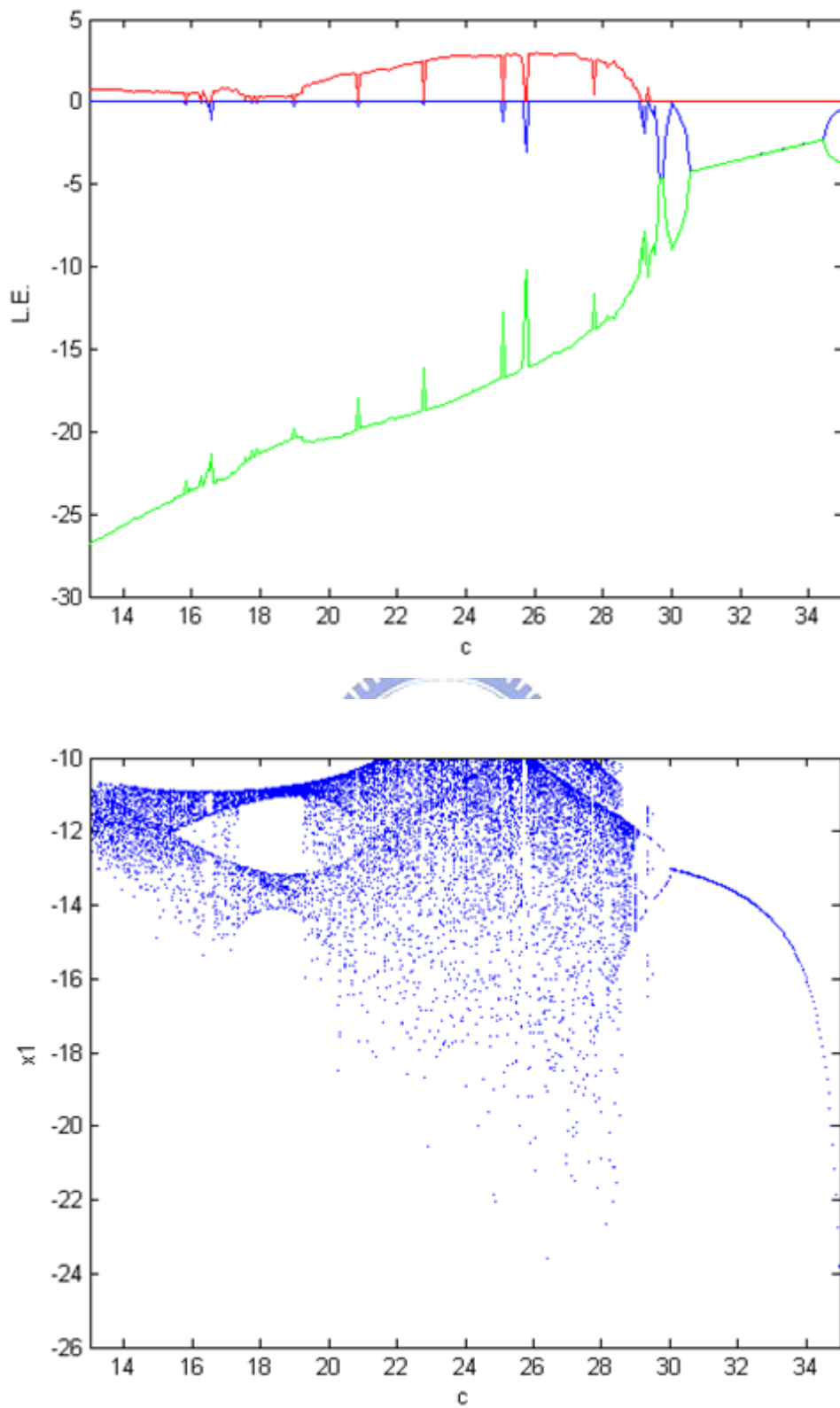


Fig. 5.3 Lyapunov exponents and bifurcation diagram of chaotic Yang Lü system with $a=36$ and $b=3$.

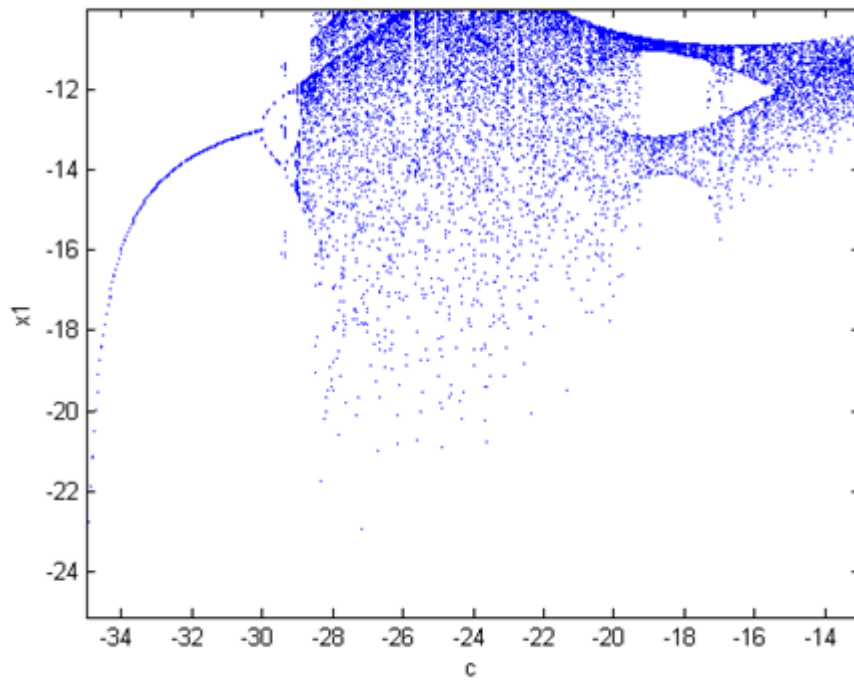
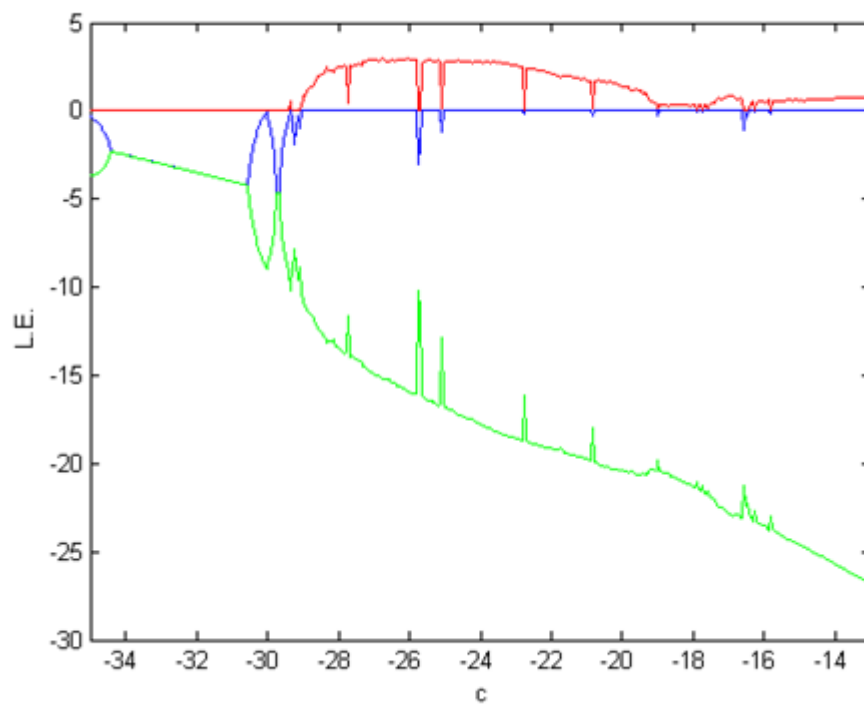


Fig. 5.4 Lyapunov exponents and bifurcation diagram of chaotic Yin Lü system with $a=-36$ and $b=-3$.

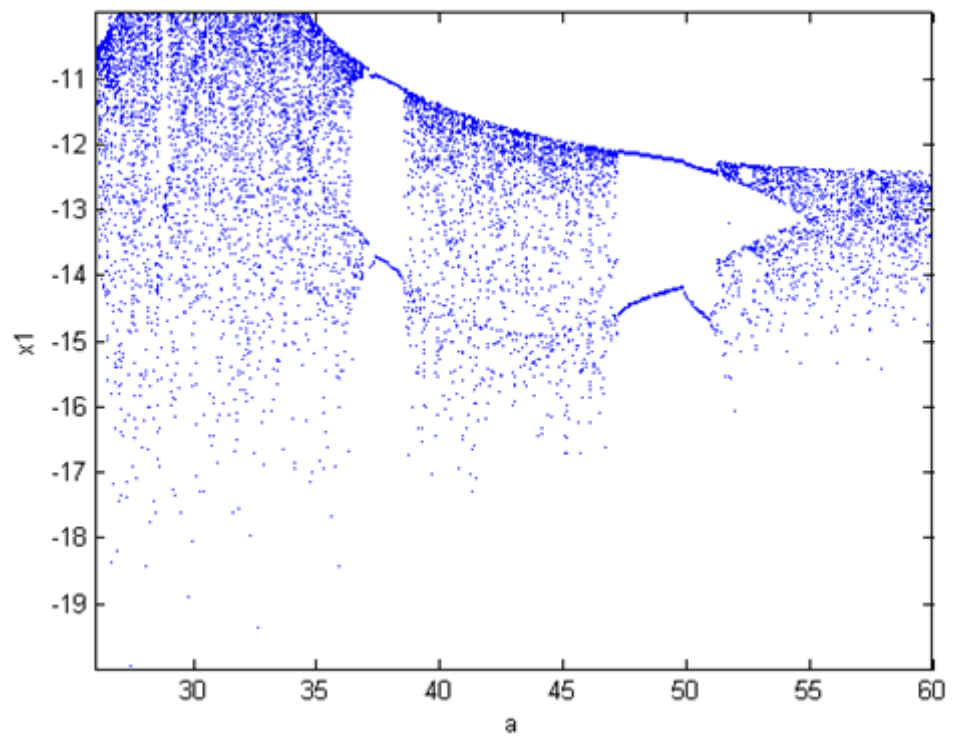
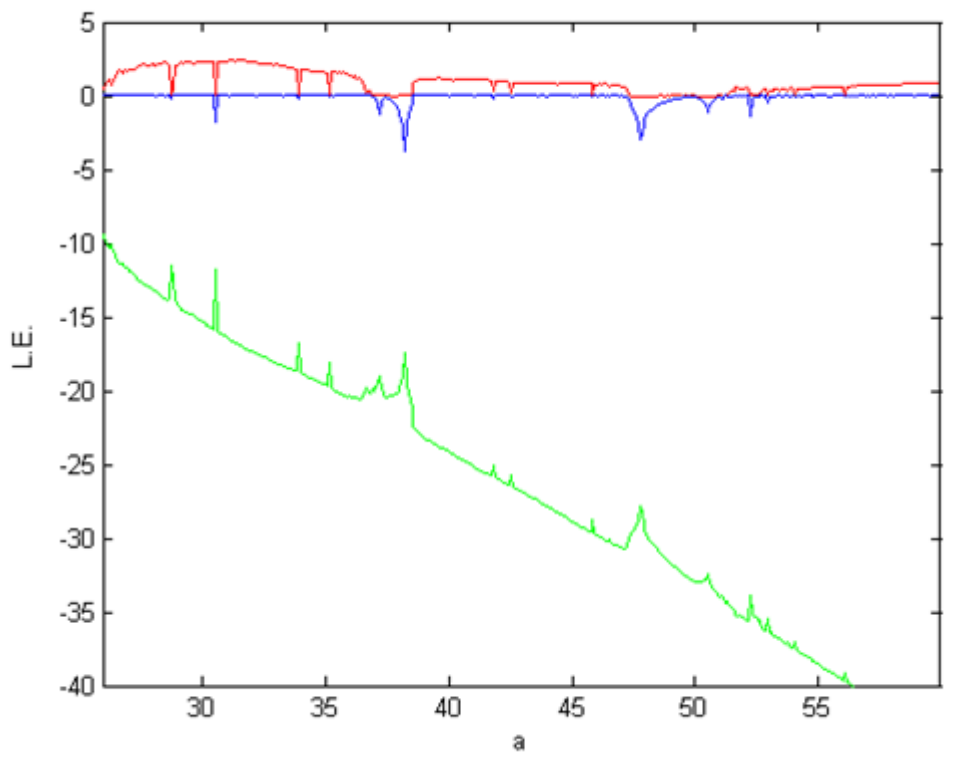


Fig. 5.5 Lyapunov exponents and bifurcation diagram of chaotic Yang Lü system with $b=-3$ and $c=-20$.

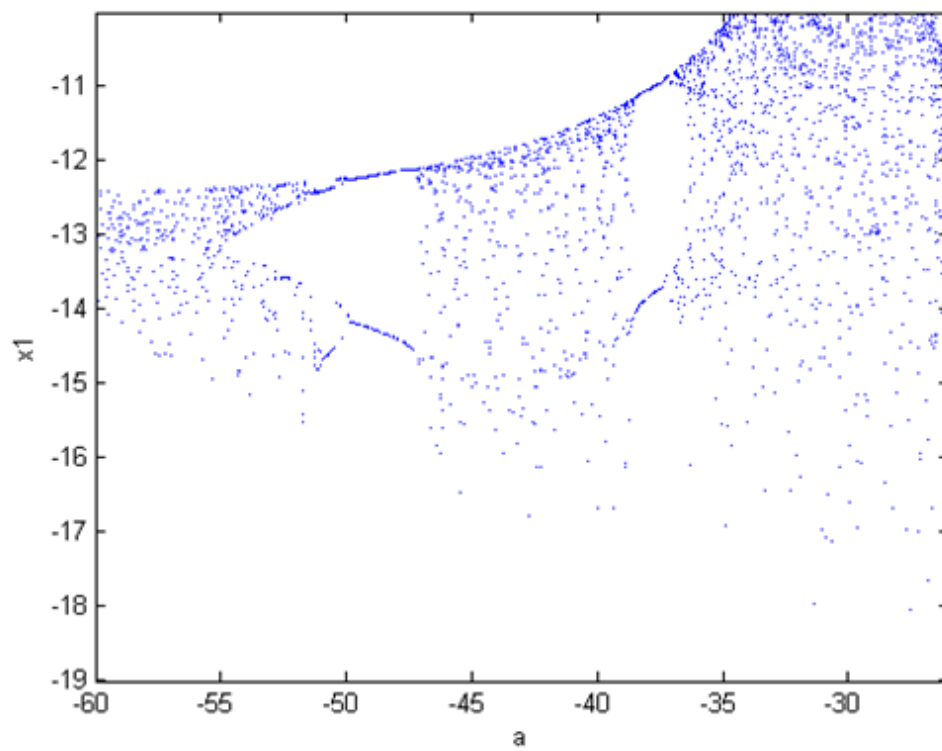
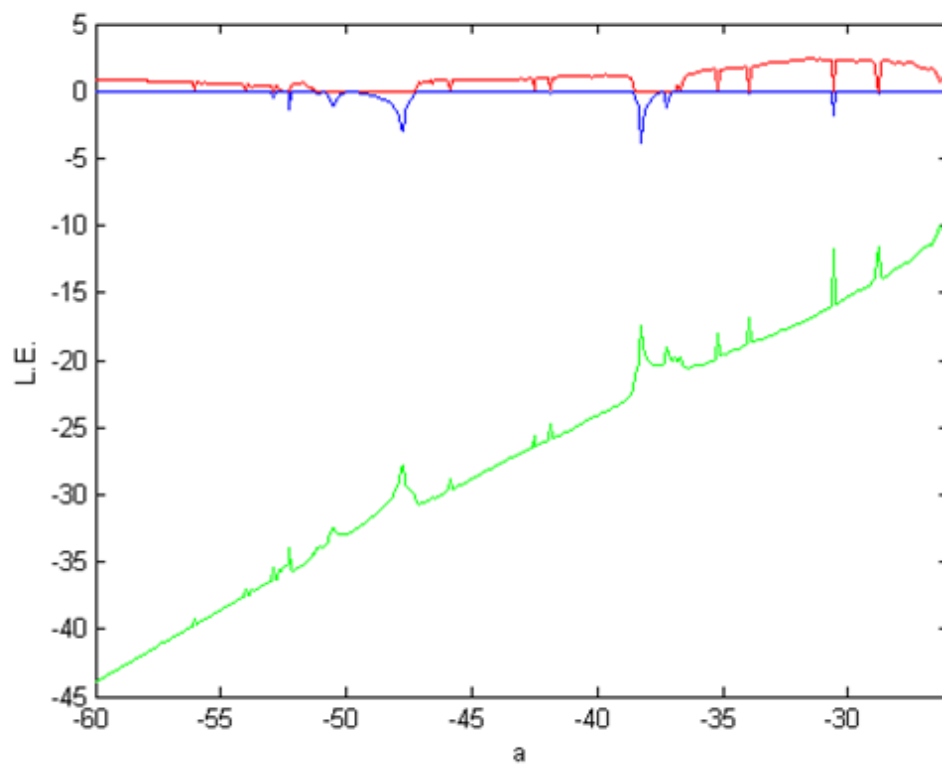


Fig. 5.6 Lyapunov exponents and bifurcation diagram of chaotic Yin Lü system with $c=-20$ and $b=-3$.

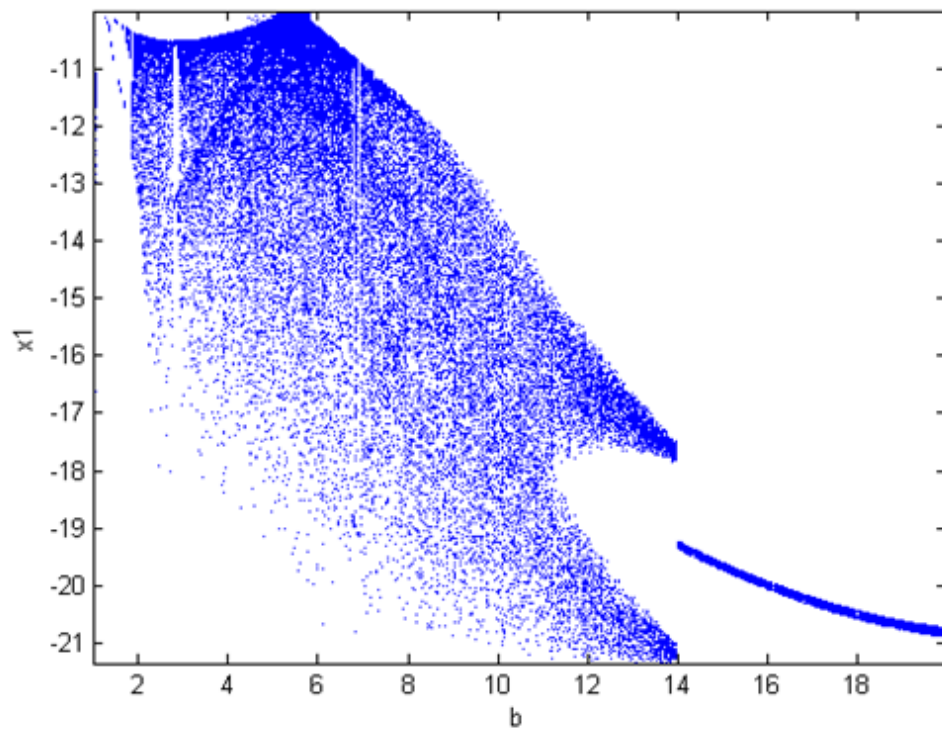
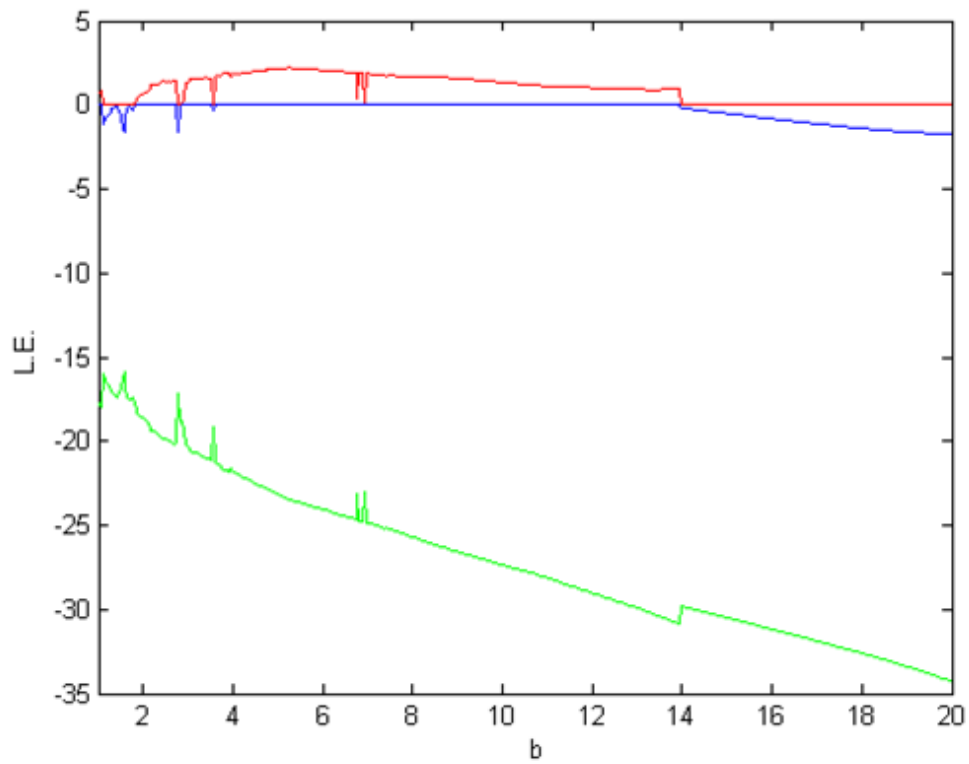


Fig. 5.7 Lyapunov exponents and bifurcation diagram of chaotic Yang Lü system with $a=-36$ and $c=-20$.

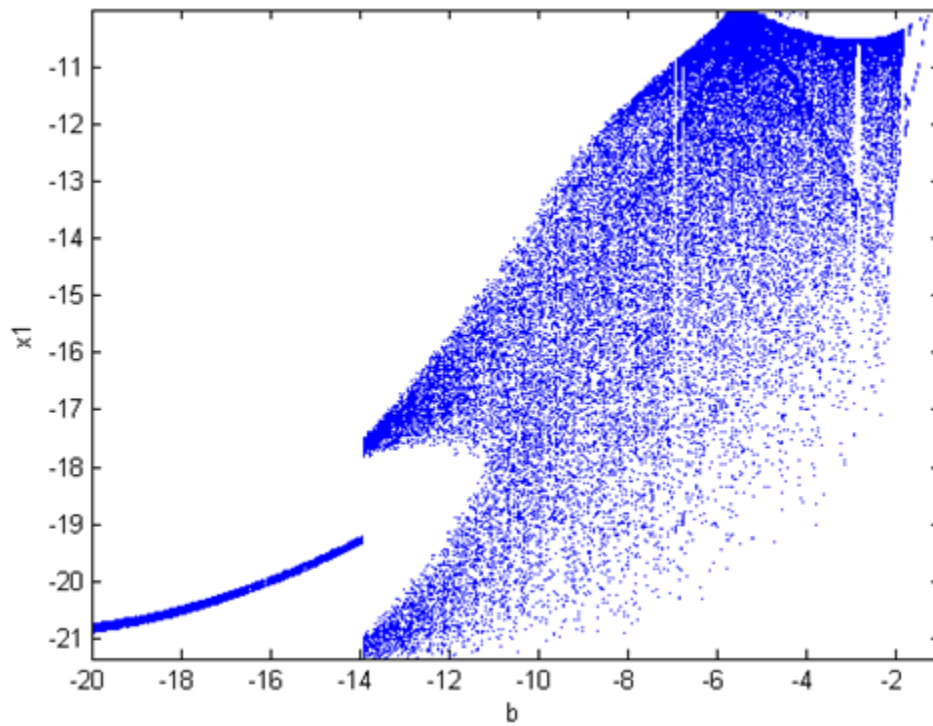
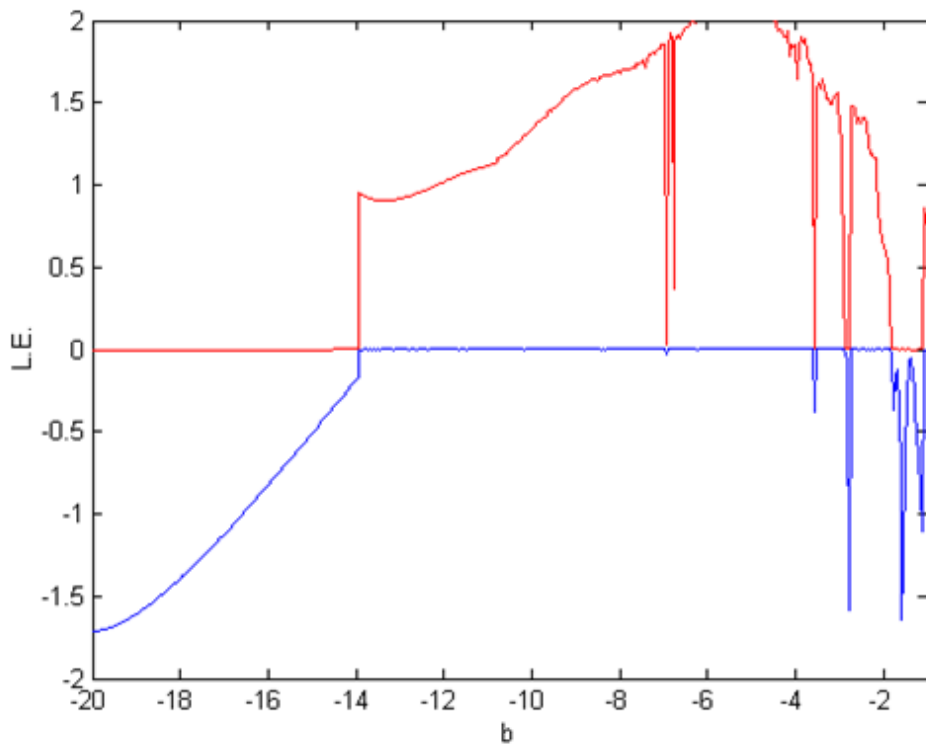


Fig. 5.8 Lyapunov exponents and bifurcation diagram of chaotic Yin Lü system with $a=-36$ and $c=-20$.

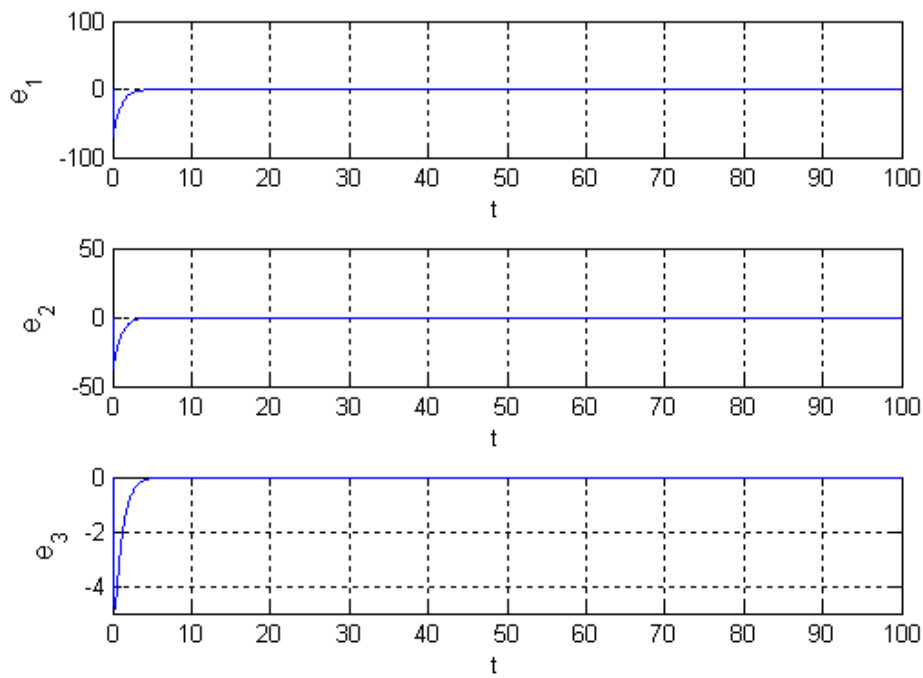


Fig. 5.9 Time histories of state errors for Yin and Yang Lü chaotic systems.

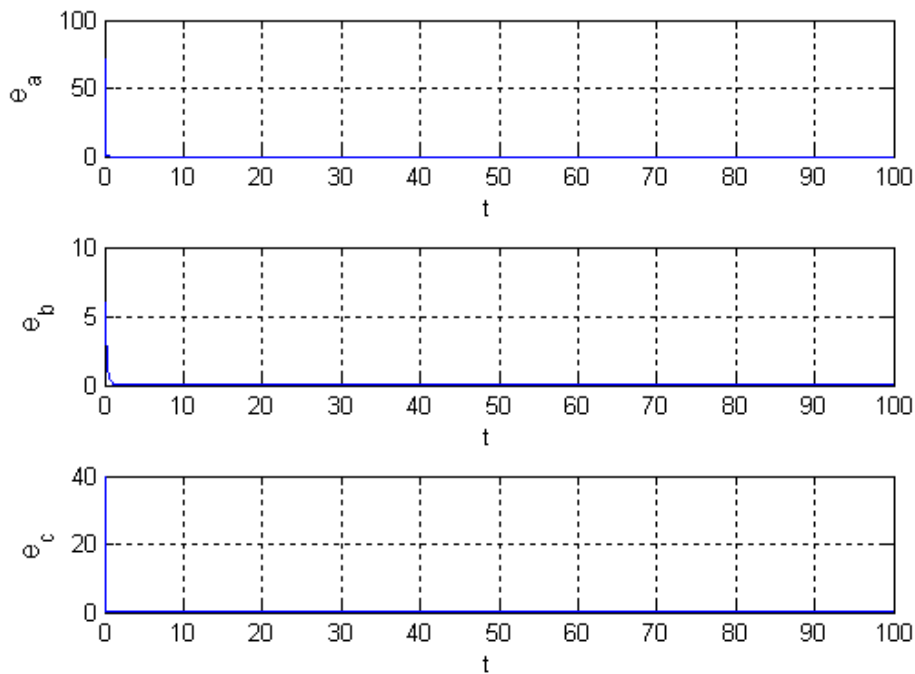


Fig. 5.10 Time histories of parameter errors for Yin and Yang Lü chaotic systems.

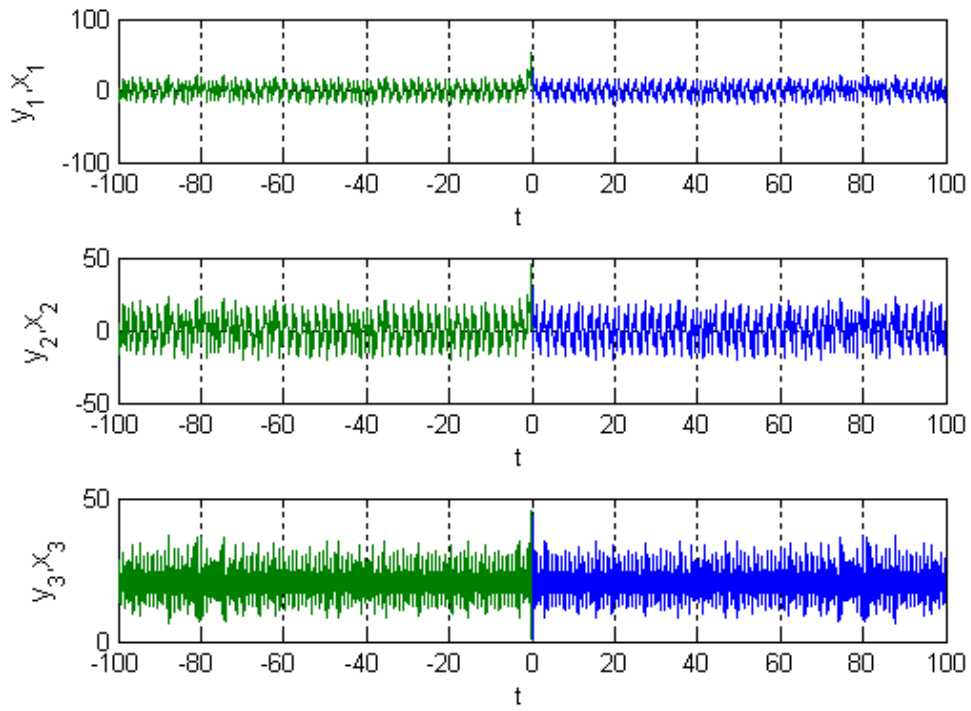


Fig. 5.11 Time histories of states of Yin and Yang Lü chaotic systems.

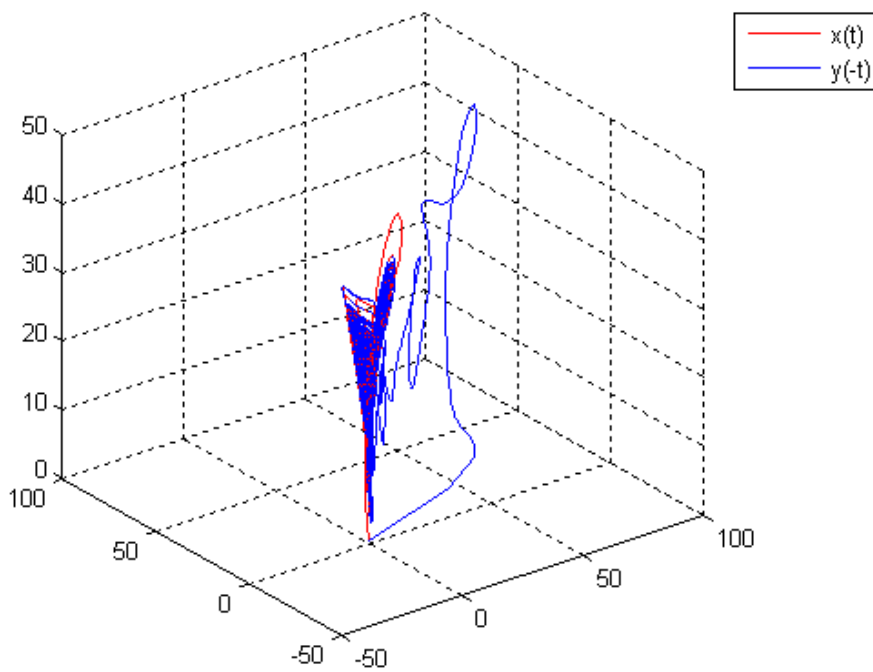


Fig. 5.12 Phase portraits of Yin and Yang Lü chaotic systems.

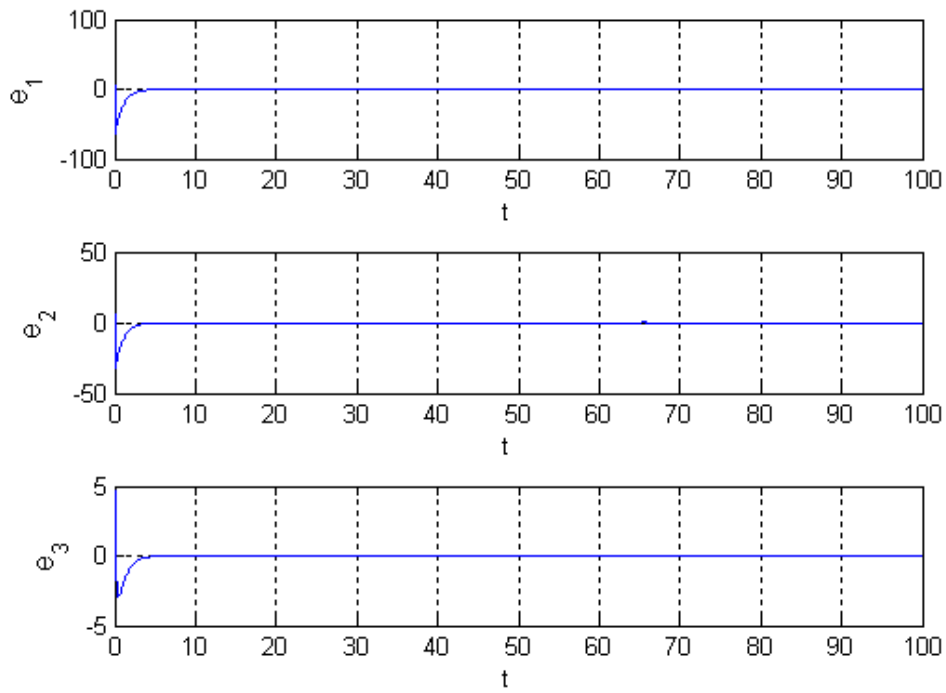


Fig. 5.13 Time histories of state errors for Case II.

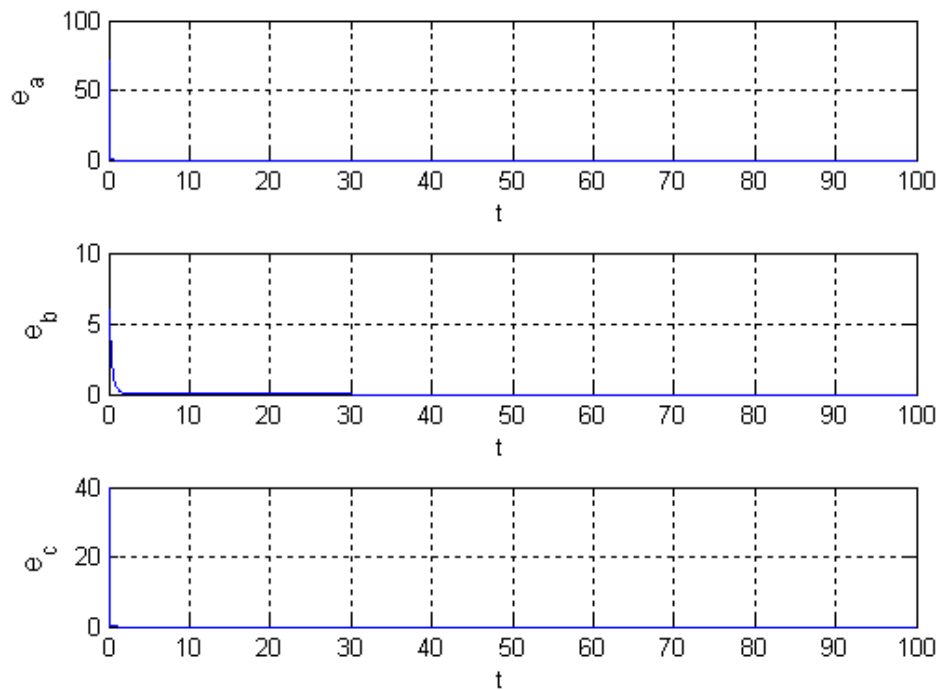


Fig. 5.14 Time histories of parameter errors for Case II.

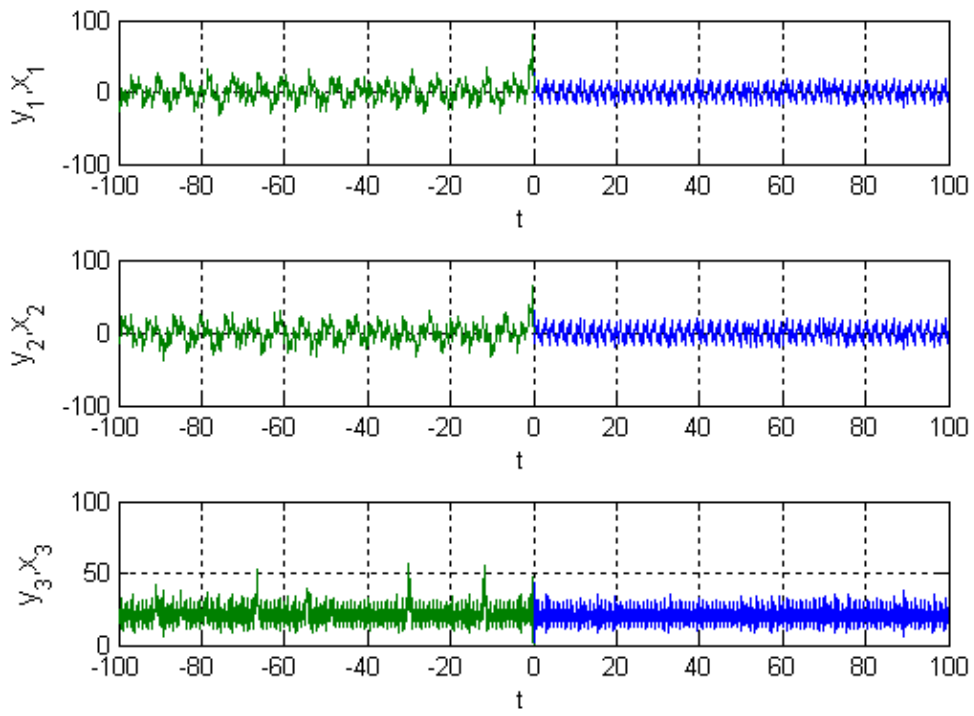


Fig. 5.15 Time histories of states for Case II.

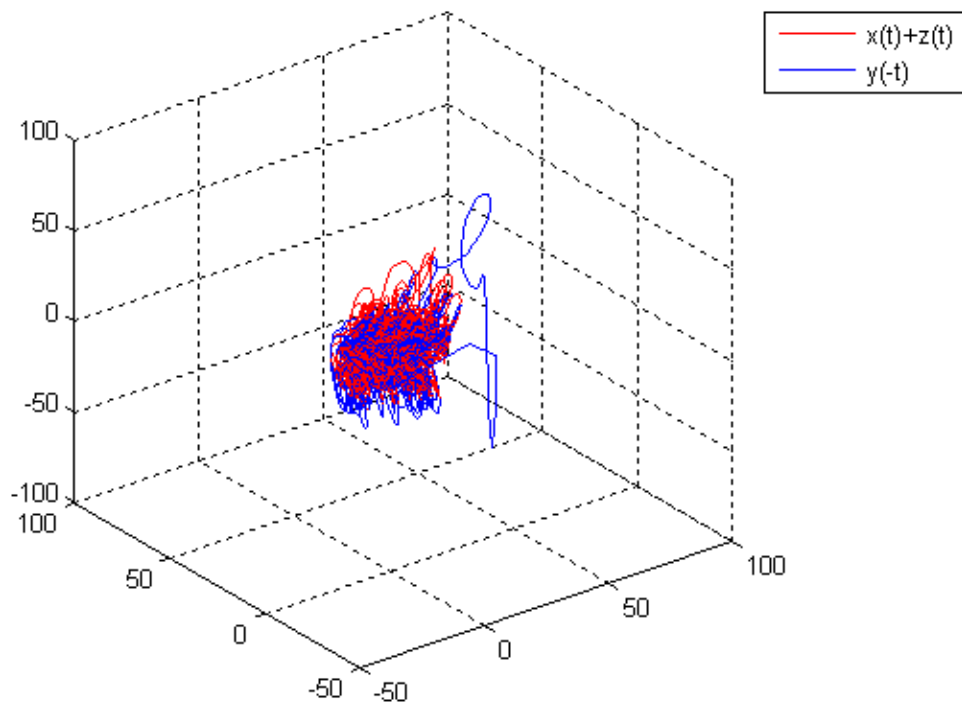


Fig. 5.16 Phase portraits for case III.

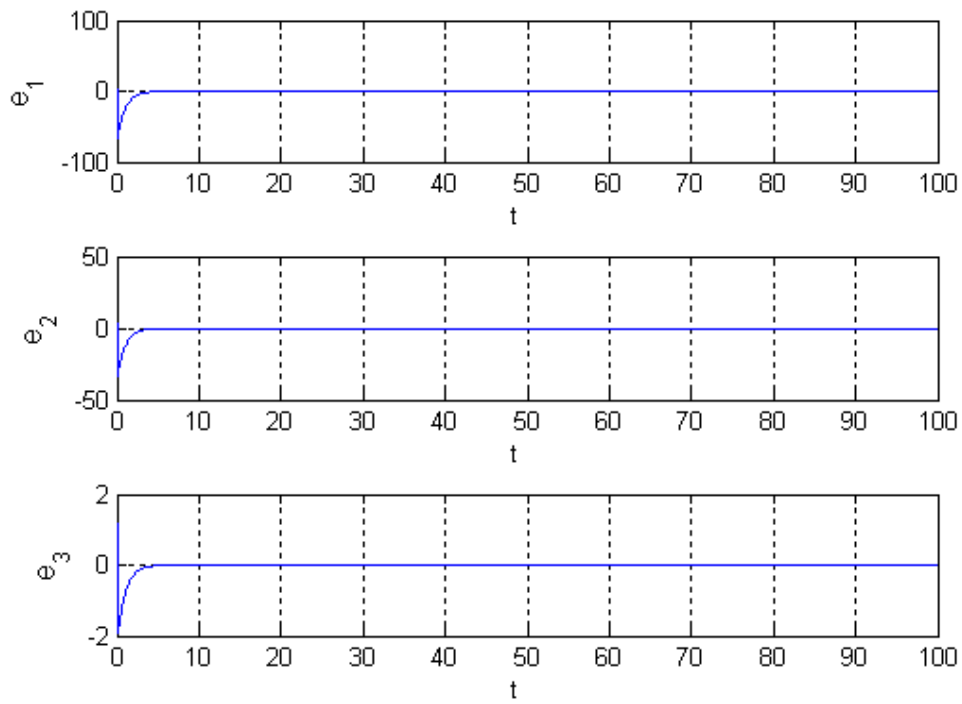


Fig. 5.17 Time histories of state errors for Case III.

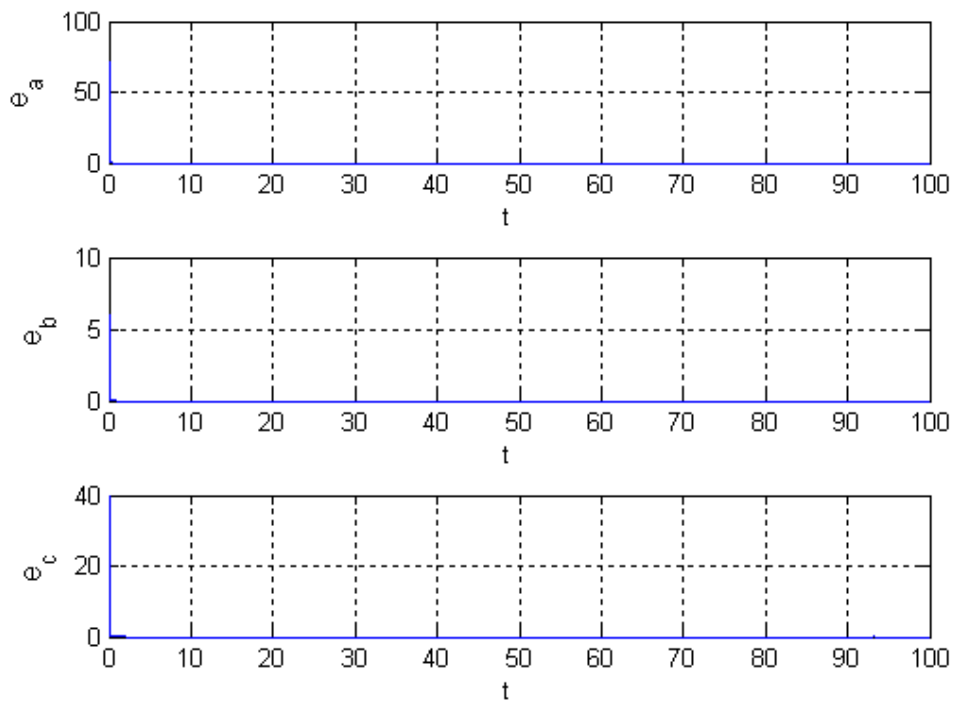


Fig. 5.18 Time histories of parameter errors for Case III.

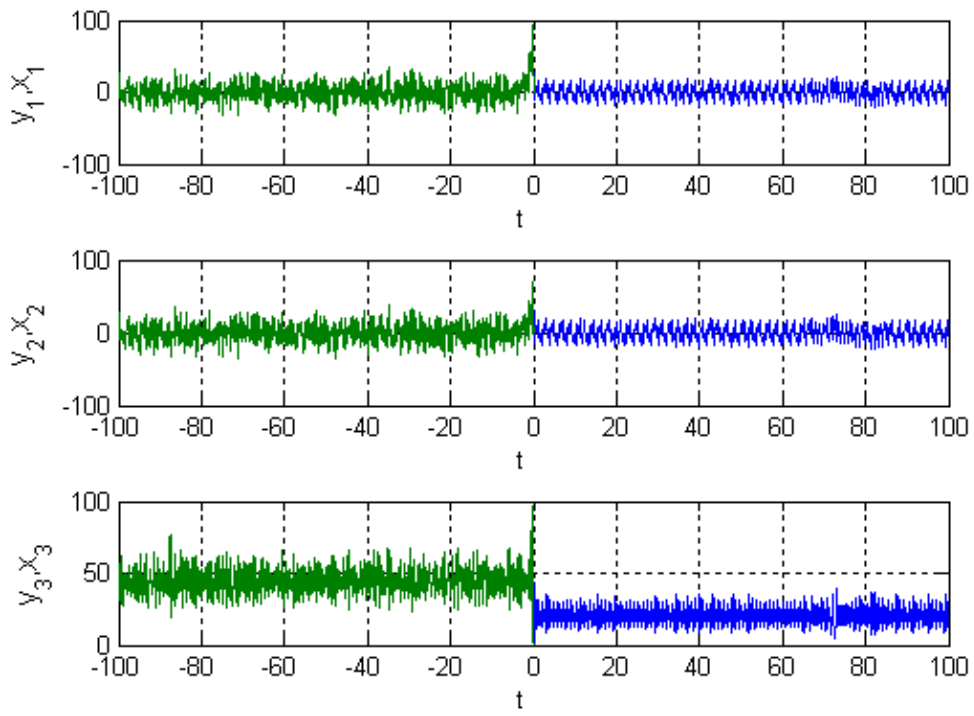


Fig. 5.19 Time histories of states of Case III.

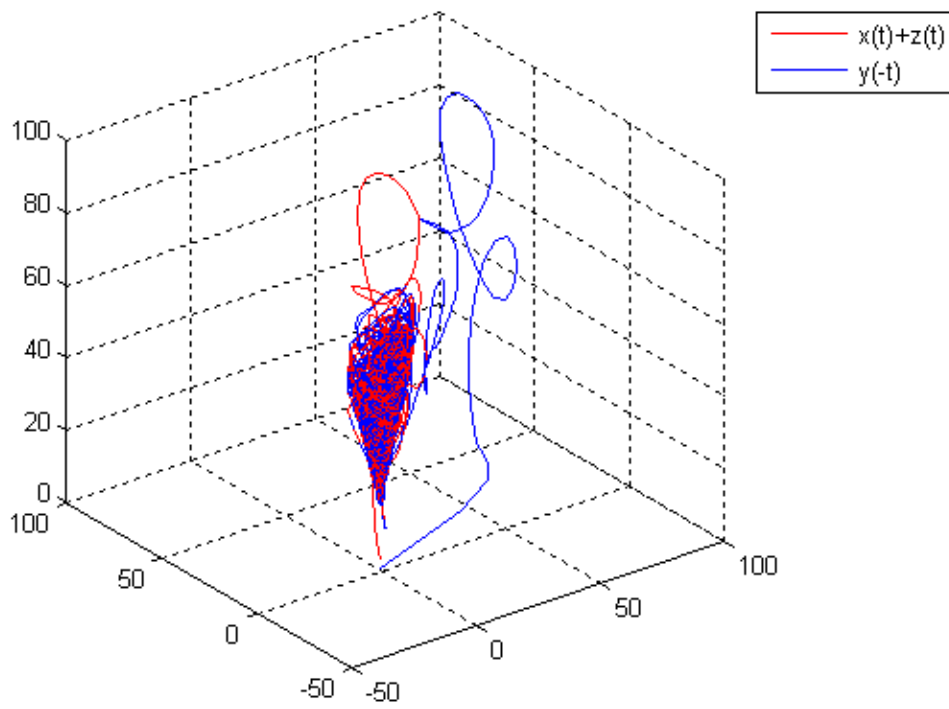


Fig. 5.20 Phase portraits for case III.

Chapter 6

Conclusions

In this thesis, the chaotic behavior of a new Double-Froude system is studied by phase portraits, time history, Poincaré maps, Lyapunov exponent, bifurcation diagrams, and parametric diagram.

In Chapter 2, a new chaos generalized synchronization method by GYC partial region stability theory is proposed. By using the GYC partial region stability theory, the controllers are of lower order than that of controllers by using traditional Lyapunov asymptotical stability theorem. The simple linear homogeneous Lyapunov function of error states makes that the controllers are simpler and introduce less simulation error. In the simulation example, generalized synchronization is extended to time delay system and to two functional chaotic systems. The new double-Froude system, generalized Lorenz system and generalized Chen system are used as simulation examples which verify the effectiveness of the proposed scheme.

In Chapter 3, a new strategy by using GYC partial region stability theory is proposed to achieve chaos control. Via GYC partial region stability theory, the new Lyapunov function used is a simple linear homogeneous function of error states and the lower degree controllers are much more simple and introduce less simulation error. A new chaotic double-Froude system and a generalized Lorenz system and a generalized Chen system are used as simulation examples which confirm the scheme effectively.

In Chapter 4, hyperchaos and chaos of a Rössler system with Legendre function parameters are studied firstly. The results are verified by time histories of states, phase portraits, Poincaré maps, bifurcation analysis, Lyapunov exponents and parametric diagram. Abundant hyperchaos is found for this system, which gives potential in

various applications, particularly in secret communication.

In Chapter 5, the Yin Lü system is firstly introduced. Via numerical simulation, the Yin Lü system is compared with the Yang Lü system and we find out there are similarity and difference between history and presence. In this Chapter, YYGS of Yang Lü and Yin Lü system are accomplished by adaptive control based on pragmatismal asymptotical stability theory. This thesis explores the another half battle field for chaos study, and would be proved to have epoch-making significance in future.



Appendix A

GYC Partial Region Stability Theory

Consider the differential equations of disturbed motion of a nonautonomous system in the normal form

$$\frac{dx_s}{dt} = X_s(t, x_1, \dots, x_n), \quad (s = 1, \dots, n) \quad (\text{A-1})$$

where the function X_s is defined on the intersection of the partial region Ω (shown in Fig. A-1) and

$$\sum_s x_s^2 \leq H \quad (\text{A-2})$$

and $t > t_0$, where t_0 and H are certain positive constants. X_s which vanishes when the variables x_s are all zero, is a real valued function of t, x_1, \dots, x_n . It is assumed that X_s is smooth enough to ensure the existence, uniqueness of the solution of the initial value problem. When X_s does not contain t explicitly, the system is autonomous.

Obviously, $x_s = 0$ ($s = 1, \dots, n$) is a solution of Eq.(A-1). We are interested to the asymptotical stability of this zero solution on partial region Ω (including the boundary) of the neighborhood of the origin which in general may consist of several subregions (Fig. A.1).

Definition 1:

For any given number $\varepsilon > 0$, if there exists a $\delta > 0$, such that on the closed given partial region Ω when

$$\sum_s x_{s0}^2 \leq \delta, \quad (s = 1, \dots, n) \quad (\text{A-3})$$

for all $t \geq t_0$, the inequality

$$\sum_s x_s^2 < \varepsilon, \quad (s = 1, \dots, n) \quad (\text{A-4})$$

is satisfied for the solutions of Eq.(A-27) on Ω , then the disturbed motion

$x_s = 0 \quad (s = 1, \dots, n)$ is stable on the partial region Ω .

Definition 2:

If the undisturbed motion is stable on the partial region Ω , and there exists a $\delta' > 0$, so that on the given partial region Ω when

$$\sum_s x_{s0}^2 \leq \delta', \quad (s = 1, \dots, n) \tag{A-5}$$

The equality

$$\lim_{t \rightarrow \infty} \left(\sum_s x_s^2 \right) = 0 \tag{A-6}$$

is satisfied for the solutions of Eq.(A-1) on Ω , then the undisturbed motion $x_s = 0 \quad (s = 1, \dots, n)$ is asymptotically stable on the partial region Ω .

The intersection of Ω and region defined by Eq.(A-2) is called the region of attraction.

Definition of Functions $V(t, x_1, \dots, x_n)$:

Let us consider the functions $V(t, x_1, \dots, x_n)$ given on the intersection Ω_1 of the partial region Ω and the region

$$\sum_s x_s^2 \leq h, \quad (s = 1, \dots, n) \tag{A-7}$$

for $t \geq t_0 > 0$, where t_0 and h are positive constants. We suppose that the functions are single-valued and have continuous partial derivatives and become zero when $x_1 = \dots = x_n = 0$.

Definition 3:

If there exists $t_0 > 0$ and a sufficiently small $h > 0$, so that on partial region Ω_1 and $t \geq t_0$, $V \geq 0$ (or ≤ 0), then V is a positive (or negative) semidefinite, in general semidefinite, function on the Ω_1 and $t \geq t_0$.

Definition 4:

If there exists a positive (negative) definitive function $W(x_1 \dots x_n)$ on Ω_1 , so

that on the partial region Ω_1 and $t \geq t_0$

$$V - W \geq 0 \text{ (or } -V - W \geq 0), \quad (\text{A-8})$$

then $V(t, x_1, \dots, x_n)$ is a positive definite function on the partial region Ω_1 and $t \geq t_0$.

Definition 5:

If $V(t, x_1, \dots, x_n)$ is neither definite nor semidefinite on Ω_1 and $t \geq t_0$, then $V(t, x_1, \dots, x_n)$ is an indefinite function on partial region Ω_1 and $t \geq t_0$. That is, for any small $h > 0$ and any large $t_0 > 0$, $V(t, x_1, \dots, x_n)$ can take either positive or negative value on the partial region Ω_1 and $t \geq t_0$.

Definition 6: Bounded function V

If there exist $t_0 > 0$, $h > 0$, so that on the partial region Ω_1 , we have

$$|V(t, x_1, \dots, x_n)| < L \quad (\text{A-9})$$

where L is a positive constant, then V is said to be bounded on Ω_1 .

Definition 7: Function with infinitesimal upper bound

If V is bounded, and for any $\lambda > 0$, there exists $\mu > 0$, so that on Ω_1 when $\sum_s x_s^2 \leq \mu$, and $t \geq t_0$, we have

$$|V(t, x_1, \dots, x_n)| \leq \lambda \quad (\text{A-10})$$

then V admits an infinitesimal upper bound on Ω_1 .

Theorem 1 [38-40]

If there can be found for the differential equations of the disturbed motion (Eq.(A-27)) a definite function $V(t, x_1, \dots, x_n)$ on the partial region, and for which the derivative with respect to time based on these equations as given by the following :

$$\frac{dV}{dt} = \frac{\partial V}{\partial t} + \sum_{s=1}^n \frac{\partial V}{\partial x_s} X_s \quad (\text{A-11})$$

is a semidefinite function on the partial region whose sense is opposite to that of V , or

if it becomes zero identically, then the undisturbed motion is stable on the partial region.

Proof:

Let us assume for the sake of definiteness that V is a positive definite function. Consequently, there exists a sufficiently large number t_0 and a sufficiently small number $h < H$, such that on the intersection Ω_1 of partial region Ω and

$$\sum_s x_s^2 \leq h, \quad (s=1, \dots, n) \quad (\text{A-12})$$

and $t \geq t_0$, the following inequality is satisfied

$$V(t, x_1, \dots, x_n) \geq W(x_1, \dots, x_n) \quad (\text{A-13})$$

where W is a certain positive definite function which does not depend on t . Besides that, Eq. (A-7) may assume only negative or zero value in this region.

Let ε be an arbitrarily small positive number. We shall suppose that in any case $\varepsilon < h$. Let us consider the aggregation of all possible values of the quantities x_1, \dots, x_n , which are on the intersection ω_2 of Ω_1 and

$$\sum_s x_s^2 = \varepsilon, \quad (\text{A-14})$$

and let us designate by $l > 0$ the precise lower limit of the function W under this condition. by virtue of Eq. (A-5), we shall have

$$V(t, x_1, \dots, x_n) \geq l \quad \text{for } (x_1, \dots, x_n) \text{ on } \omega_2. \quad (\text{A-15})$$

We shall now consider the quantities x_s as functions of time which satisfy the differential equations of disturbed motion. We shall assume that the initial values x_{s_0} of these functions for $t = t_0$ lie on the intersection Ω_2 of Ω_1 and the region

$$\sum_s x_s^2 \leq \delta, \quad (\text{A-16})$$

where δ is so small that

$$V(t_0, x_{1_0}, \dots, x_{n_0}) < l \quad (\text{A-17})$$

By virtue of the fact that $V(t_0, 0, \dots, 0) = 0$, such a selection of the number δ is obviously possible. We shall suppose that in any case the number δ is smaller than ε . Then the inequality

$$\sum_s x_s^2 < \varepsilon, \quad (\text{A-18})$$

being satisfied at the initial instant will be satisfied, in the very least, for a sufficiently small $t - t_0$, since the functions $x_s(t)$ vary continuously with time. We shall show that these inequalities will be satisfied for all values $t > t_0$. Indeed, if these inequalities were not satisfied at some time, there would have to exist such an instant $t = T$ for which this inequality would become an equality. In other words, we would have

$$\sum_s x_s^2(T) = \varepsilon, \quad (\text{A-19})$$

and consequently, on the basis of Eq. (A-9)

$$V(T, x_1(T), \dots, x_n(T)) \geq l \quad (\text{A-20})$$

On the other hand, since $\varepsilon < h$, the inequality (Eq.(A-4)) is satisfied in the entire interval of time $[t_0, T]$, and consequently, in this entire time interval $\frac{dV}{dt} \leq 0$. This yields

$$V(T, x_1(T), \dots, x_n(T)) \leq V(t_0, x_{t_0}, \dots, x_{n_0}), \quad (\text{A-21})$$

which contradicts Eq. (A-12) on the basis of Eq. (A-11). Thus, the inequality (Eq.(A-1)) must be satisfied for all values of $t > t_0$, hence follows that the motion is stable.

Finally, we must point out that from the view-point of mathematics, the stability on partial region in general does not be related logically to the stability on whole region. If an undisturbed solution is stable on a partial region, it may be either stable or unstable on the whole region and vice versa. From the viewpoint of dynamics, we

wre not interesting to the solution starting from Ω_2 and going out of Ω .

Theorem 2 [38-40]

If in satisfying the conditions of theorem 1, the derivative $\frac{dV}{dt}$ is a definite function on the partial region with opposite sign to that of V and the function V itself permits an infinitesimal upper limit, then the undisturbed motion is asymptotically stable on the partial region.

Proof:

Let us suppose that V is a positive definite function on the partial region and that consequently, $\frac{dV}{dt}$ is negative definite. Thus on the intersection Ω_1 of Ω and the region defined by Eq. (A-4) and $t \geq t_0$ there will be satisfied not only the inequality (Eq.(A-5)), but the following inequality as will:

$$\frac{dV}{dt} \leq -W_1(x_1, \dots, x_n), \tag{A-22}$$

where W_1 is a positive definite function on the partial region independent of t.

Let us consider the quantities x_s as functions of time which satisfy the differential equations of disturbed motion assuming that the initial values $x_{s0} = x_s(t_0)$ of these quantities satisfy the inequalities (Eq. (A-10)). Since the undisturbed motion is stable in any case, the magnitude δ may be selected so small that for all values of $t \geq t_0$ the quantities x_s remain within Ω_1 . Then, on the basis of Eq. (A-13) the derivative of function $V(t, x_1(t), \dots, x_n(t))$ will be negative at all times and, consequently, this function will approach a certain limit, as t increases without limit, remaining larger than this limit at all times. We shall show that this limit is equal to some positive quantity different from zero. Then for all values of $t \geq t_0$ the following inequality will be satisfied:

$$V(t, x_1(t), \dots, x_n(t)) > \alpha \tag{A-23}$$

where $\alpha > 0$.

Since V permits an infinitesimal upper limit, it follows from this inequality that

$$\sum_s x_s^2(t) \geq \lambda, \quad (s = 1, \dots, n), \quad (\text{A-24})$$

where λ is a certain sufficiently small positive number. Indeed, if such a number λ did not exist, that is, if the quantity $\sum_s x_s(t)$ were smaller than any preassigned number no matter how small, then the magnitude $V(t, x_1(t), \dots, x_n(t))$, as follows from the definition of an infinitesimal upper limit, would also be arbitrarily small, which contradicts (A-14).

If for all values of $t \geq t_0$ the inequality (Eq. (A-15)) is satisfied, then Eq. (A-13) shows that the following inequality will be satisfied at all times:

$$\frac{dV}{dt} \leq -l_1, \quad (\text{A-25})$$

where l_1 is positive number different from zero which constitutes the precise lower limit of the function $W_1(t, x_1(t), \dots, x_n(t))$ under condition (Eq. (A-15)). Consequently, for all values of $t \geq t_0$ we shall have:

$$V(t, x_1(t), \dots, x_n(t)) = V(t_0, x_{10}, \dots, x_{n0}) + \int_{t_0}^t \frac{dV}{dt} dt \leq V(t_0, x_{10}, \dots, x_{n0}) - l_1(t - t_0),$$

which is, obviously, in contradiction with Eq.(A-14). The contradiction thus obtained shows that the function $V(t, x_1(t), \dots, x_n(t))$ approached zero as t increase without limit. Consequently, the same will be true for the function $W(x_1(t), \dots, x_n(t))$ as well, from which it follows directly that

$$\lim_{t \rightarrow \infty} x_s(t) = 0, \quad (s = 1, \dots, n), \quad (\text{A-26})$$

which proves the theorem.

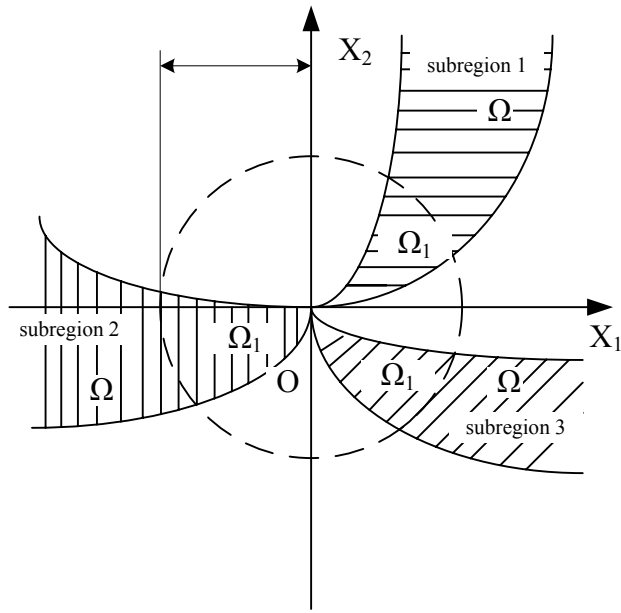


Fig. A.1. Partial regions Ω and Ω_1 .



Appendix B

Systems of Positive States

B.1 Three species prey-predator system

The three species prey-predator system which consists of two competing preys and one predator can be described by the following set of nonlinear differential equations:

$$\begin{cases} \frac{dx}{dt} = r_1(1 - k_1^{-1}x - k_1^{-1}c_2y) - \Phi_1(x, y)z \\ \frac{dy}{dt} = r_2(1 - k_2^{-1}c_1x - k_2^{-1}y) - \Phi_2(x, y)z \\ \frac{dz}{dt} = e_1\Phi_1(x, y)z + e_2\Phi_2(x, y)z - \alpha z \end{cases} \quad (\text{B-1})$$

where α, r_i, k_i, e_i and $c_i, i=1,2$ are the model parameters assuming only positive values, and the functions $\Phi_i(x, y), i=1,2$ represent the densities of the two prey species and z represents the density of the predator species. The predator z consumes the preys x, y according to the response functions [50]:

$$\Phi_1(x, y) = \frac{a_1x}{1 + b_1x + b_2y}, \quad \Phi_2(x, y) = \frac{a_2x}{1 + b_1x + b_2y} \quad (\text{B-2})$$

where $a_i, i=1,2$ are the search rates of a predator for the preys x, y respectively, while $b_i = h_i a_i, i=1,2$ where $h_i, i=1,2$ are the expected handling times spent with the preys x, y respectively. The parameters e_1 and e_2 represent, the conversion rates of the preys x, y to predator z . Obviously, when b_1 and b_2 are very small the functional of response $\Phi_i, (i=1,2)$ become linear response see Volterra functional response [51]. In the other hand as one of both b_1 and b_2 tends to zero the system approaches to hyperbolic Holling type II [52]. The prescribed model characterized by nonlinear response since amount of food consumed by predator per unit time depends upon the available food sources from the two preys x and y .

B.2 Double Mackey-Glass systems

We consider two double Mackey-Glass systems which consist of two coupled Mackey-Glass equations [53]:

$$\begin{cases} \dot{x}_1 = \frac{bx_{1\tau}}{1+x_{1\tau}^n} - rx_1 \\ \dot{x}_2 = \frac{bx_{2\tau}}{1+x_{2\tau}^n} - rx_2 - x_1 \end{cases} \quad (\text{B-3})$$

The system is a model of blood production of patients with leukemia. The variables x_1 , x_2 are the concentration of the mature blood cells in the blood, and $x_{1\tau}$, $x_{2\tau}$ are presented the request of the cells which is made after τ seconds, i.e. $x_{i\tau} = x_i(t - \tau)$, $(i = 1, 2)$. The time delay τ indicates the difference between the time of cellular production in the bone marrow and of the release of mature cells into the blood. According to the observations, the time τ is large in the patients with leukemia and the concentration of the blood cells becomes oscillatory. In this study, the delay time fixed in 20 second ($\tau = 20$) and the parameters are shown as follow: $b = 0.2$, $r = 0.1$, and $n = 10$.

B.3 Energy communication system in biological research

The so-call static state in life sciences means that the system of life is approach to a stable condition. Moreover, the relation of energy communication among the elements in a system of life is called arrangement of static state. The energy communication of elements in a system of life in static state can be divided into two forms:

(B-1) Independent form:

All the elements in a system of life can communicate energy individually with other energy systems out of theirs. The mathematics form is as follow:

$$\begin{cases} \frac{du_1}{dt} = -A_1u_1^2 + B_1u_1 + (C_{12} - D_{12}u_1)u_2 - \varphi_1 \\ \frac{du_2}{dt} = -A_2u_2^2 + B_2u_2 + (C_{21} - D_{21}u_2)u_1 - \varphi_2 \end{cases} \quad (\text{B-4})$$

where A_i, B_i, C_{ij} and D_{ij} ($i, j=1, 2, \dots, n$) are parameters, u_1 and u_2 are two different elements in a system of life and φ_1, φ_2 are modified terms. The term $(-A_iu_i^2 + B_iu_i)$ represents the energy communicated with other energy systems, and the term $(C_{ij} - D_{ij}u_i)u_j$ represents the energy communicated with the elements in the system of themselves. As a result, independent form can be $(-A_iu_i^2 + B_iu_i) \neq 0$, ($i=1, 2, \dots, n$) and $(C_{ij} - D_{ij}u_i)u_j, (i, j=1, 2, \dots, n)$ are very small in general. If the natural medium is change, such as the lack of food or the limit of living space, $(C_{ij} - D_{ij}u_i)u_j$ may be rising.

(B-2) Dependent form:

There are two different parts of elements in these systems of life. The first part of elements can communicate energy individually with other energy systems out of theirs. The mathematics form is the same to (Eq. (B-4)). The second part of elements can not communicate energy individually with other energy systems out of theirs, they have to be provided the energy by the first part of elements. The mathematics form is as follow:

$$\begin{cases} \frac{du_i}{dt} = -A_iu_i^2 + B_iu_i + \sum_{j=k+1}^n (C_{ij} - D_{ij}u_i)u_j - \varphi_i \\ \frac{du_j}{dt} = \sum_{h=1}^{m_j} (C_{jh} - D_{jh}u_j)u_h - \varphi_j \end{cases} \quad (\text{B-5})$$

$(i \in k, j \in n - k)$

where k represents the number of the first part elements and m_j represents the number of the second part elements.

In further studies, the system of food chain with three states can be described by the mathematical model as follow:

$$\begin{cases} \frac{du_1}{dt} = A_1u_1^2 + B_1u_1 + (C_{12} - D_{12}u_1)u_2 - \varphi_1 \\ \frac{du_2}{dt} = (C_{21} - D_{21}u_2)u_1 + (C_{23} - D_{23}u_2)u_3 - \varphi_2 \\ \frac{du_3}{dt} = (C_{32} - D_{32}u_3)u_2 - \varphi_3 \end{cases} \quad (\text{B-6})$$

B.4 Virus-immune system

A mathematical model of the virus-immune system consisting of the following three nonlinear differential equations is considered in this study:

$$\begin{cases} \frac{dT}{dt} = s - \mu_1T + rT \left[1 - \frac{T+I}{\Gamma} \right] - kVT \\ \frac{dI}{dt} = kVT - \mu_2I \\ \frac{dV}{dt} = \mu_3NI - kVT - \mu_4V \end{cases} \quad (\text{B-7})$$

where T , I and V represent the population concentrations of uninfected, infected target cells and virus respectively. We denote by the s constant supply of target cells from its precursor. These cells have a finite life time and μ_1 represents the average death rates of these cells. These target cells are assumed to grow logistically with specific growth rate r and carrying capacity Γ . In the presence of virus, the target cells become infected. Since virus must meet the cells in order to infect them, a mass action term is used to model infection with k as the infection rate. μ_2 denote the natural death rate of infected cells. All infected cells are assumed to be capable of producing virus. It is assumed that N virion are released by each infected cell during its lifetime. μ_3 represents the death rate of infected cells due to lysis. μ_4 is the death rate of free virus.

Appendix C

Pragmatical Asymptotical Stability Theory

The stability for many problems in real dynamical systems is actual asymptotical stability, although may not be mathematical asymptotical stability. The mathematical asymptotical stability demands that trajectories from all initial states in the neighborhood of zero solution must approach the origin as $t \rightarrow \infty$. If there are only a small part or even a few of the initial states from which the trajectories do not approach the origin as $t \rightarrow \infty$, the zero solution is not mathematically asymptotically stable. However, when the probability of occurrence of an event is zero, it means the event does not occur actually. If the probability of occurrence of the event that the trajectories from the initial states are that they do not approach zero when $t \rightarrow \infty$, is zero, the stability of zero solution is actual asymptotical stability though it is not mathematical asymptotical stability. In order to analyze the asymptotical stability of the equilibrium point of such systems, the pragmatical asymptotical stability theorem is used.

Let X and Y be two manifolds of dimensions m and n ($m < n$), respectively, and φ be a differentiable map from X to Y , then $\varphi(X)$ is subset of Lebesgue measure 0 of Y [54]. For an autonomous system

$$\frac{dx}{dt} = f(x_1, \dots, x_n) \quad (\text{C-1})$$

where $x = [x_1, \dots, x_n]^T$ is a state vector, the function $f = [f_1, \dots, f_n]^T$ is defined on $D \subset R^n$ and $\|x\| \leq H > 0$. Let $x=0$ be an equilibrium point for the system (C-1).

Then

$$f(0) = 0 \quad (\text{C-2})$$

For a nonautonomous systems,

$$\dot{x} = f(x_1, \dots, x_{n+1}) \quad (C-3)$$

where $x = [x_1, \dots, x_{n+1}]^T$, the function $f = [f_1, \dots, f_n]^T$ is define on $D \subset R^n \times R_+$, here $t = x_{n+1} \in R_+$. The equilibrium point is

$$f(0, x_{n+1}) = 0. \quad (C-4)$$

Definition The equilibrium point for the system (C-1) is pragmatically asymptotically stable provided that with initial points on C which is a subset of Lebesque measure 0 of D , the behaviors of the corresponding trajectories cannot be determined, while with initial points on $D - C$, the corresponding trajectories behave as that agree with traditional asymptotical stability [55-56].

Theorem Let $V = [x_1, \dots, x_n]^T : D \rightarrow R_+$ be positive definite and analytic on D , where x_1, x_2, \dots, x_n are all space coordinates such that the derivative of V through Eq. (C-1) or (C-3), \dot{V} , is negative semi-definite of $[x_1, x_2, \dots, x_n]^T$.

For autonomous system, Let X be the m -manifold consisted of point set for which $\forall x \neq 0, \dot{V}(x) = 0$ and D is a n -manifold. If $m+1 < n$, then the equilibrium point of the system is pragmatically asymptotically stable.

For nonautonomous system, let X be the $m+1$ -manifold consisting of point set of which $\forall x \neq 0, \dot{V}(x_1, x_2, \dots, x_n) = 0$ and D is $n+1$ -manifold. If $m+1+1 < n+1$, i.e. $m+1 < n$ then the equilibrium point of the system is pragmatically asymptotically stable. Therefore, for both autonomous and nonautonomous system the formula $m+1 < n$ is universal. So the following proof is only for autonomous system. The proof for nonautonomous system is similar.

Proof Since every point of X can be passed by a trajectory of Eq. (C-1), which is one- dimensional, the collection of these trajectories, C , is a $(m+1)$ -manifold

[55-56].

If $m+1 < n$, then the collection C is a subset of Lebesgue measure 0 of D . By the above definition, the equilibrium point of the system is pragmatically asymptotically stable.

If an initial point is ergodically chosen in D , the probability of that the initial point falls on the collection C is zero. Here, equal probability is assumed for every point chosen as an initial point in the neighborhood of the equilibrium point. Hence, the event that the initial point is chosen from collection C does not occur actually. Therefore, under the equal probability assumption, pragmatical asymptotical stability becomes actual asymptotical stability. When the initial point falls on $D-C$, $\dot{V}(x) < 0$, the corresponding trajectories behave as that agree with traditional asymptotical stability because by the existence and uniqueness of the solution of initial-value problem, these trajectories never meet C .

In Eq. (5-8) V is a positive definite function of n variables, i.e. p error state variables and $n-p=m$ differences between unknown and estimated parameters, while $\dot{V} = e^T C e$ is a negative semi-definite function of n variables. Since the number of error state variables is always more than one, $p > 1$, $m+1 < n$ is always satisfied, by pragmatical asymptotical stability theorem we have

$$\lim_{t \rightarrow \infty} e = 0 \quad (C-5)$$

and the estimated parameters approach the uncertain parameters. The pragmatical adaptive control theorem is obtained. Therefore, the equilibrium point of the system is pragmatically asymptotically stable. Under the equal probability assumption, it is actually asymptotically stable for both error state variables and parameter variables.

References

1. L.M. Pecora, T.L. Carroll, "Synchronization in chaotic systems", Phys Rev Lett 64 (1990) 821.
2. LO Chua, M. Itah, "Chaos synchronization in Chua's circuits" , J Circuits Syst Comput 3 (1993) 93.
3. LO Chua, T. Yang, GQ Zhong, "Adaptive synchronization of Chua's oscillators", Int J Bifur Chaos 6 (1996) 189.
4. G Chen, X.Dong, "From chaos to order. Singapore", World Scientific (1998) .
5. L. Kocarev, U. Parlitz, "General approach for chaotic synchronization with applications to communication" , Phys. Rev. Lett. 74 (1995) 5028.
6. S.K. Han, C. Kurrer, Y. Kuramoto, "Dephasing and bursting in coupled neural oscillators" , Phys. Rev. Lett. 75 (1995) 3190.
7. B. Blasius, A. Huppert, L. Stone, "Complex dynamics and phase synchronization in spatially extended ecological systems", Nature 399 (1999) 354.
8. M. Lakshmanan, K. Murali, "Chaos in nonlinear oscillators: controlling and synchronization", Singapore: World Scientific (1996).
9. Xinghuo Yu, Yanxing Song, "Chaos synchronization via controlling partial state of chaotic systems", Int. J. Bifurcat Chaos 11 (2001) 1737.
10. S Chen, J Lu, "Synchronization of an uncertain unified chaotic system via adaptive control", Chaos, Solitons & Fractals 14 (2002) 643.
11. JH.Park, "Stability criterion for synchronization of linearly coupled unified system", Chaos, Solitons & Fractals 23 (2005) 1319.
12. MG Rosenblum, AS Pikovsky, J Kurths, "From phase to lag synchronization in coupled chaotic oscillators", Phys Rev Lett 76(1996)1804.
13. E. Ott, C. Grebogi, JA. Yorke "Controlling chaos", Physical Review Letters 64 (1990) 1196-1199.
14. H. Y. Hu, "An adaptive control scheme for recovering periodic motion of chaotic

- systems”, *Journal of Sound and Vibration* 199 (1997) 269-274.
15. Jun-Juh Yan, Meei-Ling Hung and Teh-Lu Liao, “Adaptive sliding mode control for synchronization of chaotic gyros with fully unknown parameters”, *Journal of Sound and Vibration* 298 (2006) 298-306.
 16. Heng-Hui Chen, “Adaptive synchronization of chaotic systems via linear balanced feedback control”, *Journal of Sound and Vibration* 306 (2007) 865-876.
 17. Mei Sun, Lixin Tian, Shumin Jiang and Jun Xu “Feedback control and adaptive control of the energy resource chaotic system”, *Chaos, Solitons & Fractals* 32 (2007)1725-1734.
 18. T. Yang, L. B. Yang and C.M. Yang “Theory of control of chaos using sample data”, *Physics Letters A* 246 (1998) 284-288.
 19. T. Yang, C.M. Yang and L. B. Yang “Control of Rossler system to periodic motions using impulsive control method”, *Physics Letters A* 232 (1997) 356-361.
 20. M.T. Yassen “Chaos synchronization between two different chaotic system using active control”, *Chaos, Solitons & Fractals* 23 (2005) 131–140.
 21. Tang Fang and Ling Wang “An adaptive active control for the modified Chua’s circuit”, *Physics Letters A* 346 (2005) 342–346.
 22. Marat Rafikov and José Manoel Balthazar “On control and synchronization in chaotic and hyperchaotic systems via linear feedback control”, *Communications in Nonlinear Science and Numerical Simulation* 13 (2008) 1246-1255.
 23. Z. -M. Ge and H. -H. Chen “Double degeneracy and chaos in a rate gyro with feedback control”, *Journal of Sound and Vibration* 209 (1998) 753-769.
 24. O.E. RöSSLer, “An equation for hyperchaos”, *Phys Lett A* 71 (1979) 155.
 25. C. Barbara and C. Silvano, “Hyperchaotic behavior of two bi-directionally Chua’s circuits”, *Int J Circ Theory Appl* 30 (2002) 625.
 26. G. Grassi and S.A. Mascolo, “A systematic procedure for synchronizing hyperchaos via observer design”, *J Circ Syst Comput* 11 (2002) 1.

27. J.Y. Hsieh, C.C. Hwang, A.P. Wang and W.J. Li, “Controlling hyperchaos of the Rössler system”, *Int J Control* 72 (1999) 882.
28. K. Thamilmaran, M. Lakshmanan and A. Venkatesan, “Hyperchaos in a modified canonical Chua’s circuit”, *Int J Bifurcat Chaos* 14 (2004) 221.
29. J. Lü and G. Chen, “A new chaotic attractor coined” *Int. J. Bifurcation & Chaos* 12 3 (2002) 659.
30. J. Lü, T. Zhou and S. Zhang, “Chaos synchronization between linearly coupled chaotic system” *Chaos, Solitons and Fractals* 14 4 (2002) 529.
31. J. Lü, G. Chen and S. Zhang, “The compound structure of a new chaotic attractor” *Chaos, Solitons and Fractals* 14 5 (2002) 1.
32. J. Lü, G. Chen and S. Zhang, “Dynamical analysis of a new chaotic attractor” *Int. J. Bifurcation & Chaos* 12 5 (2002) 1001.
33. S. Chen and J. Lü, “Synchronization of an uncertain unified chaotic system via adaptive control” *Chaos, Solitons and Fractals* 14 4 (2002) 643.
34. Y. Yu and S. Zhang, “Controlling uncertain Lü system using backstepping design” *Chaos, Solitons and Fractals* 15 5 (2003) 897.
35. J. Richard Smith, “*Fathoming the Cosmos and Ordering the World: The Yi Jing (I Ching or Classic of Changes) and Its Evolution in China*”, University of Virginia Press, [ISBN 978-0813927053](https://doi.org/10.1215/00141801-2008-001) (2008).
36. Stephen Karcher, Ching I, “*The Classic Chinese Oracle of Change: The First Complete Translation with Concordance*”, London: Vega Books. [ISBN 1-84333-003-2](https://doi.org/10.1017/CBO9780511524444) (2002).
37. S. J. Marshall, “*The Mandate of Heaven: Hidden History in the I Ching*”, Columbia University Press, [ISBN 0-231-12299-3](https://doi.org/10.1215/00141801-2001-001) (2001).
38. Z.-M. Ge, C.-W. Yao, H.-K. Chen, “Stability on Partial Region in Dynamics”, *Journal of Chinese Society of Mechanical Engineer*, 15 (1994) 140.
39. Z.-M. Ge, H.-K. Chen, “Three Asymptotical Stability Theorems on Partial Region

- with Applications”, Japanese Journal of Applied Physics, 37 (1998) 2762.
40. Z.-M. Ge, “Necessary and sufficient conditions for the stability of a sleeping top described by three forms of dynamic equations”, Phys. Rev. E77 (2008) 046606 .
 41. H.K. Chen, “Global chaos synchronization of new chaotic systems via nonlinear control”, Chaos Solitons Fractals 23 (2005) 1245.
 42. D. Xu, Z. Li, “Manipulating the scaling factor of projective synchronization in three-dimensional chaotic systems”, Chaos 11 (2001) 439.
 43. D. Xu, C.Y. Chee, “Controlling the ultimate state of projective synchronization in chaotic systems of arbitrary dimension”, Phys. Rev. E 66 (2002) 046218.
 44. L. Kocarev, U. Parlitz, “Generalized synchronization, predictability, and equivalence of unidirectionally coupled dynamical systems”, Phys. Rev. Lett. 76 (1996) 1816.
 45. J.H. Park, “Adaptive synchronization of hyperchaotic chen system with uncertain parameters”, Chaos Solitons Fractals 26 (2005) 959.
 46. J.H. Park, “Adaptive synchronization of Rossler system with uncertain parameters”, Chaos Solitons Fractals 25 (2005) 333.
 47. E.M. Elabbasy, H.N. Agiza, M.M. El-Desoky, “Adaptive synchronization of a hyperchaotic system with uncertain parameter”, Chaos Solitons Fractals 30 (2006) 1133.
 48. X. Wu, Z.-H Guan, Z. Wu, T. Li, “Chaos synchronization between Chen system and Genesio system”, Phys. Lett. A 364 (2007) 315.
 49. M. Hu, Z. Xu, R. Zhang, A. Hu, “Adaptive full state hybrid projective synchronization of chaotic systems with the same and different order”, Phys. Lett. A 365 (2007) 315.
 50. Y. Kuang, “Basic properties of mathematical population models”, Biomathematics 17 (2002) 142.
 51. A. EI-Gohary and M. Yassen, “Optimal control and synchronization of Lotka-Volterra model”, Chaos, Solitons & Fractals 12 (2001) 2087.
 52. J. Sugie and M. Katayama, “Global asymptotic stability of a predator-prey system of Holling type”, Nonlinear Analysis 160 (1999) 105.

53. M. C. Mackey and L. Glass, "Oscillation and chaos in physiological control systems", *Science* 197(4300) (1977) 287.
54. Y. Matsushima, *Differentiable Manifolds*, Marcel Dekker, City, 1972.
55. Z.M. Ge, J.K. Yu and Y.T. Chen, "Pragmatical asymptotical stability theorem with application to satellite system", *Jpn. J. Appl. Phys.*, 38 (1999) 6178.
56. Z.M. Ge and J. K. Yu, "Pragmatical asymptotical stability theorem partial region and for partial variable with applications to gyroscopic systems", *The Chinese Journal of Mechanics*, 16 (2000) 179.
57. J. H. Park, "Adaptive synchronization of Rössler system with uncertain parameters", *Chaos, Solitons and Fractals*, 25 (2005) 333.
58. E. M. Elabbasy, H. N. Agiza and M. M. El-Desoky, "Adaptive synchronization of a hyperchaotic system with uncertain parameter", *Chaos, Solitons and Fractals*, 30 (2006) 1133.
59. A. El-Gohary and R. Yassen, "Adaptive control and synchronization of a coupled dynamo system with uncertain parameters", *Chaos, Solitons and Fractals*, 29 (2006) 1085.
60. H. Fotsin and S. Bowong, "Adaptive control and synchronization of chaotic systems consisting of Van der Pol oscillators coupled to linear oscillators", *Chaos, Solitons and Fractals*, 27 (2006) 822.